STUDIES ON CHROMATIN CONFORMATION OF RADIOSENSITIVE (XRS) CHINESE HAMSTER CELL LINES

Arthur Ng

A Thesis Submitted for the Degree of PhD
at the
University of St Andrews

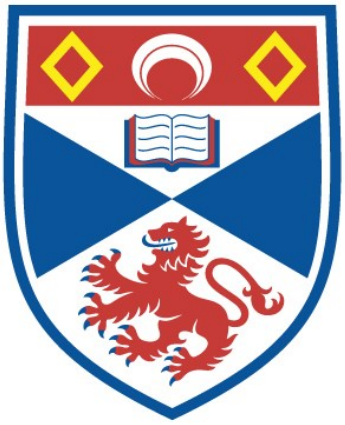

1998

Studies on Chromatin Conformation of Radiosensitive (*xrs*) Chinese Hamster cell lines

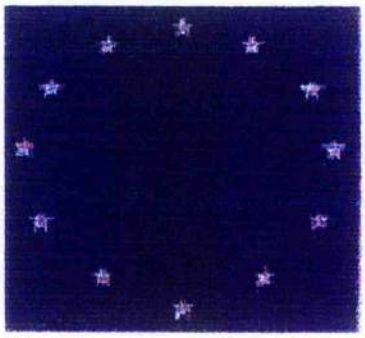

By

Arthur Ng MSc (Aberdeen)

Abstract

The objective of this project was to investigate the chromatin structure of the mutant Chinese hamster ovary cell line, *xrs,* the project consisted of two parts by: a radiobiological study, and a protein chemistry study and to specifically ask, whether or not the increased susceptibility of the *x* family of mutants compared to wt could be attributed to modifications to structure of chromatin or are the modifications a pleiotropic effect of the mutated gene.

The radiobiological study used the change in DNA radiosensitivity with progressive removal of DNA bound proteins as a probe to investigate the chromatin conformation of CHO KI and *xrs*. The DNA alkaline unwinding assay, showed that there was a difference in sensitivity to ionising radiation (IR)-induced damage between *xrs*-5 and CHO KI after treatment with various concentrations of salt (0.25-0.75 M NaCl) and γ-rays (0.25-0.75 Gy), 0.75M NaCl and 0.75 Gy gave maximal effects. The sensitivity difference between mutant and wt was less obvious with NaCl treatment at 0.75 Gy γ-irradiation but nonetheless apparent. This radiosensitivity could be attributed to structural modifications in the mutant cell lines. These structural modifications are represented graphically in two algebraic forms i.e. a quadratic ($y=mx^2$) and a quartic sine ($y= ax^4 + bx^3 + cx^4 + dx+ C$) in CHO KI and *xrs*-5 respectively. The decrease in unwinding in hypertonic solutions was thought to be attributable to either ongoing fast ssb repair, a faster unwinding population , or, loss of DNA supercoiling due to high salt and irradiation, or negative interaction between one unwound DNA population and a adjacent break points leading to saturation. Partial reversion of *xrs*-5 did not alter the unwinding profile markedly. As deduced from the observation that despite the partial reversion the mutant was consistently more susceptible to IR-induced DNA damage compared to wt. The difference in DNA radiosensitivity in this assay of mutant compared to wt may not nesscarily reflect the radiosensitivity of the *xrs* cells.

The protein chemistry study showed that there was a difference observed between protein extracts of mutant *xrs-6* and wt, with respect to histone-related proteins. Specifically, a species of 31 kDa was detectable in extracts of wt but not *xrs*-6 mutant cells. The possible identity of this polypeptide and the rôle of candidate proteins in chromatin structure and radiosensitivity is discussed.

Declaration

I declare that this thesis is of my own composition and has not been submitted previously, either partially or totally, for a degree.

The work recorded in this thesis has been conducted by myself , with references to the work of others being indicated and sources of information specifically acknowledged.

Arthur Ng MSc (Aberdeen)

Acknowledgements

'There comes a time in one's scientific endeavours when one must account for all and give due regard to the veracity and verve of others.'

Therefore I wish to thank my supervisor, Dr P.E. Bryant, for the opportunity to study in the cloistered halls of St Andrews amongst the luminaries and dignitaries whom bring the light of knowledge to illuminate the darken corners of ignominy and ignorance. I wish to express my thanks to the European Union for funding this project.

Equally I wish to thank Dr Elena Notarianni for her help and support during my darkest days and particularly I give thanks for her proofreading skills which has ensured this *magnum opus* expresses *veritas*.

I wish to thank, Mr Angus Gleig and Mr John MacIntyre equally, for their technical assistance and valued support. I wish to thank Mr Sean Earnshaw for the photography and my continued readership of the tabloid press. Mr Dave Shields and the Computer Sciences department, University of Liverpool for the use of their facilities. Granthams of Preston, Lancashire for their assistance with the computer reprographics. University of Liverpool Colour Printing Unit for the colour photocopying, ACE Cards and Stationers of Liverpool for the use of their photocopying facilities and the University of St Andrews and Dundee Bindery for the binding of this dissertation.

I wish to express my appreciation to my family for their support and encouragement throughout. In particular I wish to thank my brother, Simon Ng, for his financial support and for allowing me to pick his mathematical mind on esoteric matters.

Finally I want to thank all the people of St Andrews both Town 'n' Gown for their kindness and friendship. In particularly I want to thank the regular's of the Cellar Bar and in equal measure Lafferty's for the pleasant atmosphere and 'where everybody knows yer name.' (Cheers-theme tune).

Index

PAGE NUMBERS

List of Abbreviations

Abbreviation	Components
AUT	Acid :Urea:Triton polyacrylamide gel
DAB	diaminobenzidine tetrahydrochloride
DNA	Deoxyribose Nucleic Acid
DMSO	Dimethyl sulphoxide (Sigma)
ds	double-stranded
dsb/DSB	double-strand breaks
'EasiGel'	acrylamide/bis-acrlamide stock solution:
Fds	Fraction of double-strands
Fss	Fraction of single-strands
HA	Calcium Hydroxyapatite (BioRad)
HBBS	Hank's balanced salt medium (GibCo BRL)
HEPES	4-(2-hydroxyethyl)piperazine-1-ethanesulfonic acid
HPLC	High Pressure Liquid Chromatography
IR	Ionising Radiation
MEM-CsFe	Eagle's modified minimal essential salts medium, supplemented with new born calf serum plus Fe^{++} salts. (GibCo BRL)
MEM-FCS	Eagle's modified minimal essential salts medium, supplemented with fetal calf serum . (GibCo BRL)
NP40	Nonidet P 40 (Sigma)
PBS	Phosphate Buffered Saline (GibCo BRL)
PVDF	Polyvinyldecafluoride
RE	Restriction Endonuclease
RelXLIN	Relative number of DNA cross-links
SDS	sodium dodecyl sulphate (BDH Merck)
SDS-PAGE	Sodium dodecyl sulphate polyacrylamide gel elecrophoresis
Sörensen's salt	Sodium dihydrogen orthophosphate (BDH Merck)
SSB/10^9 Daltons	Single strand Breakage equation

ss	**single-stranded**
SPB	**Sodium phosphate buffer**
TE	**Trypsin** **EDTA**
TBS (obtained from Scotlab)	**Tris-buffered Saline**
TBST	**Tris-buffered Saline Tween-20**
TEMED	**N,N,N',N'-tetramethylethylenediamine**
wt	**wild type**

Buffer Components

Buffer	Components
Acid electrode buffer	**0.1M glycine** **1M glacial acetic acid**
alkaline unwinding solution	**0.03M sodium hydroxide (BDH Merck)** **0.15M sodium chloride (BDH Merck)**
AUT	**1M glacial acetic acid** **8M urea** **8mM Triton X100**
blocking buffer	**1% powdered skimmed milk in TBS**
Boiling Mix	**0.015M Tris pH 7.5 (BDH Merck)** **4.2% sodium dodecyl sulphate BDH Merck)** **0.075 % 2-Mercaptoethanol (Sigma)** **3% glycerol (Sigma)** **few grains of Bromophenol blue (Sigma)**
DAB	**diaminobenzidine tetrahydrochloride (Sigma):** **a tablet (10 mg) dissolved in 15 ml 0.05M Tris pH 7.6 and 1.7 ml 0.3% nickel sulphate**
Destain	**10% acetic acid and 20% ethanol**
'EasiGel'	**acrylamide/bis-acrlamide stock solution:** **30% w/v acrylamide** **0.8% w/v bis-acrylamide** **37.5:1**
HBSS	**Hanks balanced salts solution (GibCo BRL):** **2mM magnesium sulphate** **4mM potassium chloride** **0.6mM potassium phosphate monobasic** **3.5mM sodium bicarbonate** **8M sodium chloride** **0.6mM sodium phosphate monobasic $2H_2O$**
Ljungman's Lysis Solution/ Extraction buffer	**0.5% Triton X100 (Sigma)** **4mM Tris base pH 7.5 (BDH Merck)** **150mM potassium chloride (BDH Merck)** **5mM magnesium chloride (Sigma)** **0.25-2M sodium chloride (BDH Merck).**
MEM-CsFe	**Eagle's modified minimal essential salts medium, supplemented with 10% new born calf serum plus 27 μg/ml Fe^{++} salts. (GibCo)**
MEM-FCS	**Eagle's modified minimal essential salts medium, supplemented with 10% fetal calf serum (GibCo)**
NP40	**10 % Nonidet P 40 (Sigma)**
PBS	**obtained from GibCo BRL for Tissue Culture.** **140 mM NaCl** **2.5 mM KCl** **8.1 mM Na_2HPO_4** **1.5 mM KH_2PO_4**

PBS	**Phosphate buffered saline (10X) used in antibody probing:** **70.1g sodium chloride** **4.4g sodium dihydrogen orthophosphate** **12.8g disodium hydrogen orthophosphate** **2g potassium chloride**
Prestained Molecular Weight Markers (obtained from BioRad)	**The sizes correspond to the following proteins:-** **Myosin (206 kDa)** **β-galactosidase (125 kDa)** **Bovine Serum Albumin (88 kDa)** **Ovalbumin (47.7 kDa)** **Carbonic Anhydrase (34.9 kDa)** **soyabean trypsin inhibitor (29.6 kDa)** **lysozyme (20.4 kDa)** **Aprotinin (7 kDa)**
Protein Stain	**0.01% Coomassie blue 250G in 10% acetic acid and 20% ethanol**
Reswelling buffer	**10 mM Tris pH7.4** **10 mM NaCl**
SDS	**0.087M sodium dodecyl sulphate (BDH Merck)**
SDS-PAGE	**12% Sodium dodecyl sulphate polyacrylamide gel elecrophoresis:** **2.5% 'EasiGel' (ScotLab)** **0.375M Tris pH 8.8** **0.1% SDS** **12.08 ml double distilled water**
Sörensen's salt	**Sodium dihydrogen orthophosphate(BDH Merck)**
Sodium Phosphate buffer (SPB)	**0.125-0.25M Na_2HPO_4 pH 6.8. (BDH Merck)** **0.125-0.25M NaH_2PO_4 pH 6.8. (BDH Merck)**
TBS (obtained from Scotlab)	**0.05M Tris pH 7.5** **0.15M NaCl .**
TBST	**0.05M Tris pH 7.5** **0.15M NaCl .** **0.1% Tween-20 (Sigma)**
TE	**obtained from Sigma and BDH Merck** **0.05%Trypsin** **0.7nM Na EDTA**
Tris- glycine electrode buffer	**0.05M glycine** **0.005M Tris pH 9.1** **0.1% SDS** **2 L double distilled water**
Western Transfer Buffer	**0.025M Tris pH 9.1** **0.19M glycine** **0.1% SDS**

List of Suppliers and Addresses

Amersham International P.LC.
Amersham Place
Little Chalfont
Buckinghamshire
HP7 9NA
UK

Apple Computer Inc.
20525 Mariani Ave.
Cupertino, CA 95014-6299 USA

BDH Merck Ltd
Broom Rd.
Poole
BH12 4NN
UK

Beckman Instruments Inc.
2500 Harbor Blvd.
Box 3100
Fullerton
CA 92634
USA

Becton Dickinson
1 Becton Dr.
Franklin Lakes
NJ 07417
USA

Bio-Rad Laboratories
3300 Regatta Blvd
Richmond
CA 94804
USA

Boehringer Mannheim UK Ltd.
Bells Lane
Lewes
BN7 1LG
UK

Carl Zeiss Inc.
1 Zeiss Dr.
Thornwood
NY 10594
USA

Claris Corporation
5201 Patrick Henry Dr.
Santa Clara, CA 95052
USA

Computer Associates International Inc..
1 Computer Associates Plaza
Islandia
NY 11788-2000
USA

Corning Inc.
HP-AB-03
Science Products Div.
Corning
NY 14831
USA

Coulter Electronics
1950 West 8th Ave.
Marcus Building (195-10)
Hialeah
FL 33010
USA.

Dynatech Laboratories Inc.
14340 Sullyfield Cir.
Chantilly
VA 22021
USA.

Fisons P.LC.
Bishop Meadow Rd.
Loughborough
Leics. LE11 0RG
UK

GibCo BRL
Life Technologies Ltd.
P.O.Box 35
Trident House
Renfrew Rd., Paisley PA3 4EF
UK

Heraeus Instruments Inc.,
111-A Corporate Blvd,
South Plainfield,
N. J. 07080
USA

Hoefer Scientific Instruments
654 Minnesota St.
P.O.Box 77387
San Francisco
CA 94107
USA

ICN Biomedicals Inc.
3300 Hyland Ave.
Costa Mesa
CA 92626
USA

Hewlett-Packard Ltd.
Cain Rd.
Bracknell
Berks. RG12 1HN

NUNC Inc.
2000 North Aurora Rd.
Naperville
IL 60563
USA
Promega Ltd
Epsilon House
Enterprise Rd.
Chilworth Research Centre
Southampton SO1 7NS
UK

Scotlab Ltd.
Kirkshaws Rd.
Coatbridge
Strathclyde ML5 8AD
UK

Shandon Southern) Life Sciences Intl.
93-96 Chadwick Rd.
Runcorn
Cheshire WA7 1PR
UK
Whatman Inc.
9 Bridewell Pl.
Clifton
NJ 07104
USA

Millipore Corp.
80 Ashby Rd.
Bedford
MA 017430
USA

Pharmacia Biotechnology Inc.
800 Centennial Ave.
Piscataway
NJ 08854
USA
Sarstedt Inc.
Rt.#2 St James Church Rd.
Newton
NC 28601
USA

Schleicher & Schuell
10 Optical Ave.
P.O.Box 2012
Keene
NH 03431
USA
Sigma Chemical Co.
P.O.Box 14508
St Louis
MO 63178
USA
Wheaton
1000 North 10 th St.
Millville
NJ 08332
USA(

Chapter 1:
General Introduction

This dissertation represents a study of the structure of chromatin in Chinese hamster ovary cell lines. These cell lines were derived from a parental line, CHO KI, and the daughter cell lines, *xrs*, were either proficient (CHO KI) or deficient (*xrs*) in DNA double-strand break repair and V(D)J recombination (1,2,3,4). These cell lines have different responses to ionising radiations (5,6,7,8). The aim of the project was to quantify the response of the CHO KI and *xrs* cell lines to ionising radiation-induced damage and to attempt to correlate the response with changes in chromatin structure.

This chapter is divided into five sections:

(i). Chromatin Structure.

(ii). Chinese Hamster Ovary Cell Lines.

(iii). DNA Unwinding and the modified Ahnström & Erixxon Assay.

(iv). Micronucleus Assay.

(v). Chromatin Conformational Proteins.

(vi). Experimental 0bjectives.

(i) CHROMATIN STRUCTURE

The cell's growth and differentition processes lead to changes in the chromatin conformation. The eukaryotic DNA is packaged with scaffolding proteins to form a chromosome and hence the total genetic information is termed the genome. Chromosome conformation is a very good compromise between compaction and accessibility. The precise nature of chromosomal compaction has implications on the mutability and reparability of the structure. The reparability of the structure reflects genomic stability in that misrepair or defective repair gives rise to chromosome aberrations or chromosome loss (9).

The haploid human genome contains 3 x10^9 bp DNA organised as 46 chromosomes (22 pairs of autosomes and 2 sex chromosomes), thus 24 different DNA molecules each containing from 50 x 10^6 to 250 x 10^6 bp. When uncoiled the DNA is 21.7 to 8.5 cm long. In diploid organisms, there are two copies of each chromosome, one maternal and one paternal except for the sex chromosomes where the gamete receives an Y chromosome from the father and an X from the mother.

The DNA of all chromosomes is packaged into a compact structure with the aid of specialised proteins, the histones and non-histonal proteins together these proteins and DNA form chromatin (Fig.1). Histones associate with DNA to form nucleosomes. Nucleosomes are usually packed together by linker histones (histone H1) to form regular higher-order structures. Histones rarely dissociate from the DNA and they influence accessibility to the chromosome. In the nucleosome 146 bp DNA is wrapped in 2 turns around a core particle of eight histones, the histone octamer. The positioning of the nucleosomes on the DNA is dynamic and depends on two influences; the propensity of the DNA to form tight loop at A-T rich sites, and, by the presence of other DNA bound proteins e.g. Topoisomerase II.

Figure 1 shows a diagram of the currently accepted model for the higher order packaging of a metaphase chromosome in which one arm (q) has been magnified to show a looped region arranged radially around a scaffold core and magnification of the loop domain shows one chromatin loop attached to the nuclear lamina by a matrix attachment complex. The matrix is organised into a series of loop domains with specific sites for DNA replication/repair and transcription. Each DNA molecule forming a linear chromosome must contain a centromere, two telomeres and many replication origins. In metaphase the chromosomes become visible under the light microscope and the centromere can clearly be seen as the two arms of the chromatids extend in preparation for mitosis. In Fig.1 the telomeres are indicated, under light microscopy these structures are only made visible using Flouresence *In Situ* Hybridisation (FISH) with fluorescent-tagged telomeric probes. Electron microscopy (EM) of one arm shows the chromatid arranged as a concentric ring of radial loops around a central bilipid matrix (scaffold) membrane. Each loop is anchored to the nuclear matrix. The nuclear matrix contains the residual components of the pore-complex, lamins, the nucleolus and the intranuclear fibres that form the nucleus. Approximately 10% of the total nuclear protein is the nuclear matrix. Evidence for this radial loop model, shown in Fig.1, as proposed by Gasser & Laemmli (1986) (10) is given in the paper by Pienta & Coffey (1984) (11) and supporting evidence provided by the papers of Jackson & Cook (12,13,14). Alternative models are discussed by Wolffe (1995) (14) and briefly discussed later in this section.

Figure 2 shows the high degree of compaction necessary to form an arm of a eukaryotic chromosome. As can be seen from Fig.2, packaging of the naked DNA (2 nm) depends upon interaction with specialised proteins, histones and non-histonal chromosomal proteins. Compaction of the nucleosomal arrays can be mediated by variation in the concentration of mono- and divalent cations in the cytosol (10,11). Consequently 6 nucleosomes form the 10 nm 'beads on a string' model in the presence of low salt (0.2 mM EDTA, 1mM diethanolamine chloride). At moderate strength salt (0.2 mM EDTA, 5mM diethanolamine chloride) chromatin compacts to form a flat wide ribbon of 25 nm width. At physiological ionic strength (100 mM NaCl) chromatin condenses to form an irregular rod of 30 nm in diameter, which is the form found in the eukaryotic nucleus. The six nucleosomes are positioned at each turn of the linker DNA and each turn is pitched at 11 nm; thus each nucleosome is 11 nm wide. Fifty turns form the radial loop (10). Eighteen loops per turn form the miniband, and approximately 106 minibands are stacked around the central axis to form the chromatid. One loop is 0.25 μm in length and the width of the one miniband is 0.84 μm (11).

The linker histone (Histone H1) may align down the longitudinal axis of the 30 nm solenoid/filament or preferentially bind to one end of the nucleosome. The resultant assymmetry gives directionality to the fibre axis, which might propagate

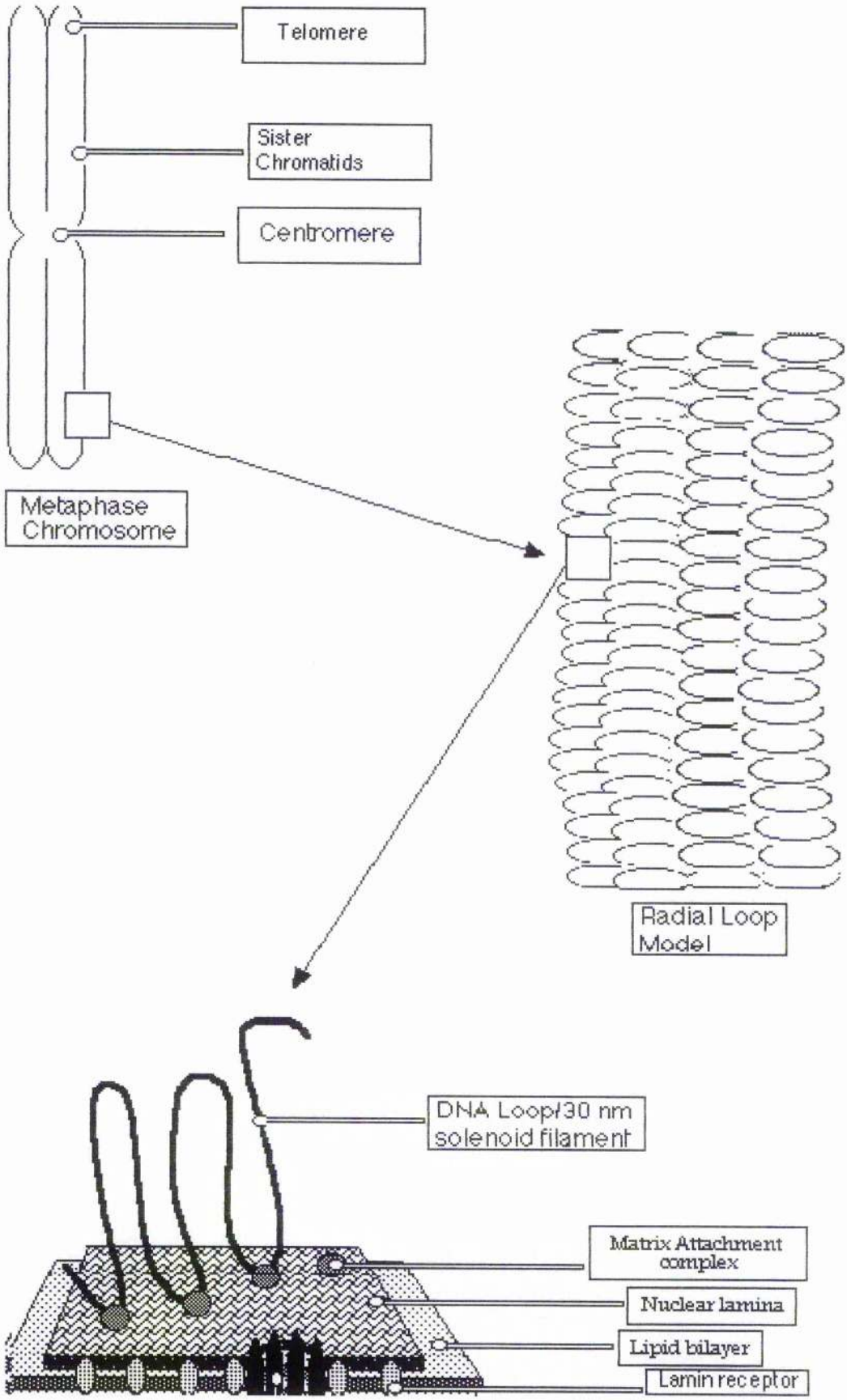

Figure 1:
Higher order chromosome organisation as represented by the radial loop model of Gasser and Laemmli (1986) (10).

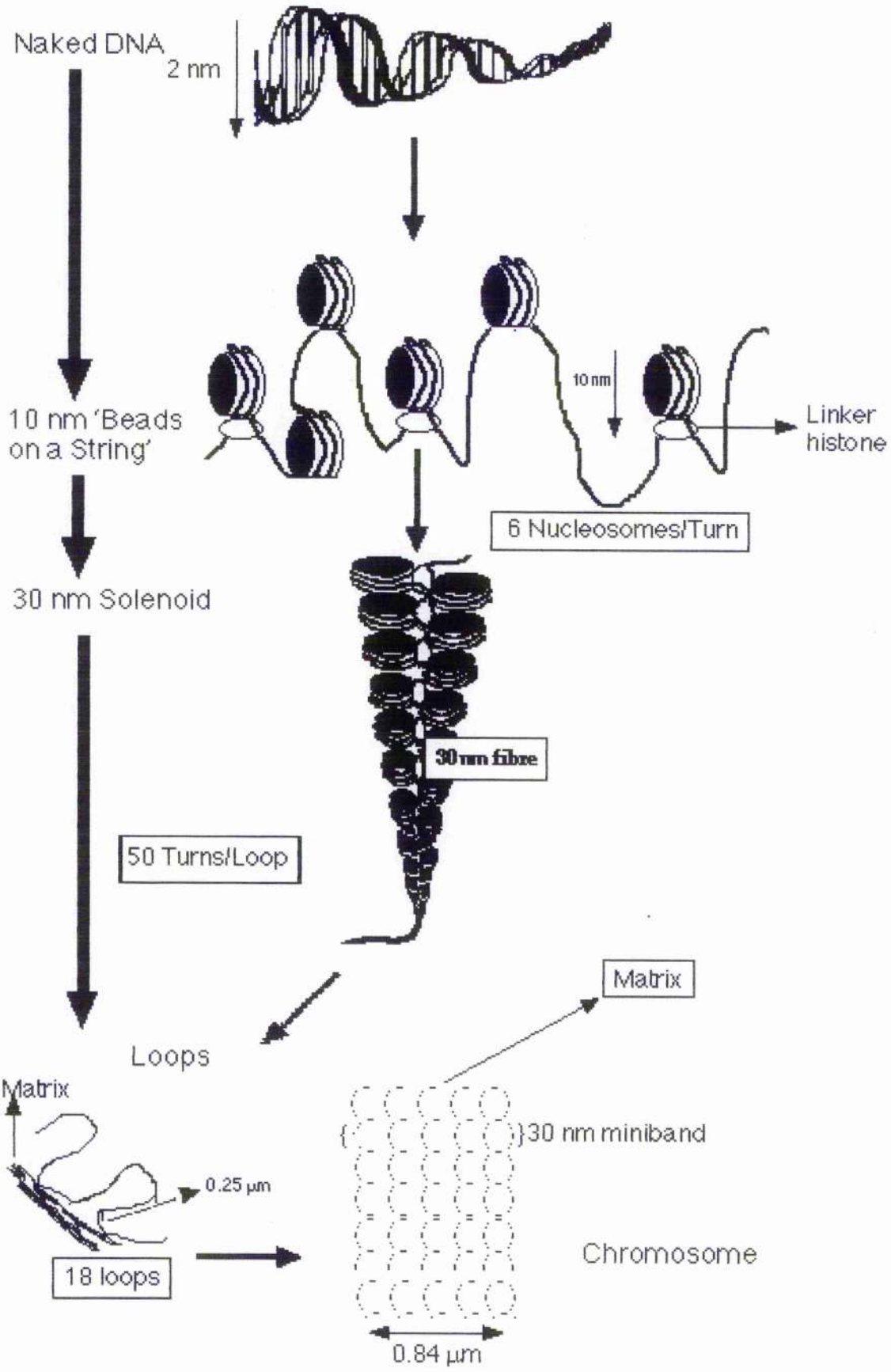

Figure 2:
The compaction of eukaryotic chromatin as DNA supercoiled loops, and the formation of a radial loop structure (Pienta & Coffey 1984 (11)).

over a large region of the chromatin (>1 kb), and polarity to the linker histone. This provides constraints upon the folding capacity of the nucleosomal array providing considerable specificity to the interaction between linker histone and linker DNA. As the linker histone:DNA interaction determines the degree of charge shielding along the phosphodiester backbone, only 60 000 nucleotide pairs can be compacted into a 10 μm nucleus. This was the minimal number of nucleotide pairs that can be compacted as the charge shielding is a function of the net charge neutralisation provided by the basic amino acids of the scaffolding proteins (histones and HMG 1/2).

Other chromatin conformations are possible; one possible conformation detected, (in EM studies of native chromatin at physiological ionic strengths), is bead-like discontinuities or globular nucleosome clusters termed 'superbeads' (16). These superbeads can contain between 8 and 48 nucleosomes. The presence of superbeads show that the chromatin structure does not adopt a single fixed form and that this fluidity indicates that the structure is dynamic.

Alternative helical conformations to the solenoid model are possible: the condensed zig-zag ribbon of two parallel rows of nucleosomes mediated by linker histones and coiling of this ribbon forms the 30 nm fibre (17 & 18). Cryo-electron microscopy has shown a chromatin fibre which follows an irregular path with smoothly bent regions interspersed with sharp bends forming a fibre that is a 2 nucleosome wide ribbon that zig-zags with little face-to-face contact and an acute linker DNA.

Another model, 'coiled linker', assumes that the linker DNA are not limited to the central axis of the 30 nm fibre but follow the orientation of the nucleosome chain, and thus the linker DNA lies between adjacent nucleosomes then the linker histones binds on the coiled DNA of the core particle. The linker DNA thus binds to the bound linker histone forming the chromatosome (19).

An alternative model to the radial loop is one whereby the 30 nm fibre is compacted to form a multiple helical folded condensed 250 nm fibre (20). Instead of a radial loop conformation arranged as a stacked miniband around a central scaffold a more haphazard arrangement of local looping of 50-100 kb forming hierarchical folded domains of 50 to 200 nm is favoured, and, these loops are thought to assemble and disassemble during mitosis.

(ii) CHINESE HAMSTER OVARY CELL LINES

The hamster cell lines are a good model for examining DSB repair not only as they are easy to culture and good hosts for exogenously transfected DNA, but especially because there are mutants (*xrs)* with defective components of the DNA repair pathways, e.g.. Ku 80 and,DNA-PK (p350), which has been demonstrated to be defective in Severe Combined Immune Deficient (SCID) cells (21).

The *xrs* family cell lines were derived from the wild type (wt) parent, CHO KI and were first isolated by the 'toothpick' method (5). The family members are characterised into six cross-complementation groups according to the positional mutation in the expression of the Xrs protein and their sensitivity to DNA damaging agents: X-ray; Bleomycin (a radiomimetic i.e.single-(ssb) and double-strand (dsb) break agent); UltraViolet (UV); Methyl methanesulphonate (MMS,a ssb agent); N-Methyl-N'-nitro-n-nitrosoguanidine (MNNG); and, EMS (6). The cross-sensitivity to the radiomimetic Bleomycin would indicate that chromosome aberrations occured at first mitosis at G_o/G_1 similiar to that detected after irradiation. These aberrations are:- dicentric/acentric fragments, reciprocal translocation, interstitial deletion, and, terminal deletion (22).

Repair kinetic studies (Jeggo 1990, Collins 1993) had shown that the six mutants had a decreased ability to repair double-strand breaks (dsb) and dsb rejoining followed biphasic kinetics i.e. it has a fast and a slow component. As the mutants showed no variation in the initial rejoining rate i.e.a loss of the biphasic nature; therefore the defect was expressed differently, either as an absence of one rejoining enzyme or rejoining might occur by a separate pathway, to the wild type. As these mutants showed a DSB rejoining defect similar to the yeast *rad*52 mutant (which was defective in X-ray induced recombinational repair) the defect is likely to lie within the mutants' Non-Homologous End Joining (NHEJ) pathway. Following irradiation at 0.95 Gy there was more chromatid gaps and breaks in the *xrs* family than in the CHO KI parent which would indicate that unrepaired DSB can lead to a chromatid gap or break in these mutants (8). The primary defect in *xrs* cells is a biochemical change in the mechanism of DNA repair (1,2,3). Cytogenetic studies on *xrs* found that the number of unrepaired double-strand breaks (at t=20 mins) in these mutants was greater than the parent cells and correlated with an increase in chromosome breaks. Therefore there were at least two pathways to process dsbs, one requiring the *xrs* gene product and a second leading to the formation of chromosome exchanges. Thus unrepaired dsbs might appear as chromosome or chromatid breaks at mitosis, and any unrejoined dsbs induced in G2 would either appear as breaks or interact with other dsbs to produce chromatid exchange aberrations (22). The mutation in the *xrs* family can be reverted by 5-azacytidine and thus the defective repair autosomal gene was determined to be a single copy Cytosine-methylated and unexpressed gene (23). Transfection studies have shown that the defect was transient (24) i.e. the deficiency was reversible and could be corrected by cross -complementation in culture or correctable by transfection with the gene for Ku antigen(24).

The *xrs* family have been physically mapped to the human gene XRCC5 situated on chromosome 2q33-35, encoding a DNA end-binding protein Ku80 (2). These cells are deficient in DNA dependent Ku-mediated double-strand break repair and V(D)J recombination (3). V(D)J recombination is a site-specific gene rarrangement process used by developing vertebrate B and T cells to produce

alternative immunoglobulin and T-cell receptors (TCR). In this process varible (V), diversity (D) and joining (J) subexonic gene segments are combined after initial blunt-ended DNA double-strand breakage at recombination signal sequences (RSS) flanking the V,D and J segments by recombination activating gene (RAG) products, RAG1 and RAG2. The diversity of TCR is provided by the shuffling of the V and D segments and J segment combines at RSS blunt-ends to form the coding ends. Functionality is restored by DSB-dependent DNA ligase repair joining the coding ends to the constant domain. The DSB processing in V(D)J recombination is thought to involve Ku70 and repair of DSB involves Ku70 linked with Ku 80 in a protein kinase (p350) complex. The *xrs* family have a cross-sensitivity to topoisomerase II inhibitors e.g. etoposide (VP16) which might indicate DNA supercoiling alterations in the mutant cell lines (25). This antitumour drug (VP16) stabilises topoisomerase II in the DNA bound state after the enzyme has induced dsb's and as such could be classed as dsb radiomimetic (26). Thus inability to repair dsbs would make *xrs* mutants sensitive to VP16, and as one rôle of topoisomerase II is the regulation of chromosome condensation and condensation is effected by changes in supercoiling therefore treatment with VP16 could lead to over-condensation (25).
Family member *xrs-5* has been found to have chromatin structural abnormalities (27) and higher rates of radiation-induced, unrepaired dsb than the wt parent (28). *Xrs*-6 has been shown to have elevated sister chromatid exchange's after X-irradiation (an index of chromosome instability or mutability) (29). Recently Ku80 knockout mice have been bred showing both whole animal and cellular phenotypic differences to wild type mice. The most notable observation was that the homozygous mice were 40-60% smaller than their normal littermates, and the characteristic *xrs* radiosensitivity, dsb and V(D)J rejoining deficiencies of murine cells cultured from these mice. Thus Ku80 might have a rôle in growth regulation (30) and absence of Ku80 might have a rôle in radiosensitivity .

(iii) DNA UNWINDING AND THE MODIFIED AHNSTRÖM & ERIXXON ASSAY

In this section the theory behind the development of the DNA unwinding assay is discussed and the notion is developed of the DNA loops or the anchoring complex as one locus for ionising radiation-induced DNA damage.
The format for this section is to review the literature pertaining to DNA unwinding and to describe the DNA unwinding assay. This assay would provide the prima facie evidence for the differences in chromatin structure of the *xrs* family having a rôle in their radiosensitivity.

Acceptance of the loop model e.g. the radial loop model (10) implies acquiescence to the further DNA compaction by supercoiling, and quantitative methods are available to investigate, this higher order packaging and to measure

the reponse of these DNA loops to clastogenic agents (Instigators of chromosome breakage) such as ionising radiation.

Looping of solenoidal chromatin into domains of 60 000 bp periodicity (average loop size) increases compaction by a factor of 680. The final 10-20 kb can be partly achieved by DNA supercoiling. Supercoils allow for the generation of local regions or domains which are self-regulating i.e. small regions of DNA can be 'melted' or unwound for replication/repair and larger global domains can be opened for transcription. The local regulator of these supercoils can be assumed to be DNA topoisomerase I and II (31, 32). The nuclear matrix has been implicated in the spatial control of replication, gene transcription and DNA damage repair. Thus the interaction (attachment) between the supercoils and the nuclear matrix may be important in the response of chromatin to ionising radiation-induced DNA damage (33).

The interface between DNA loop domains and the nuclear matrix are mediated by nucleoprotein interactions, and these mediators allow maintenace of contiguous regions with different superhelical densities. The degree of supercoiling within a segment profoundly affects gene transcription, thus any gene bracketed between two intact matrix attachment regions would be protected from position effects and be a independent, fully functional unit. The attachment points are non-random, providing spatial and temporal specificity for nucleic acid metabolism at the matrix (31,34,35). Tight attachment points provide structural stability and loci for segregation of daughter chromatids at mitosis. Looser attachment points allow for transcriptional and replicational loci.

The nuclear matrix can be cross-linked to the DNA by the nuclear lamina via the action of *cis*-platinium. (37) Thus infering that there is a close apposition of DNA to the nuclear lamina. Ionising radiation will cross-link the nuclear matrix proteins to transcriptionally-active genes and these proteins can be found associated with replication forks.

Many genes have adjacent matrix attachment region (MAR) in their upstream noncoding sequences. These MARs show considerable sequence homology across species and contain multiple copies of the DNA topoisomerase II consensus sequence. MAR binding proteins are tissue specific controlling gene transcription via topological modifications upregulating activation, replication and repair (31).

Numerous quantitative methods are available to measure the response of γ-irradiation on DNA loop superhelicity and or loop:nuclear matrix interactions. Five techniques commonly used by radiobiologists are:

(a) Sedimentation;
(b) Fluorescent halo method;
(c) Comet assay;
(d) FACS/FCM;
(e) DNA Unwinding;

For the purposes of this radiobiological study, method (e) was used. Prima facie evidence for DNA loop differences in the *xrs* family was shown by family member *xrs*-5 (Yasui *et al* 1991), and the sensitive DNA unwinding assay of Ahnström & Erixon 1981 was thought to provide a good baseline for further study. The evidence obtained by the unwinding assay for *xrs*-5 having a different chromosome condensation from the wild type CHO KI cell line would be supported by the data from the micronucleus assay. Additionally the micronucleus assay would give an indication as to the biochemical state of the cell line i.e. if there is a reversion of the mutant cell line to the radioresistant wt parent, CHO KI ?

In summary, nucleoid DNA has been shown to be supercoiled and thus torsionally constrained. As ethidium bromide binds to supercoiled DNA avidly, and it's fluorescence has been observed outside of the nuclear envelope, then the DNA must form loop domains which contact the nuclear periphery. The fluorescent halo dynamics show that unscissioned DNA has a biphasic character i.e. the supercoils flip from negative superhelical turns to positive superhelical turns, moving from a tightly condensed, closed circle configuration to an open, 'nicked' form. The 'nicked' form is the characteristic form taken by irradiated chromatin. The 'nicked' form is classically refered to as the unwound state of form or decondensed form (Cook & Brazell 1975 (36)).

As the loops are at the nuclear periphery and interact strongly with the nuclear matrix then radioresponses of the loops are further compounded by nuclear matrix responses to the ionised particle (OH radical). Hence strand break lesions are one type of radiation-induced damage, another type of DNA damage is DNA-DNA, and, DNA-protein cross-links (Oleinick & Chiu 1994 (37)).

Ahnström & Erixxon (1981) developed a method for exploiting the unwinding property of DNA under weak alkaline (+ low salt) conditions and unwinding initiation at radiation-induced single strand breaks, to measure strand breakage (38). Ljungman modified the Ahnström unwinding method using the effect of histone depletion at high salt (NaCl) concentrations to quantify DNA cross-links in conjunction with the formation of different chromatin substrates (in cellular, nuclear and nucleoid monolayers preparations) (39). Ljungman *et al* (1991) (40) and Nygren *et al* (1995) (41) found that a major radioprotectant was the DNA-bound protein, with a minor contribution from soluble intracellular scavengers. Nygren *et al* (1995) postulated that double-strand breaks (dsbs) were caused by multiple-hit ionisation clusters close to the DNA, and the main radioprotective mechanisms was the physical barrier proffered by the large DNA-bound protein aggregate plus minimal intra-protein water for generation of hydroxyl radicals. This finding was consistent with the hypothesis for dsb generation postulated by Goodhead (1994) (42).

A number of algebriac expressions have been derived from Ahnström & Erixxon (1981) and Ljungman (1991) studies which aids the interpretation of superhelical DNA response to ionising radiation. In this study only the Ljungman (1991) strand breakage expression was used:

$$Fss = dpm\ ssDNA / (dpm\ ssDNA + dpm\ dsDNA) \quad (1)$$

Where Fss is fraction of single stranded DNA. To determine the pattern of change in DNA damage at various NaCl concentrations for each cell line the relative slope was determined:

$$\text{Relative slope} = Fss\ (test) / maximal\ Fss \quad (2)$$

For comparative analysis the ratio of the relative DNA sensitivity of *xrs*-5 to CHO KI was determined using the following expression:

$$\text{Ratio of relative DNA sensitivity} = rel.slope\ (xrs\text{-}5) / rel.slope\ (CHO\ KI) \quad (3)$$

If there is no difference between *xrs*-5 and CHO KI then the ratio of the relative DNA sensitivity would be equal to 1.0 and a plot of the ratio of relative DNA sensitivities would give a curve of the form $y = mx^2$.

These expressions are used in this study to investigate (a)the nature of DNA binding protein interactions with the superhelical loops and thus determine if there is a difference in the binding between CHO KI and *xrs*-5, and (b) whether or not any difference can be attributed to chromatin structure, and thus could account in part for the mutant's radiosensitivity.

(iv) MICRONUCLEUS ASSAY

This section describes the cytokinesis block micronucleus assay developed by Fenech and Morley (1985) (43). Under a light microscope the micronucleus could be observed as small (2μm in diameter) membrane bound nuclear material arrayed at the nuclear periphery.

Micronuclei are formed from acentric chromosome fragments or whole chromosomes that have not been incorporated in the main nuclei at cell division. Enumeration of micronuclei in mitogen-stimulated lymphocytes provides a simpler and statistically more precise method than karyotypic analysis for quantitation of chromosome damage. This was a more precise method because it was easier to score whole micronuclei than to count silver halide grains in an autoradiogram and presumably one micronucleus was formed per lesion per dose of mitogen added. By necessity the cell has to undergo one mitotic division in order for a micronucleus to be expressed. The number of micronuclei scored in a given number of lymphocytes depends upon:

(a) the proportion of cells that have responded to the mitogen;
(b) the proportion of stimulated cells that have divided, and;
(c) the fate of micronuclei in cells which have divided more than once.

These three factors can vary between individual and within individual patients thus conventional micronucleus assays are imprecise. As a result the cells which have undergone one division, and the micronuclei within them, could not be differentiated from the total population of cells (lymphocytes). To overcome these limitations, Fenech & Morley (1985) developed two methods to identify cells which have undergone the first mitosis: autoradiographic and cytokinesis block.

The autoradiographic method was flawed as the radiolabel alone generated micronuclei. In the cytokinesis block (Cyt-B) method only Chinese Hamster Ovary cells blocked with a certain concentration cytochalasin B (3.0 μg/ml) produced micronuclei. These were easy to identify owing to their binucleate appearance, and a large number of binucleates could be produced optimally when cells are treated with 3.0 μg/ml cytochalasin B after 44h culturing and scored after 72h for micronclei. Unlike the autoradiographic method cytochalasin B did not produce micronuclei, and, the method was simple to perform and reliable. The authors found that there was a linear relationship between irradiation dose and number of micronuclei. Normal lymphocytes in the presence of Cytochalasin B have been shown to produce polyploid metaphase chromosomes and no chromosomal aberrations, but neoplastic cells have shown to have more chromosomal abnormalities such as persistent nuclear division and chromosomal pulverisation. A few micronuclei have been observed in mononuclear interphase cells, suggesting that the drug was biased towards certain cell populations which tended to form micronuclei easily, but they found no evidence for this suggestion instead they accounted for this latter observation as due to either some cells dividing pre-blockage or cells escaping blockage.

This assay was used in this study to establish the radiosensitivity of the Chinese hamster cell lines, specifically to assay damage in terms of numbers of micronuclei formed, and to ensure that the *xrs* had not spontaneously reverted to the radioresistant wild type CHO KI form. The mutant cell lines (*xrs*) would be expected to express more micronuclei linearly with dose of ionising radiation (IR) (γ-^{137}Cs) than the parental cells. The cytokinesis block micronucleus assay; degree of sensitivity, ease of use, reproducibility, and applicability to cancer risk assessment, has been reviewed by Tucker and Preston (1996). They had found that the technique was reasonably easy to apply but caution is required in data interpretation as there are many mechanism of micronuclei formation depending upon the clastogenic agent and as a further caveat symmetrical chromosome alterations e.g. reciprocal translocations can not be detected by this method (44).

(v) CHROMATIN CONFORMATIONAL PROTEINS

This section is concerned with the structural proteins which function to package the chromatin into higher order structures such as the 30 nm fibre and the supercoiled DNA loops, and, which anchor, these loops to the nuclear matrix. The format for this section is to describe the two major protein groups involved and to discuss their possible rôle in the phenomena of radiosensitivity as mediators of the conversion of DNA double-strand breaks into chromatid and chromosome aberrations.

Conformational proteins in chromatin can be grouped into two types according to amino acid sequence and charge (45):

(A) Histones.

(B) Non-Histonal Proteins (NHP).

(A) *Histones*

There are five classes of histones in eukaryotic cells: H1, H2A, H2B, H3 and H4. The structure of these histones vary from a random coil form to a globular structure. Their sequences are asymmetric with basic and/or acidic variable terminal regions, and apolar and constant central domains. These constant domains range from highly conserved in H3 and H4 to less conserved in H1. Histones H3 & H4 cross-link to form a tetramer, and H2A and H2B to form a dimer.The tetrameric histones cross-link with the dimeric histones to form the core **'wedge'** particle and histone H1 binds forming a **'winged helix'** domain to stabilise the nucleosome. The post-translational chemical modifications in these histones serve to **silence** gene activity (acetylation) or to activate regulatory genes (phosphorylation). Major interactions between histones and DNA occur through the binding of the positively charged side chains and the negatively charged phosphate groups in the duplex minor groove. The histone residues (glutamate or aspartate) may be loci for the binding of the highly acidic residues of the non-histonal chromosomal proteins (NHP) (45). The aromatic rings, tyrosine and phenylalanine have the capacity to interact with the DNA bases or to intercalate between adjacent bases (46).

Stabilisation of the histones with respect to the DNA requires some degree of chemical modification. These modifications can take the form of methylation, acetylation, phosphorylation and ubiquitination. (46,47).

Histone phosphorylation is a major reversible modification which converts seryl- and threononyl- residues from neutral to negatively charged residues. Histone H1 is the most extensively phosphorylated of the five histones, and three forms of phosphorylation have been classified:

(1) cAMPlysation of seryl 37 affecting adjacent regions only;

(2) *in vitro* phosphorylation of seryl 105 by histone kinase2;

(3) global phosphorylation of H1 seryl and threononyl residues through the cell cycle, and growth associated phosphorylation.

The reduction in the net positive charge are thought to modulate the conformational transitions required for DNA processing and chromosome condensation. All these histones can be visualised as bands on an acid:urea:Triton PAGE gel (48).

(B) *Non-histonal proteins*

Non-histonal Proteins (NHP) have been called **acidic** proteins to distinguish them from the **basic** histones. The NHP include enzymes required for DNA replication, and histone modification e.g. histone kinases and **'housekeeping'** enzymes. Other NHP include the 'scaffold' proteins e.g. lamins A, B, and C and DNA topoisomerase II, that determine the shape and organisation of the metaphase/interphase chromosome. Another group of NHP are the high electrophoretic mobility group proteins (HMG) (49). Structural intergrity and intranucleosome metabolic activity is maintained by the NHP molecules. The former function is represented by the presence of scaffold proteins, HMG proteins and DNA topoisomerases (I and II), and the latter activity is represented by the **'housekeeping' enzymes**. The HMG proteins in particular HMG14 and 17 have a high affinity for nucleosomal DNA and may influence chromatin folding and thereby indirectly increase access of regulatory proteins to RNA polymerase. HMG14 and 17 may act as unwinding enzymes opening up the duplex to RNA polymerase activity. HMG1 and 2 may be structural mediators in nucleosome assembly by local destabilisation in competition with histones H2A/H2B (45,49). These proteins may substitute for linker histones, and have also been implicated in the mediation of transcription and/or components of nucleoprotein structures. The asymmetric distribution of basic and acidic groups prevalent in the histonal proteins is a prominent feature of HMG proteins, which implicates a close interaction between these proteins and thus emphasises their mutual rôle in DNA loop assembly and interaction with the nuclear matrix.

A fourth NHP is Ubiquitin which has been shown to be associated with the histones, especially histone H2 in the form of protein A24; and it is speculated that ubiquitin is associated with active chromatin, and A24 with 'silenced' chromatin. Ubiquitin is a globular protein with a high number of apolar residues, is universally distributed in cells, stable, and its sequence is highly conserved.

A fifth NHP is chromatin assembly factor I (CAFI) is required for nucleotide excision repair in Xenopus egg extracts after UV-irradiation (50). hCAFI may be acting during or immediately after repair to efficiently restore the nucleosomes which may free the repair mechanism from the reassembled chromatin fibre: hCAF1 may interact with the histones by recognition of nascent histone H4, possibly by transient modifications of the histones; and, by interacting with the replication machinery.(50).

A sixth NHP that is intimately involved in cell cycle checkpoints is the mitosis promoting complex (MPF) of cyclin B and $p34^{CDC2}$. Low-dose irradiation is known to induce G_2 arrest by dephosphorylation of the tyrosyl 15 residue of the catalytic subunit, $p34^{CDC2}$. Barth *et al* (1996) showed that γ-irradiation at 1 Gy interrupted the initiation of the autocatalytic loop between MPF and the phosphatase cdc25-C in HeLa cells, leading to G2 arrest (51).

It has been postulated by Oleinick and Chiu (1994) and Mullenders *et al* (1987) that the close apposition between the conformational proteins and the nucleosomal DNA suggests the sites of irradiation damage and repair mechanisms must be in part within the loop system or close to the matrins/lamins. Therefore the repair components must be close to the lesions and have a sequence or shape similarity to the damaged components to bypass the 'sentry proteins' (52) to affect repair. Such repair components could be the linker histones mediated by HMG 1 or HMG1 and 2 alone (53,54).

(vi) EXPERIMENTAL OBJECTIVES.

The remit for this project under the CEC Nuclear Fission Safety Programme (Chromatin Structure, Repair and Aberrations) was to study (a) the rôle of nuclear matrix DNA binding proteins and (b) the histone H1 family of proteins, and their phosphorylation, in the conversion of radiation mediated DNA damage to chromosomal aberrations. The remit entailed utilisation of (i) cell culture techniques, (ii) DNA damage assessment by the Ljungman modification (39) of the Ahnström & Erixxon (38) alkaline unwinding method, and, (iii) protein separation and analysis by one dimensional PAGE, Western blotting and Acid-Urea PAGE for histone isolation.

Specifically the experimental aim of the project was to (1) examine and compare the radiosensitivity of the wild type CHO KI cells and the mutant *xrs*-5 by DNA unwinding and micronucleus assay. (2) To correlate the radiosusceptibility of one member of the *xrs* family, *xrs*-6 to differences in the chromatin structure by the isolation of proteins and compare these proteins to those proteins from the wild type parent. This cell line has a defect in DSB repair specifically attributable to the absence of Ku80.

Chapter 2:
Materials and Methods

Radiobiology protocols

(1) *Alkaline unwinding assay For single strand and double-strand breaks*:

Initial experiments were conducted based on the technique of Ljungman (39). A generalised protocol was subsequently developed, as described below. Details of specific buffers, concentrations and ionic strengths (pH) are given in the Abbreviations and Buffer Components section.

Cells were grown routinely in 75 ml tissue culture flasks (NUNC) for 17-24h, at 37°C, in a 5% CO_2/humidified incubator, to a density of 20-30 x 10^6 cells per flask in the presence of 0.1 μCi/ml of tritiated Thymidine (Amersham). The cells were harvested by treatment with 3 ml TE in PBS. Monolayers were prepared by seeding 7-8 x 10^4 cells into sterile 24-well microtitre plates (Corning, New York) or as a cell suspension washed twice with 0.15M sodium chloride solution and γ-irradiated (10-30 Gy), then treated as described as below in the alkaline lysis paragraph.

The cell monolayers were cultured for 17-24h after which the spent medium was aspirated. Duplicate wells were treated with 1 ml Ljungman lysis solution (See Abbreviations and Buffer Components section for definition) for 10 mins, aspirated and briefly treated with 0.5 ml 0.15M sodium chloride as an equilibration solution. After this treatment plates were exposed to different doses (Gy) of γ-irradiation. To provide a measure of background damage, unirradiated control wells were processed concurrently, and the background values of Fss obtained were subtracted from those obtained for the irradiated wells, to yield the effect for irradiation over constitutive levels of damage.

The equilibration solution was aspirated to waste, and all wells were treated with 0.3 ml alkaline unwinding solution (See Abbreviations and Buffer Components section for definition) for 40 mins in the dark at 4°C. Samples were neutralised with 1 ml 0.02M Sörensen's salt (See Abbreviations and Buffer Components section for details), sonicated (MSE sonicator setting 10, 10s) and the DNA solubilised with 0.15 ml SDS (See Abbreviations and Buffer Components section for concentration) and stored frozen at -20°C till analysed by Hydroxyapatite (HA) chromatography as described below.

(2) *HA Chromatographic analysis of single-stranded and double-stranded fragments:*

The sample DNA was equilibrated to 21°C and loaded onto 0.15g HA columns, which were pre-wetted with 2.5 ml 0.0125M sodium phosphate buffer (SPB) pH 6.8 and pre-warmed at 60 °C. The bound DNA was washed once with 2.5 ml 0.0125M SPB to elute the SDS and unbound tritiated Thymidine. The single-stranded fraction was eluted from the columns with two washes of 2.5 ml 0.125M

SPB, and the eluate collected in scintillation vials containing 0.5 ml 5M hydrochloric acid to neutralise the phosphate ions. The ds fraction was eluted from the columns with two washes of 2.5 ml 0.25M SPB, and collected in scintillation vials plus 0.5 ml hydrochloric acid. A 6 ml aliquot of InstaGel plus (Hewlett-Packard LKB) scintillant was added to each sample, which was vortexed to mix, and the resultant colloidal suspension counted for tritiated thymidine disintegrations per minute (dpm) in a scintillation counter (Pharmacia-LKB, Sweden). The data was manually analysed and then transferred to CricketGraph III for plotting and presentation.

(3) *Salt concentration and irradiation dose for cell monolayers*

Wt CHO KI cells were grown and harvested as above. The cells were resuspended in 10 ml fresh medium and the cell density adjusted to 7 x 10^4cells per well and seeded into 24-well microtitre plates (Corning, New York) and cultured for 17-24h. The medium was aspirated to waste and the attached cells washed with 1.5 ml HBBS, aspirated to waste and treated with 1 ml Ljungman lysis solution (See Abbreviations and Buffer Components section for definition) with either 1 or 2M sodium chloride 20 minutes at 4 °C. The lysis solution was aspirated to waste and the cells washed twice with 1 ml 0.15M sodium chloride, and after the last wash the cells were exposed to 0, 0.25, 0.5 or 1 Gy. The monolayers were subjected to DNA alkaline unwinding assay as described above in section (1) and (2)

(4) *The micronucleus assay to confirm the radiosensitivity of xrs-5 cells.*

Cells were grown as described above in the alkaline unwinding protocol, and after 24h the cells were harvested with 3 ml TE, the density was adjusted to 2 x 10^5 cells per ml of medium and cells were seeded into 25 ml tissue culture flasks. The cells, in the presence of supernatant, were exposed to γ-irradiation at 1 or 2 Gy, and the medium aspirated to waste and replaced with fresh medium containing 3 μg/ml cytochalasin B. The cells were harvested using 2 washes of 1 ml TE, resuspended in 3 ml fresh medium at an adjusted density of 2 x 10^4 cells per ml of medium. The suspension was applied to the funnel of a Cytospin sample application cup (Cytospin, Shandon), and the cells were cytospun onto frosted-glass grease-free microscope slides at 800 rpm for 10 mins. The slides were allowed to air dry for 24h and fixed in methanol (99%) for 10 -30 mins, dried completely in a flow hood (~ 20-30 mins) and stained with 6% Giemsa in Sörensen's buffer II pH 6.8. The slides were blotted dry on 'Post-Up' filter paper and the micronuclei scored under oil immersion using X100 magnification and Köhler illumination. The frequency of micronuclei per 100 cells was plotted against dose in Grays.

Protein Chemistry protocols

(A) *Isolation of mitotic cells.*

Cells were seeded into 75 ml tissue culture flasks (NUNC) at a concentration between 0.7- 2 x 10^5 in 10 ml medium and cultured for 48-72h, at 37°C, in a 5% CO_2/humidified incubator, to reach a total number of 20-30 x 10^7 cells per flask. Cells at a density of 2 x 10^7 were seeded into 500 ml roller bottles (NUNC), fresh medium (containing 2mM HEPES) was added to a final volume of 110 ml, and, cells were cultured overnight on a 37°C roller set at 2.5 rpm. The spent medium was replaced with fresh pre-warmed medium and returned to the roller machine for a further 24h. After 24h the spent medium was replaced with 50 ml fresh pre-warmed medium with 2mM HEPES and 0.1 μg/ml Nocodazole (400 μg/ml stock) and cells were roll-incubated at 37°C for 1h. The discarded medium contained asynchronous or apototic cells detached from walls of the roller bottle. The roller bottle was spun for 2 minutes on a small electric motor set at 200 rpm, to release any loosely attached cells into the medium and the spent medium was discarded. Fresh 50 ml of medium was added and reincubated for 1h. After 1h the synchronised mitotic cells were harvested by spinning the bottle again for 2 mins and centrifugation of the suspension at 1200 rpm. The cell density of the harvested mitotic cells were determined using a Coulter counter (Coulter Electronics) as a 1/100 dilution with spent medium. The cell pellet was resuspended with 1.5 ml cryomedium containing MEM-CsFe or -FCS with 1 μg/ml Colcemid and 10 % DMSO and stored at -20°C. Subsequently five or six harvestings were made with 50 ml fresh media, and all collections were transferred to cryovials for storage under liquid nitrogen (storage was required as the procedure was designed for harvesting cells in bulk and 24h storage was considered ideal for both preparation and collection of mitotic cells). Each harvest producing around 3-4 x 10^6 mitotic cells sufficient for protein extraction.

Action of Nocodazole

Nocodazole (400 μg/ml stock) was used as the drug is acting on the microtubules forming the mitotic spindle, specifically preventing their degradation so that the chromatid daughters fail to separate and instead congregate at the poles or remain at the equatorial plate and consequently synchronise cells at metaphase (3).

(B) *Isolation of mitotic chromosomal proteins.*

Three vials of each cell line (CHO KI or *xrs*-6) of equal cell density, approximately 3 x 10^6/ml, in1.5ml medium, were rapidly thawed to induce cell lysis. The contents of each vial were transferred to 10 ml 'V' centrifuge tube

(Scotlab) on ice (4°C). The cells were pelleted at 1200 rpm, 0°C for 10 minutes and the medium discarded. The pellet was resuspended, washed three times in HBSS, respun and the washings discarded.

The pellet was resuspended in 1 ml cold reswelling buffer and transferred to a siliconised 7 ml Wheaton tissue grinder with piston A chilled on ice. The pellets were homogenised with 150 μl 10 % NP-40 and the disruption of cell membranes was confirmed with inverted phase contrast microscopy of 10 μl of homogenate.

The homogenate was layered onto a cold (4°C) 35% Sucrose gradient in a siliconised polypropylene 2ml vial (Promega) and centrifuged for 5 mins at 3200 rpm in a Sorvall swinging bucket GLC-2B centrifuge (MSE, Fisons). The homogenates separated into six layers of which the bottom contained the chromosomal pellet (66).

The protein concentration was determined, by the Bradford assay (BioRad, 67) using Bovine serum albumin (BSA) as the standard. An aliquot of 10 μl protein extract was dispensed into a well of a 96 well Terasaki tissue culture plate (Corning), 20 μl of Bradford reagent (BioRad) was added, mixed by aspiration and made upto 230 μl with sterile double-distilled water (Millipore). The reaction was allowed to incubate for 15-20 minutes and the protein absorbance determined on a microtitre plate reader (DynaTech) and the protein concentration estimated by extrapolation from the BSA standard curve.

(C) *Protein separation by SDS-PAGE and visualisation by Coomassie staining.*

The protein isolates were resuspended in 50-100 μl of boiling mix. The resuspended protein was boiled at 95°C for 5 minutes prior to loading onto a 12% SDS-PAGE gel. The gel was pre-run for 10 mins in a Tris- glycine electrode buffer, then loaded. The gel was resolved at 20-25 mA per gel for approximately 1.5h. Pre-stained molecular weight markers (M) were used to estimate size (kDa) and relative mobility. The gel was stained in Coomassie blue 250G for 2h, destained, and, rinsed with double distilled water. The stained gel was stored with 1-5 ml of electrode buffer prior to photography with a polaroid camera using Kodak black and white film. The photographic print was scanned with DeskScan II (Hewlett-Packard) and manipulated in the drawing package ClarisWorks 4.0 (Claris) for presentation

(D) *Western blotting procedure.*

The protein extracts were sonicated (setting 10 for 5 secs.), to disrupt the DNA-bound proteins and 5 μg/ml of sonicated protein was loaded onto another 12% SDS-PAGE gel and resolved for 1.5h.

During resolution a piece of nitrocellulose membrane (Schleicher & Schuell) (70 long x 84 mm wide) was excised with four similarly proportioned pieces of 3MM

Whatman chromatography paper (Merck) and these were immersed in Western transfer buffer for 1h. After resolution the PAGE gel was gently transferred to the transfer buffer. Western transfer was performed by the semi-dry method and the electrophoretic blotter was supplied by Hoefer Scientific Instruments (Pharmacia, Sweden). Two pieces of equilibrated 3MM paper was transferred onto the Mylar mask (anode) The equilibrated gel was placed onto the 3MM paper. The nitrocellulose membrane was laid on top of the gel. The remaining two pieces of 3MM paper was laid on top of the membrane and the semidry blotter lid (cathode) was replaced. Transfer was initiated by connecting the anode and cathode through Shandon Vokam power pack (Life Sciences) and transfer occurred at constant 25V for 2-3h from anode to cathode. Any trapped air was removed by gently applying a 12 inch polycarbonate rolling pin. Transfer efficiency was determined by the transfer of prestained markers.

(E) *Anti-Histone probing of the Western blot*

The blotted membrane was placed into blocking buffer overnight at 4°C. The blocked membrane was washed with twice with 0.1% Tween-20 in TBS (TBST) to block any non-specific binding sites on the membrane. The mouse anti-histone monoclonal antibody (Boehringer-Mannheim clone H11-4) was reconstituted with 500 μl sterile double distilled water. The antibody (at a concentration of 1μg/ml) was added to fresh 20 ml TBST, mixed by inversion and decanted onto the membrane. The membrane was incubated at 21°C for 2h with gentle agitation. Any non-specific binding to the mouse IgG1 antibody was blocked by washing twice with TBST and twice with TBS. The secondary antibody (2μg/ml) , an anti-mouse IgG1 covalent conjugated to horse radish peroxidase (Sigma Immunochemicals), was added to fresh 10 ml TBS, inverted to mix and decanted onto the membrane. The membrane was incubated at 21°C for 1h with gentle agitation. The colour development agent, DAB, was prepared. Any unbound or loosely bound antibody was removed by four washes with TBST. The developer solution was filtered with Whatman No.1 (BDH) then 100 μl of developer was diluted with 10 ml TBS and 3 μl 30% hydrogen peroxide was added to the immunoblot. The immunoblot was agitated until visible black/brown bands appeared (approximately 1-5 mins) then the immunoblot was washed with Phosphate buffered saline (PBS) (GIBCO) and rinsed with distilled water, and photographed. The photograph was scanned into ClarisWorks 4.0 and the processed image was shown in Fig.21. Figure 21 shows Western blotting analysis for histones in protein extracts, using an mouseanti-HeLa-histone antibody.

(i) *Acid digestion of nuclei to release histone proteins*.

Nuclear extracts were prepared as in section (B) The nuclei was pelleted by centrifugation at 3,000 rpm, 0°C for 10 minutes and the medium discarded. The pelleted nuclei was resuspended in 1 ml 0.22M hydrochloric acid overnight at 4°C. The suspension was centrifuged at 1200 rpm, 0°C for 5 minutes and 100 µl boiling mix (including 6M urea, and, excluding SDS and Tris-HCl) was added to the supernatant, boiled for 5 minutes, chilled on ice(4°C), and stored at -20°C.

(ii) *Acid Urea Triton X100 Gel.*

For a discontinuous 30 ml resolving gel the components were:- 7.5 ml 30% 'Easy Gel', 1.8 ml glacial acetic acid, 0.15 ml TEMED, 0.09 ml concentrated ammonium hydroxide, 14.4g urea, and, adjusted with distilled water to 27.4 ml. After the urea had dissolved in the mixture, 0.6 ml 25% Triton X 100 was added, and 0.004g riboflavin in dim light. The gel mixture was cast into 75 x 90 mm MiniProtean II (BioRad) slab gel and the bottom of the gel was sealed with 10 ml of gel mixture polymerised with 0.3 ml 10% ammonium persulphate, to prevent leakage. The cast gel was polymerised by exposure to four 60W fluorescent striplights and the polymerised gel was immersed into the electrophoretric tank containing acid electrode buffer. The samples were loaded, and, the gel was resolved at a constant current (10mA) for 1.5h. The gel was stained in 0.1% Coomassie blue R in 5% acetic acid/40% ethanol and destained in 5% acetic acid/20% ethanol.

Chapter 3:
Radiobiology

This chapter describes experiments to examine DNA damage in wild type (CHO KI) and mutant (*xrs*) cell lines, induced by IR utilising the Ljungman (1991) modification of the Ahnström & Erixxon (1981) alkaline unwinding method and the Fenech & Morley (1985) cytokinesis-block micronucleus assay. This chapter is divided into two sections: Experiments involving (A) alkaline unwinding assay, and (B) micronucleus assay.

(A) DNA Damage Measurement By the Alkaline Unwinding Technique, in Nucleoid and Nuclear Monolayers.

The experiments were designed to address the condensation differences and change in susceptibility to IR-induced damage in the *xrs* family of mutants from the wild type CHO KI as a response of chromatin to different monovalent ion concentrations (NaCl) and weak alkali, and to elucidate reasons for these differences. CHO KI and *xrs*-5 has been shown to have the same susceptibility to IR-induced damage (Jeggo 1990, MacLeod & Bryant 1990) and only partial histone denudation of the chromatin by the simultaneous action of monovalent and divalent ions that any higher order chromatin structural differences be observed (Johnson & Bryant 1994).

Nucleoids and Nuclear Monolayers

When cells are grown to confluence on a plastic dish to form a one cell thick layer this is termed a cellular monolayer if the monolayer is treated with hypotonic buffer containing (0.15-0.75M) monovalent ions (Na^+Cl^-) some DNA bound proteins are released and this chromatin structure is termed the nuclear monolayer and if the monolayer is treated with hypertonic buffers containing 1-2M salt (NaCl) then the chromatin structure is denuded of protein, except for the nuclear matrins and MAR proteins, the residual monolayer is termed a nucleoid. Figure 3 shows a diagram of the three types of monolayer, and, the conditions for formation of nuclear and nucleoid monolayers. These nuclear and nucleoid monolayers were made by treating cell monolayers to hypertonic buffers (2M NaCl) and detergent (0.5% Triton X 100) (nucleoid), and/or, hypotonic buffers (0.15M NaCl) plus detergent (Nuclear monolayer). The cells are permeabilised by the simultaneous action of sodium chloride and Triton X100. Nygren (1995) proposed that the permeabilisation also removed the soluble sulphydryl scavenger proteins responsible for the oxygen effect (41).

These monolayers are valuable tools to examine chromatin as:
(i) DNA-bound proteins could be removed stepwise by increasing the concentrations of salt which dramatically increased the susceptibility of DNA to γ-irradiation-induced strand breaks;

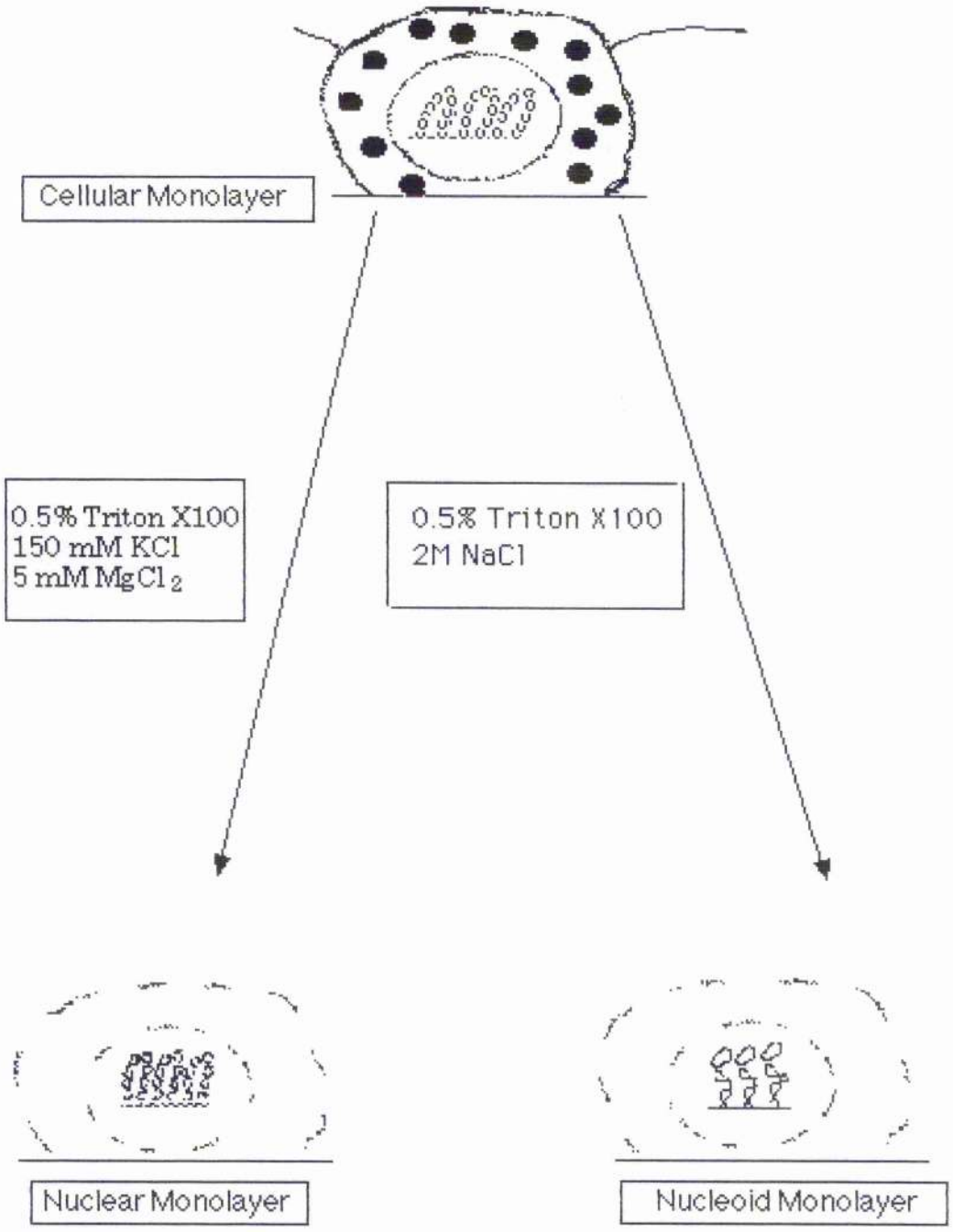

Figure 3:
Diagram to show the formation of cellular, nuclear and nucleoid monolayers by the manipulation of non-ionic detergent and salt (Ljungman 1991 (39)).

(ii) Chromatin compaction in nuclear monloayers could be modified by the addition or removal of cations;
(iii) All samples have the same concentration and spatial distribution of DNA;
(iv) Monolayers have very low constitutive levels of DNA strand breaks.

These monolayers were used in this study as: (a) logistically comparable for high throughput assay, and (b) data obtained from treatment of these monolayers,salt and IR, would have a high degree of sensitivity with a low background of constitutive damage.

The alkaline unwinding assay has proven useful for examining DNA damage in lysed cells (38), nuclear monolayers and nucleoids (39). Thus it was decided to apply this assay to examine the susceptibility of mutant hamster cell lines, specifically the line *xrs*-5 to IR-induced DNA damage after treatment with increasing salt concentrations and to correlate the data with chromatin conformation.

Theory of alkaline unwinding assay

The technique relies upon the action of mild alkali (0.03M NaOH) on "de-proteinised" DNA, involving electrophilic attack upon the phosphate backbone of the DNA duplex and, consequently, inducing partial unwinding of the two DNA strands (denaturation). Where DNA breaks (single and double) have been induced by IR, unwinding will be initiated at these points. The principle of the assay is shown in (Fig.4). Figure 4 in which the DNA duplex nicked by the action of ionising particles or OH-radicals (55) producing single-stranded DNA sites for alkaline unwinding. Neutralisation and sonication of the DNA lead to double-stranded (ds) and single-stranded (ss) fragments for HA chromatographic separation. After neutralisation with sodium phosphate buffer (0.02M) to arrest unwinding, sonication is used to give single-stranded (damaged) plus double-stranded (undamaged) fragments which are separable by hydroxyapatite (HA) chromatography, by exploiting their different elution properties in the presence of low concentrations of sodium phosphate buffer (Fig.5). Figure 5 shows two diagrams of components of the calcium hydroxyapatite chromatographic method. Fig.5(A) shows the column which was packed with two different (mixed) grades of HA and the DNA percolates through the column to bind to the HA, and, elution rate is controlled by the 100 μm filter and the different grades of HA. Fig.5(B) depicts the constant (60°C) heating block with holes cut and routered for the 2ml polypropylene syringe barrels, and, the collection tray beneath.

Ss and ds fragments are eluted at 0.125M and at 0.25M phosphate buffer, respectively (56). The strand breakage can be expressed in the form of the fraction of single strands (Fss), using equation (1) from the Introduction chapter section (iii):

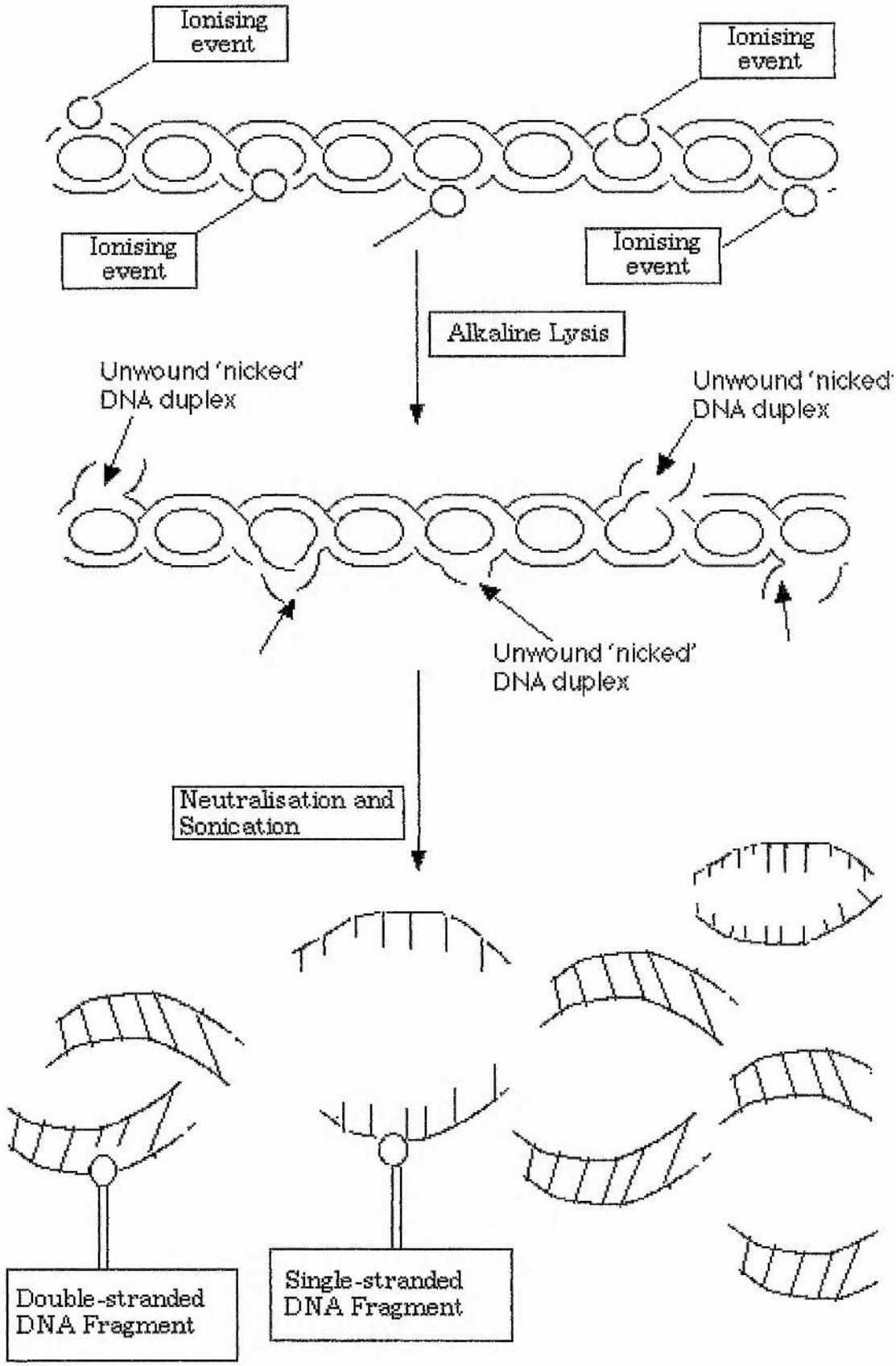

Figure 4:
Diagrammatic representation of the alkaline unwinding assay of Ahnström & Erixxon (1981).

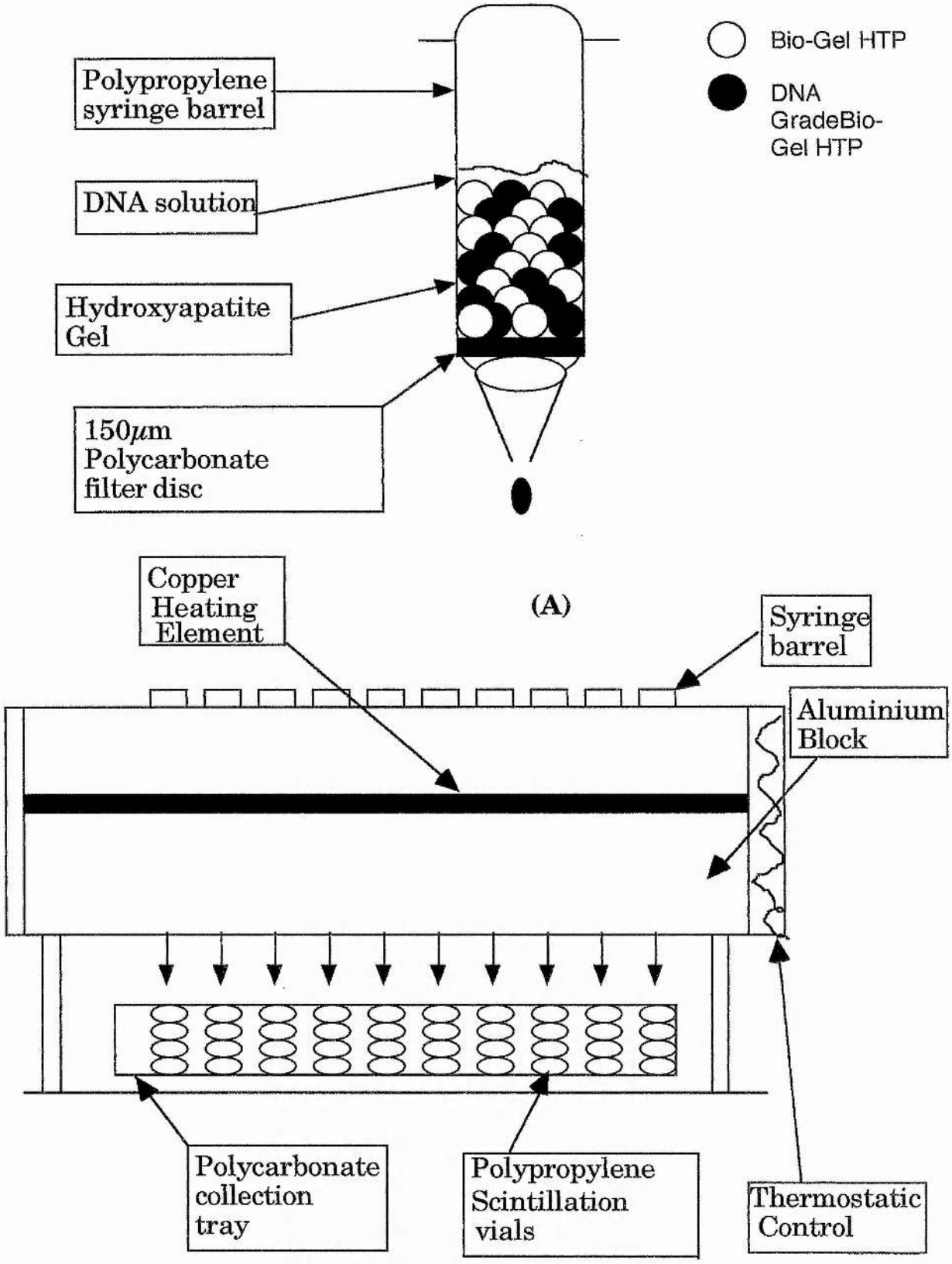

Figure 5:
Apparatus for the alkaline unwinding assay and HA Chromatography.

Fss = dpm single stranded(s) / (sum of dpm (s) + double dpm (d))

In 'nicked' DNA, as produced by IR or restriction enzyme (RE) digestion, the rate of unwinding would be faster proportionally at the lesion than at the tightly-coiled ds region, due to the induction of ssb (57).

(1) **Preliminary experiments to establish the sensitivity of wt and mutant DNA to IR under various conditions**

Preliminary experiments were performed to assess the viability of the alkaline unwinding assay, with respect to dose of irradiation and alkaline lysis conditions for wt cells in suspension, and in monolayers. Unwinding conditions in suspension were then used to assess baseline IR sensitivity in both cellular monolayers (CHO KI and *xrs*-5).

IR-induced damage in wt cells.

Wt CHO KI cells were cultured and harvested as described in section (1) of chapter 2. The cell pellet was resuspended in 10 ml fresh medium, transferred to a centrifuge tube and centrifuged at 1200 rpm (Heraeus Instruments) 10 mins , 0-2°C. The medium was aspirated and the cell pellet resuspended in 0.15M sodium chloride. Suspensions were exposed to 0, 10, 20, or 30 Gy on ice to prevent repair, and the cells collected by recentrifugation. The supernatant was aspirated, the cells were treated subjected to DNA alkaline unwinding assay with 1 ml alkaline unwinding solution as described above in sections (1) and (2) of chapter 2.

Figure 6 shows that for the alkaline lysed cells, CHO KI, Fss curve was approximately linear with irradiation dose. The curve did not start at zero, as the background was Fss=0.08, and this was within the accepted limits of the assay as applied to cell suspensions and reflects the condition of the cells in culture (58). This constitutive level of damage may have been due either to presence of replication fork DNA or to apototic/necrotic cells which would contain damaged DNA or another potentially significant source of background IR-induced DNA damage may be low level microbial nuclease activity. For the alkaline unwinding experiments, the constitutive Fss value were subtracted, for comparison of the two cell lines. In conclusion unwinding was optimal at 0-10 and 25-40 Gy and, after treatment with 1ml of 0.03M sodium hydroxide for 40 minutes . The reduction in size from tube assay to microtitre plate allowed for a reduction in liquid volume,

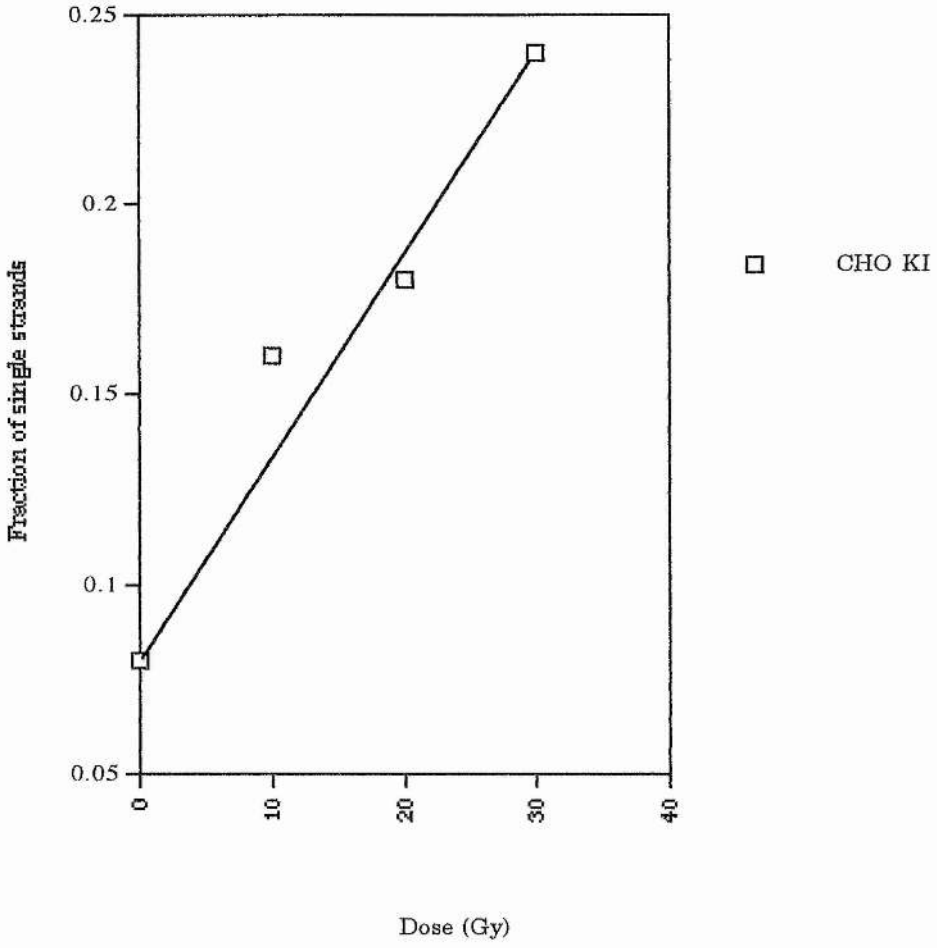

FIGURE 6:
Graph showing Fss against dose of γ-irradiation, for wt CHO (KI) cells in suspension. (n=1).

reduced surface area for irradiation, and a reduction in dosage therefore it was decided to irradiate from 0-1 Gy. To detect any low level microbially induced DNA damage 1ml of supernatant medium could be centrifuged at 1200 rpm and the cell pellet examined for microbial contaminants under phase Contrast and/or bacterial vital stainning.

Response of cellular, nuclear and nucleoid monolayers to low-dose IR

In these preliminary experiments the response of wt CHO KI monolayers to IR was assessed. Cell cultivation and harvesting were performed as described in chapter 2 sections (1) and (2), seeding of microtitre plates and treatment with Ljungman lysis solution is described in chapter 2 section (3).

Figure 7 depicts the graphs of cellular, nuclear and nucleoid monolayer responses to low doses of γ-irradiation. The response of nucleoids to low dose irradiation is approximately linear (r =0.96). The tangential curve at 1M NaCl in the extraction buffer (r =0.994) clearly shows that as the proteins are increasingly denuded from the chromatin with salt treatment, more damage is incurred. Although the cellular monolayer response was biphasic (i.e. tangential) the low damage observed in the cellular monolayers (r^2=0.938) was due to the absence of salt-induced removal of chromatin proteins, and thus greater protection of DNA from damage. In conclusion the chromatin structure became more susceptible to IR-induced damagedas proteins are removed by increased salt treatment.The value 'n' refers to the number of experiments performed

Response of CHO KI and xrs-5 cellular monolayers to high dose irradiation

A baseline response needed to be established for the two cell lines and as such the conditions for lysed cells (Fig.6) was used as a model for assessing baseline unwinding for cell suspensions. This was to ensure that lysis conditions were comparable for both cell lines. CHO KI and *xrs*-5 cells were cultured and seeded as described in chapter 2 sections (1). The cell suspensions were treated as described in chapter 2 sections (1) and (2).

Figure 8 showed that the Fss profile for wt and mutant was not different for the same range of IR (10-40 Gy) from each other or from Fig.6 as both gave approximately linear lines when standard deviation bars are taken into account. Although the mutant Fss profile seemed relatively lower at each point than the wt CHO KI suggesting that *xrs*-5 cell suspensions might be less damaged by IR than wt or the damage process in the mutant was expressed differently (59). However the Fss difference between mutant and wt may not be statistically significant when the standard deviation from the mean for both cell lines is taken into account as the errors overlap. As the sample size is small (n=3), a true estimate of the error remains indeterminate and thus any difference between the response of mutant to

IR as compared to the wt is speculative and would require further experimentation especially at the higher IR doses. The value 'n' refering to the number of experiments performed.

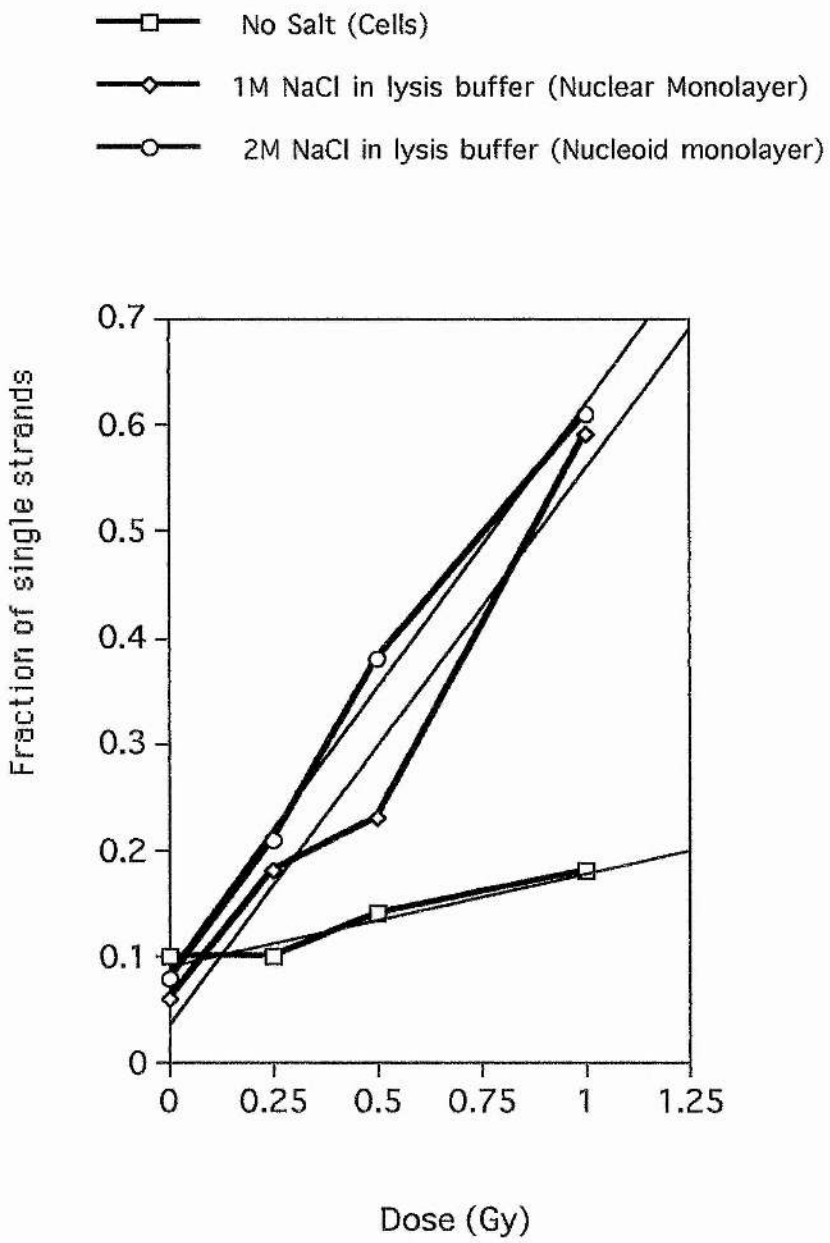

Figure 7:
Graph of Fss against dose of irradiation, in wt CHO KI monolayers (n=1). The variable 'n' refers to the number of experiments.

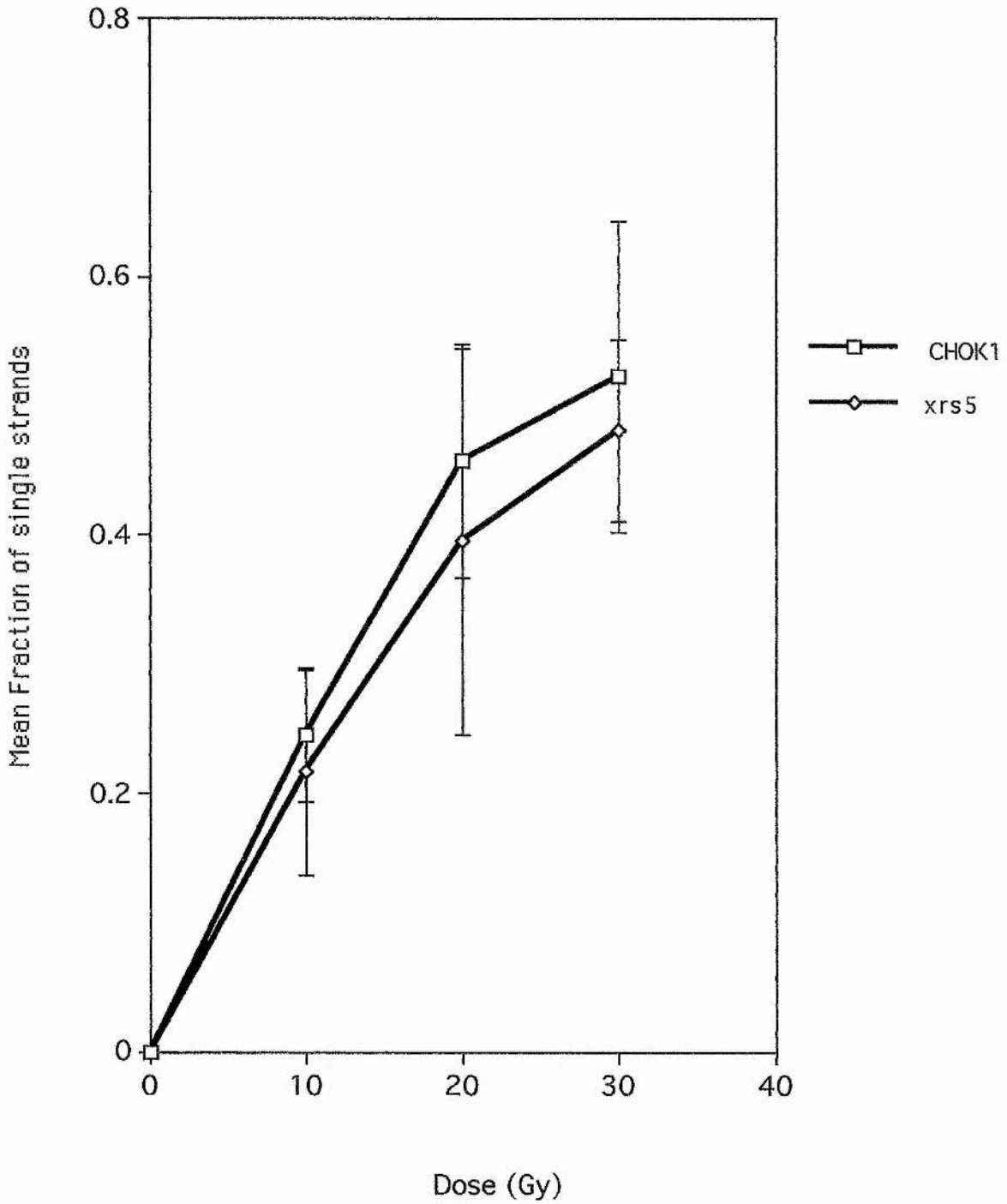

Figure 8:
Graph of Fss against dose of IR, in wt CHO KI and *xrs*-5 cell monolayers (n=3). The variable 'n' refers to the number of experiments. The error bars represent ± sd.

In conclusion the preliminary experiments were performed in order to ascertain Fss for wt and mutant cells under various conditions of salt (1 and 2M NaCl in the extraction buffer) and irradiation dose (0-40 Gy) to establish the sensitivity of DNA in wt and mutant. From these preliminary experiments it is deduced that in both cell lines, for IR doses between 10 and 40 Gy,there was a linear response for cell suspensions (Figure 6 & 8) and the difference between Fig.6 & 8 to Fig.7 was due to the use of nucleoids (Fig.7).

The replication fork DNA would affect unwinding rates which would be observed as an increase in the background unwinding profile. Cells undergoing DNA replication would actively uptake nucleotide substrates more than quiescent (G_0) cells thus the tritiated thymidine would be selectively incorporated into replication forks leading to unequal labelling of cells and could under-represent the unwinding profile of nucleoid monolayers. Replication fork DNA would be considered more radiosensitive as the supercoiling around replication sites would be low as the chromosome region would decondensed hence there would be deproteinated DNA readily accessible for ionised particles to assault consequently replication fork DNA duplexs would be primary sites for strand breakage and provides the bulk of the tritium-labelled DNA detected by the unwinding assay.

It should be emphasised that although the error bars (± s.d.) were large, the pattern of the error curves, both maximal (+) and minimal (-) error, showed the same trigonometric distribution (biphasic) as the signal curve (Fig.6). Also, if the data were generated by noise alone then the scatter of datum points would be random, rather than follow an approximately linear form. Thus it is deduced that the data represents a real response of wt CHO KI and *xrs*-5 to IR-induced damage.

(2) Effects of varying salt (NaCl) concentration in the lysis buffer and low dose γ-irradiation on wt CHO KI and *xrs*-5 Fss values.

Lower doses were chosen despite the concurrent increase in errors as the initial experiment (Fig.7) had shown a linear relationship between protein denudation from the chromatin and increased radiosensitivity and it was assumed that the radiosensitivity mutant would show a steeper rise in strand breakage in the presence of monovalent cations at lower irradiation doses than the wt. The presence of any soluble scavengers was assumed to be removed by the presence of the potassium salt (K^+Cl^-) and the nonionic detergent (Triton X 100).

Wild type and mutant cells were cultured and harvested as above. The medium was aspirated to waste and cells treated with 1 ml Ljungman lysis solution with 0.25, 0.5, 0.75, 1 or 2M sodium chloride for 10 minutes at 4 °C. The lysis solution was aspirated to waste, and the monolayers washed twice with 1 ml 0.15M sodium chloride. After the last wash the samples were exposed to 0, 0.25, 0.5 or 0.75 Gy. The DNA in the monolayers were subjected to alkaline unwinding assay, as described in the Materials and Methods chapter. These experiments were

repeated two or three times, and Fss plotted against dose (CHO KI n=3; *xrs*-5 n=2). (Fig.9 & 10).

The object of this experiment was to compare the Fss for wt and mutant cell, nuclear, and nucleoid monolayers by varying the concentration of NaCl in the Ljungman lysis buffer: cellular monolayers would be produced in the absence of lysis buffer, nuclear monolayers using 0.25-0.75M NaCl in the extraction buffer, and nucleoid monolayers using 1 and 2M NaCl in the extraction buffer. These NaCl concentrations correspond with the elutriation of histone H1 at 0.5M NaCl in the extraction buffer, histones H2A and H2B at 0.95M NaCl in the extraction buffer, and histones H3 and H4 at 2M NaCl in the extraction buffer. As the NaCl concentration increased there would be a corresponding increase in IR-induced strand breakage (Fss). There was an increase in Fss for both CHO KI and *xrs*-5 from 0.25-0.75M NaCl in the extraction buffer for the dose ranges 0.5-0.75 Gy whilst 1 and 2M NaCl in the extraction buffer produced a lower Fss profile over the dose range 0.25-0.75 Gy (Figures 9 & 10). Both cell lines showed a biphasic response and maximal unwinding at 0.75M sodium chloride. In the mutant there was an initial Fss decrease for 0.5M NaCl in the extraction buffer at the dose 0.25 Gy which could correspond to low level single strand breakage repair. One possible explanation for the plateau or 'shoulder' initiated at 0.25 Gy in *xrs*-5 and 0.5Gy in CHO KI could be ongoing repair which could occur according to the explanation given in the above section i.e.temperature fluctuations during irradiation step. Unwinding might be inhibited at higher salt concentrations in the extraction buffer due to structural changes in the chromatin such as relaxation of torsional tension that allows the DNA to be wound tighter (39,40) or accumulated ongoing 'slow' repair leading to an overall reduction of residual damage in hypertonic solutions i.e. repair may have initiated at 0.25Gy and repair might have been halted with the deproteinisation of the chromatin with increased NaCl concentration but there was sufficient repaired DNA to produce a signal though not enough repair enzymes were present (replicases) to reproduce the intact chromatin structure. Additionally the nuclear matrix proteins (matrins) are relatively salt resistant, and so would suppress the effect of salt on denuding protein from the remaining higher order chromatin structure (34). However the preliminary experiments (Fig.7) showed approximate linearity of Fss against dose at the higher NaCl concentrations, whilst Figures 9 and 10 showed biphasic kinetics, reflecting the change from nucleoids (Fig.7) to nuclear monolayers (Fig.9 & 10). Additionally the change of reaction vessel from centrifuge tube (Figs.7 & 8) to microtitre plate (Figs.9 & 10) meant that there was a concurrent change of shape from spheroid to fibroblast and thus different shapes would have different sensitivities to IR (55). The difference between the Figures 7 and 9 & 10 might be attributed to efficacy in the inhibition of repair i.e. conditions for studying unwinding in CHO KI and *xrs*-5 without repair were optimal in Fig.7. It is notable that the last points in figures 9 and 10 are in

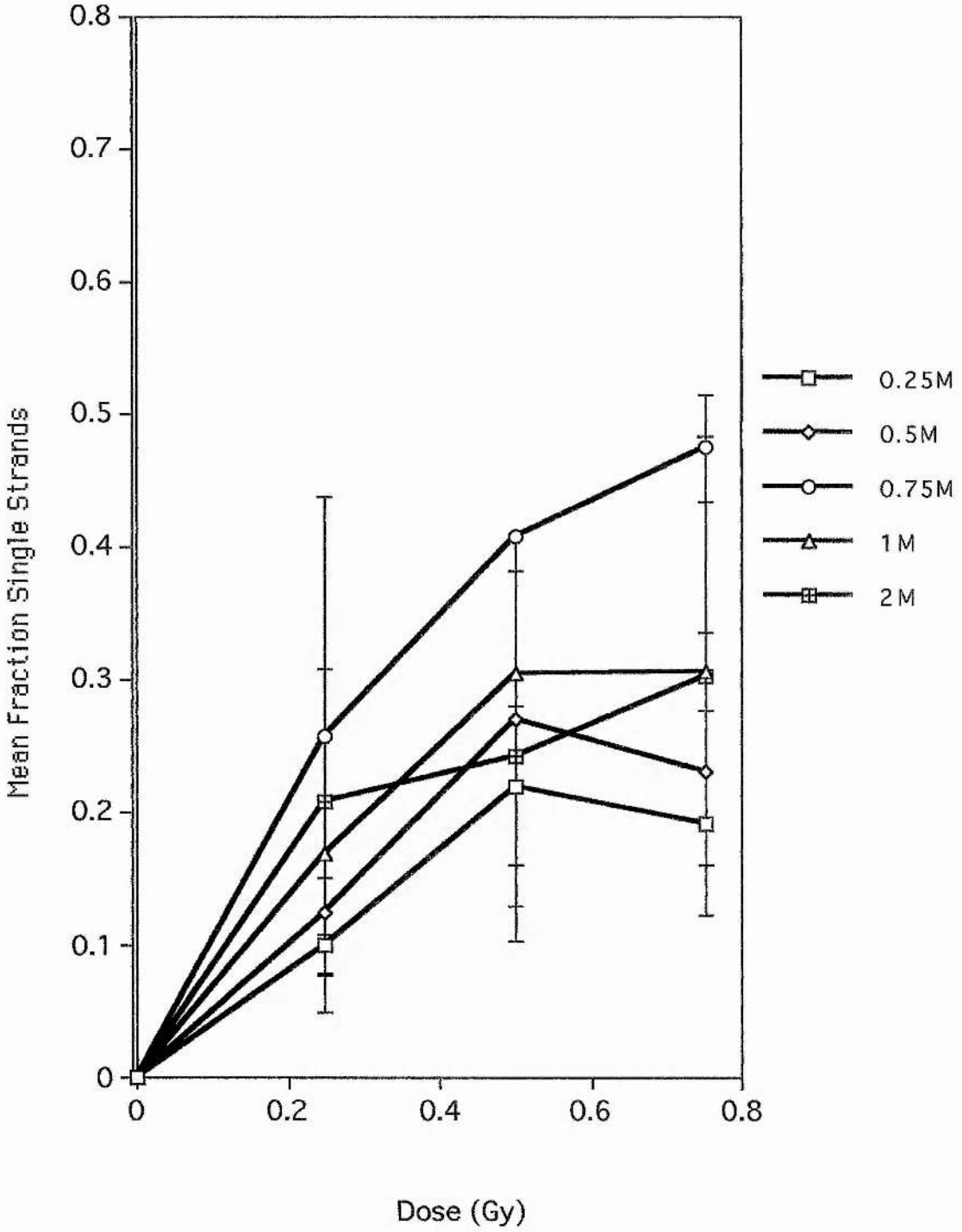

Figure 9:
Graph of Fss against dose of irradiation, in wt CHO KI for various salt solutions (0.25-2M NaCl) during cell lysis and IR. The error bars represent ± sd and n=3.

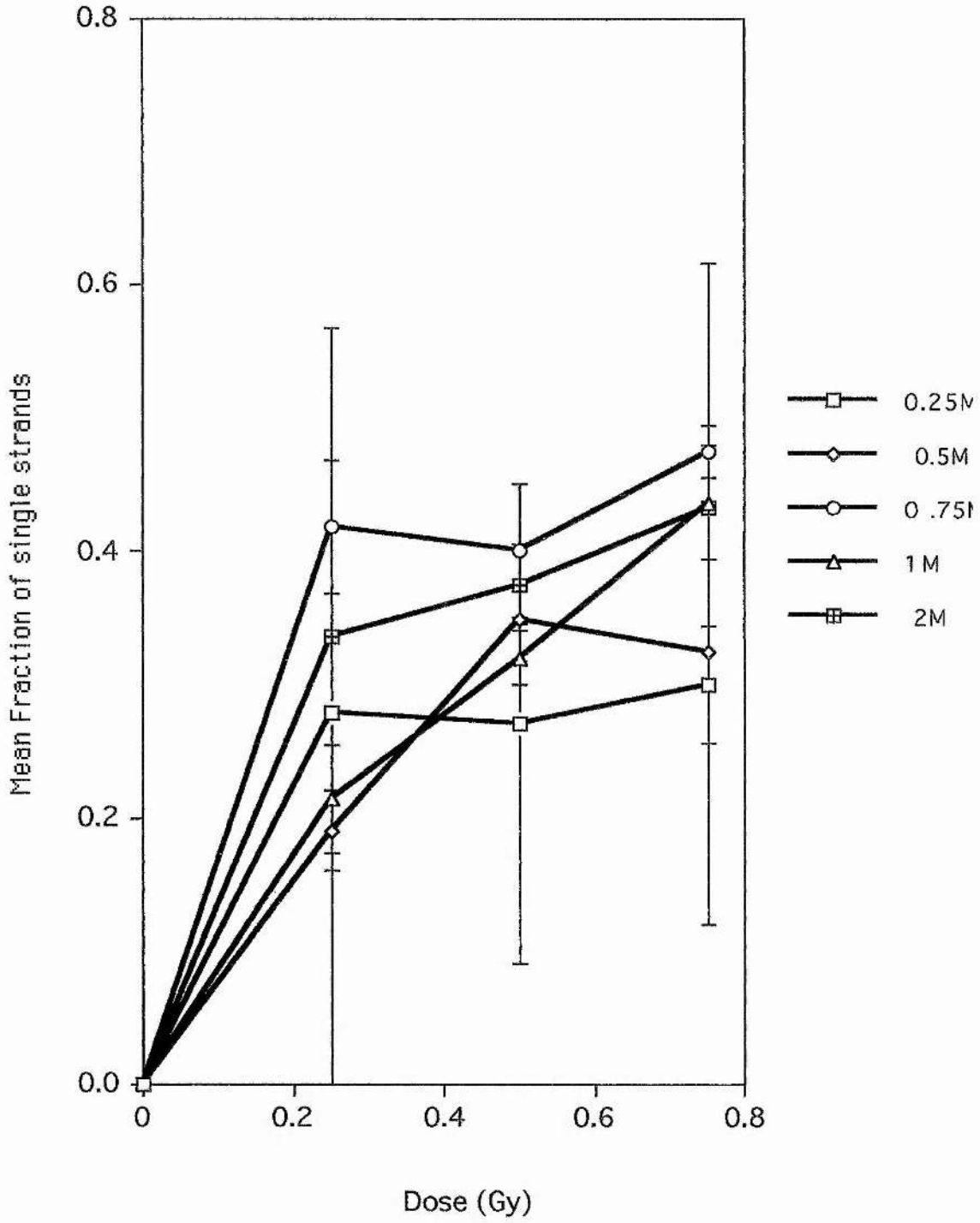

Figure 10:

Graph of Fss against dose of irradiation, in *xrs*-5 for various salt solutions (0.25-2M NaCl) during cell lysis and IR. The error bars represent ± sd and n=2.

the same order for both wt and mutant, and at 0.75 Gy unwinding was optimal for each NaCl concentration.

The right-handed skew in hypertonic extraction medium might be indicative of three different populations of cells with different unwinding rates of which the central portion of the curve could be attributed to replication fork DNA or cells undergoing replication or reversion of the mutant to the wt. Alternatively these cells could be observed as cell undergoing replication repair, as kinetically this portion of the curve appears static. Ongoing repair might occur if there was a temperature fluctuation at the irradiation stage when the cells were moved between the irradiator to the laboratory bench during the alkaline step whereby cell could have been warmed upto about 10-21 ^{o}C. However this stasis could be the result of equilibrium between early unwound duplex strands and late partially unwound supercoiled DNA rather than ongoing repair, which should not occur at 0 ^{o}C. The observed saturation in the data for both cell lines could be explained by the **'babbel'** hypothesis. In this hypothesis unwinding is proposed to proceed for a limited distance from the breakage point and then halt and further breaks are initiated from a secondary points. If these multiple break points are adjacent to each other its possible for break point interactions (**'babbel'**) to occur leading eventually to saturation which is graphically displayed as a decrease in Fss value. See 'Perspective' chapter for an in depth analysis of the three explanations for the decreased Fss values in hypertonic solution (**'two speed', 'one country, two systems'** and **'AC/DC'** hypotheses) and the biological implications of the mathematical treatment. Due to the non-linear nature of the dataset further mathematical treatment (ratios) of Figs.9 & 10 has to be treated with a caution as the processed data may only represent a small portion of the dataset and due to the non-linearity makes any assumption based on the processed data subjective and hence error prone.

Figure 11 shows, using equation (2) from the Introduction chapter section (iii), the relative slope plot for *xrs*-5 and CHO KI at various NaCl concentrations for three different irradiation (IR) doses. The relative slopes for CHO KI cells showed that greater DNA damage was induced linearly in response to protein denudation by various NaCl concentrations at low γ-irradiation dose (0.25Gy). With higher irradiation dose (0.5 Gy) on CHO KI cell, damaged was induced on treatment with hypotonic extraction medium (0.25M NaCl) and proceeded to decline in a quartic cosine form ($\pm ax^4+bx^3+cx^2+dx+C$) over the other NaCl concentrations. The polynomic form of the data could be simplified to a logarithmic form indicate that each point had a large variation and that the biological effects at each data point was complex. The distribution of points around 1.0 would suggest that the polynomic curve could be simplified to a logarithmic distribution of the form $y=mx^2$ and in this form it is clear that increasing dosage leads to an insignificant decline in relative slope. At 0.75Gy the relative slope follows a quartic sine form which can be simplified to a logarithmic form and in this simplified form

□	CHO KI @ 0.25 Gy	y = 0.137x + 0.417 r = 0.984
◇	CHO KI @ 0 .5 Gy	y = -0.203LOG(x) + 0.902 r = 0.716
○	CHO KI @ 0.75 Gy	y = 0.174LOG(x) + 0.972 r = 0.805
△	xrs5 @ 0.25 Gy	y = -0.161LOG(x) + 0.703 r = 0.275
⊞	xrs5 @ 0.5 Gy	y = -0.121LOG(x) + 0.850 r = 0.417
◈	xrs5 @ 0.75 Gy	y = 0.015x + 0.972 r = 0.331

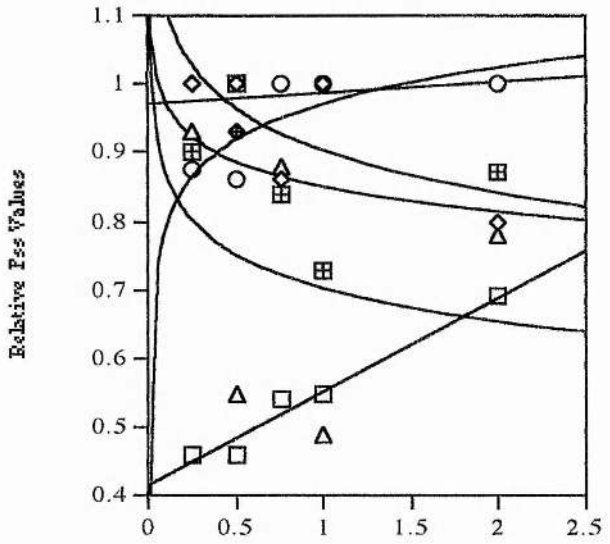

Figure 11:
Graph showing the relative Fss slopes of CHO KI and *xrs*-5 against NaCl concentration at three IR doses.

there is an initial increase from 0.25M NaCl followed by saturation at 0.75M NaCl with no change in relative slope at the higher NaCl concentrations. Therefore at 0.75Gy CHO KI became sensitive to IR damage with 0.25M NaCl treatment and higher NaCl treatment (0.75-2M NaCl) produced no further enhancement of the initialtial damage. The relative slope of *xrs*-5 cells showed that protein denudation from the chromatin occurred at 0.25Gy irradiation dose and treatment with hypotonic extraction medium (0.25M NaCl) and DNA damage proceeded to decline in a quartic sine form over the other NaCl concentrations. In the simplified logarithmic form it is clear that there was an overall decrease in relative slopes for all doses examined and with increasing dosage the relative slope became less steep, indicating that the mutant became relatively less sensitive to IR damage. Therefore this decline could be the result of ongoing repair or reversion in the mutant. Notably as in the case of CHO KI at 0.5Gy irradiation,the mutant similarly followed a declining quartic cosine function rather than a quartic sine function. This change in polarity may suggest that there was a corresponding superhelix polarity change, from positive (+) to negative (-).

Figure 12 shows, using equation (3) from the Inroduction chapter section (iii), a ratio of DNA radiosensitivity plot for *xrs*-5 with various NaCl concentrations at three different γ-irradiation doses. All three plots fitted a logarithmic form ($y=(\pm)mx^2$) distributed around 1.0 and that there was a polarity change from negative to positive with exposure to 0.5Gy irradiation dose. This showed that there was a trend toward no difference between mutant and wt radiosensitivity with increasing NaCl which could infer possible partial reversion of the mutant to the wt radiosensitivity. Only partial reversion was indicated as there was a marked difference in radiosensitivity at 0.25Gy especially at 0.25M where the mutant was twice as radiosensitive as compared to the wt. The declining logarithmic curves at 0.25 and 0.75Gy could represent the effect of ongoing repair whilst the initial low sensitivity of the 0.5Gy curve with treatment with 0.25M NaCl concentration in extraction buffer could indicate supercoiling polarity change.

□ Ratio of sens @ .25 $y = -1.005\text{LOG}(x) + 1.216$ $r = 0.754$

◇ Ratio of sens@.5 $y = 0.112\text{LOG}(x) + 0.958$ $r = 0.272$

○ Ratio of sens@.75 $y = -0.168\text{LOG}(x) + 1.020$ $r = 0.888$

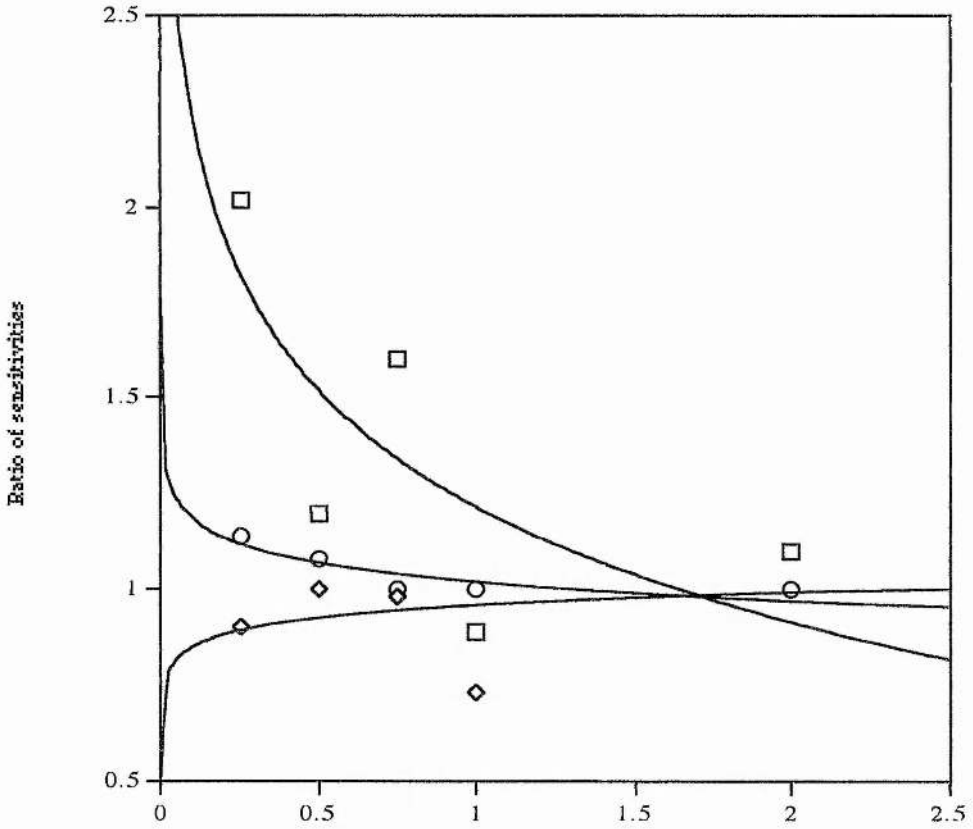

Figure 12:

Graph showing the ratio of the relative sensitivity of *xrs*-5 to CHO KI for different NaCl concentrations at three different IR doses.

To reduce the handling errors and increase throughput 24 well Terasaki tissue culture plates were used, which allowed for analysis of one parameter (salt) rather than the two parameters (salt and irradiation) due to the reduced number of samples. Thus the cells were exposed to a single dose of 0.75 Gy, which was the optimal dose for unwinding (Figs. 9 and 10). The biphasic model needed further investigation and a single parameter kinetic would provide an insight into the biophysics of the model, resolving questions as to whether or not the model was valid or an artefact generated by the quantitiation.

(3) **Effect of varying NaCl concentration in the extraction buffer at a single IR dose (0.75 Gy) on Fss values .**

Wt and mutant cells were cultured and treated as in Materials and Methods section (1). After the last wash, monolayers were exposed to 0.75 Gy and subjected to alkaline DNA unwinding assay, as described in chapter 2 sections (1) and (2). Separate, unirradiated control plates were processed at the same time as the irradiated plates, and their Fss values were subtracted from the irradiated plates to yield the effect of salt over background levels of damage. The experiments were replicated three times (n=3) for both CHO KI and the *xrs*-5 cells. The mean fractions of single strands were plotted against concentration of NaCl in the extraction buffer (M). (Fig.13).

Figure 13 shows that the wt follows logarithmic kinetics ($y=x^2$) ($r=0.981$) and the mutant follows a quintic cosine function ($r=1.0$), with four turning points i.e.two real root and two complex roots. It is the real root which is important in terms of the biology as the complex roots become negligible when plotted with wider axes as the curve approximates a straight line. Initially the mutant has a higher Fss value than the wt reaching a maximal value of 0.46 after treatment with 0.5M NaCl then proceeded to decline exponentially to a value of 0.38 after treatment with 0.75Gy then rising logarithmically to reach saturation at 0.468 after treatment with 2M NaCl whilst the wt rises logarithmically with increasing NaCl concentration skewing toward saturation at an Fss value of 0.6 after treatment with 2.0M NaCl. Maximal damage was manifest in the mutant at 0.5M NaCl, whilst maximal damage in the wt at 2.0M. These results appear to contradict the data obtained for Fig.9 & 10 whereby maximal unwinding (damage) at all doses occurred at 0.75 M. This anomaly could be attributed to experimental error or a population of pre-replicative DNA. This could mean that the DNA duplex was unwound faster in pre-replicative nuclear monolayers (Fig.13) than post-replicative nuclear monolayers (Figs.9 and 10). Alternatively damage may initially occur at 0.5M NaCl then longer term damage occurs over larger doses at 0.75M NaCl. In a simplified logarithmic form, the initial increase in Fss values at 0.25-0.5M NaCl is discounted for the curve fit to yield a curve of the linear quadratic form $y=mx^2+C$. In this simplified model it appears that overall the Fss values are much lower for the mutant as compared to the wt implying that there was a

□ Av CHO FSs $y = 0.337LOG(x) + 0.477$ $r = 0.981$

◇ Av Xrs5 FSs $y = 0.108LOG(x) + 0.435$ $r = 0.713$

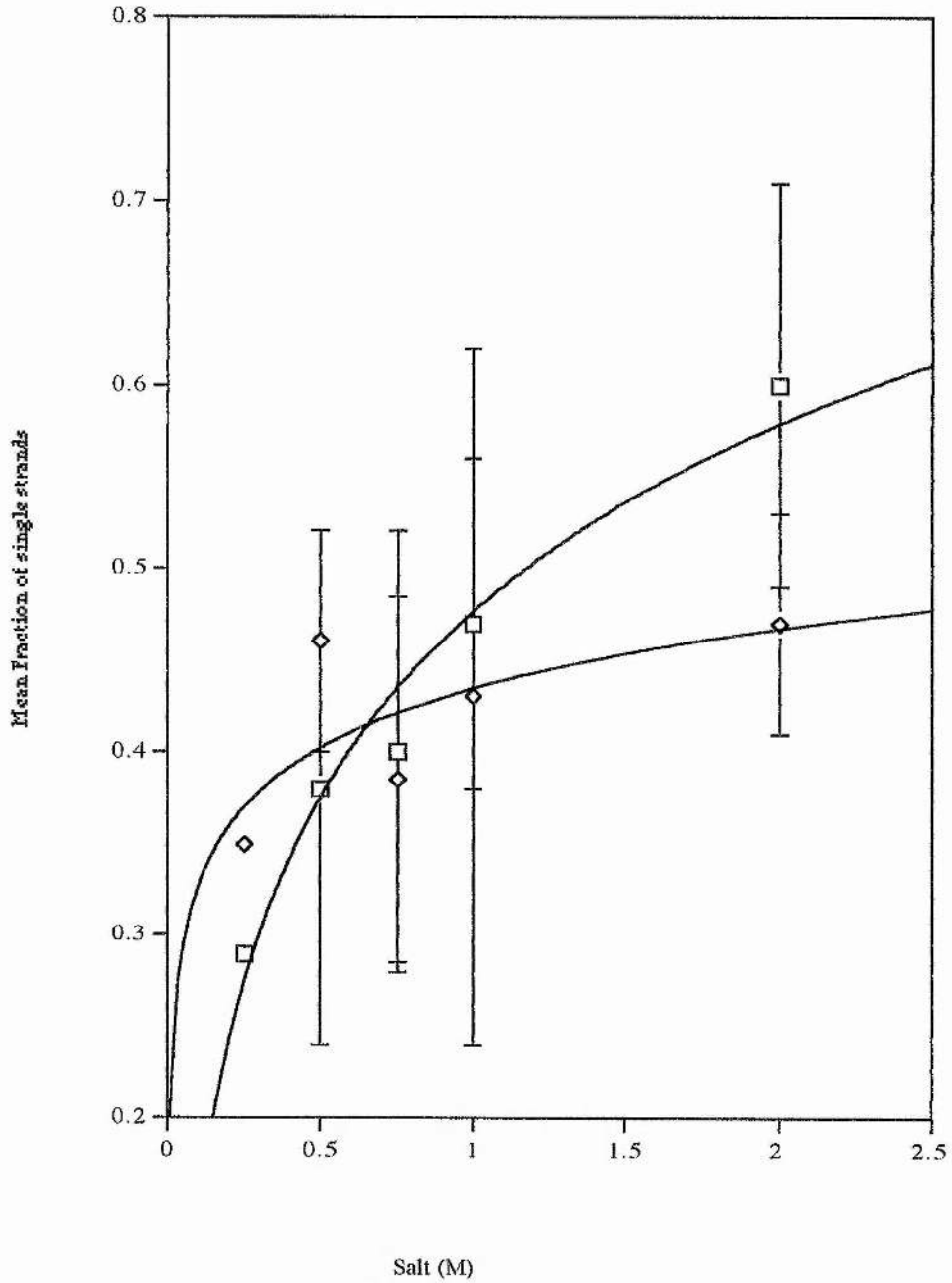

Figure 13:

Graph of Fss against salt concentration for CHO KI and *xrs*-5, at a single IR dose (n=3) where 'n' refers to the number of experiments performed. The error bars represent ± sd.

reduction in unwinding and a lower sensitivity to IR-induced damage after treatment with NaCl in the extraction medium. This could be prime facie evidence for ongoing repair or subversion of the growth medium by a radioresistant (revertant?) population of *xrs* 5 cells.

Figure 14 shows the relative Fss slope plots for CHO KI and *xrs*-5 at various NaCl concentrations and after irradiation with 0.75Gy. The plot showed that *xrs*-5 had higher relative Fss values than CHO KI ranging from a factor of 2 (in nuclear extraction medium) to 1 (in nucleoid extraction medium). CHO KI plot fitted a logarithmic function (r=1.0) whilst *xrs*-5 fitted a quintic cosine function (r=1.0) although it is possible to fit the *xrs*-5 relative Fss values to an approximate logarithmic function. The exponential decline in Fss value after treatment with 0.75M NaCl could be attributed to partial reversion to the wt. Reversion was only partial as the 1.0M NaCl treatment produced a higher relative Fss plot (factor of 1) than the wt. A logarithmic plot of *xrs* 5 relative slopes showed the difference between mutant and wt converged with extraction in hypertonic medium reflecting possible development of a revertant population or ongoing repair which reduces the IR-sensitivity after treatment with Na^+Cl^- monovalent extraction buffer.

The inherent nature of the raw data and the format of the two variables determine the polarity of the quartic/quintic equation, hence if the gradient was positive then the quartic equation has a sine function, and if the gradient was negative, then a cosine quartic function applies.

Figure 15 shows the graph of *xrs*-5 ratio of relative DNA sensitivity for various NaCl concentration at 0.75Gy which fits a reciprocal linear quadratic function approximately. This plot indicates that as a result of ongoing repair the radiosensitivity of *xrs*-5 decreases with increasing NaCl treatment.

Generally there is inherent inaccuracy in these types of assay as the background damage is high (Fss= 0.05-0.1) and these could arise from several factors. The major one of which is replication fork DNA and also contaminants within the reagents or growth medium such as bacterial (mycoplasma). Alternatively aberrant ionic strength changes within the cells caused by intrinsic cellular response to components in the growth/lysis medium could lead to an increase in the background level of DNA damage. Therefore the assay requires more stringent reproducible methods to check the validity of the data.

In summary the unwinding profile of the cell lines is fundamentally biphasic but it is manifested in two different forms in the two cell lines; wt CHO KI cells follow a logarithmic kinetic of the form ($y= mx^2$) and the mutant approximates a quartic cosine function. At high salt in the extraction buffer (1 and 2M NaCl) both cell lines exhibited linear kinetics, reflecting repair. The biological implications are discussed in the Perspective chapter.

□ CHO $y = 0.565LOG(x) + 0.794$ $r = 0.983$

◇ *xrs*-5 $y = 0.225LOG(x) + 0.927$ $r = 0.710$

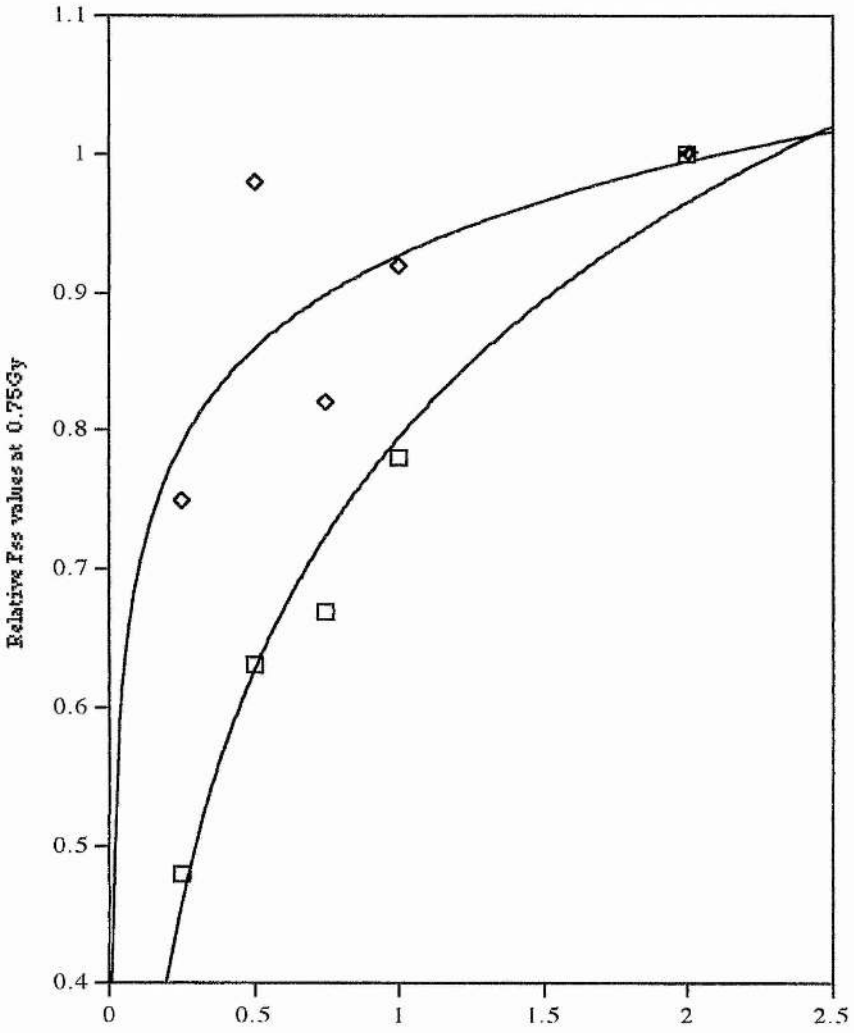

Figure 14:
Graph showing the relative Fss slopes of CHO KI and *xrs*-5 against NaCl concentration at a single IR dose.

□ Ratio of relative plots *xrs*-5/CHO KI $y = 0.228x^2 - 0.866x + 1.816$ $r = 0.953$

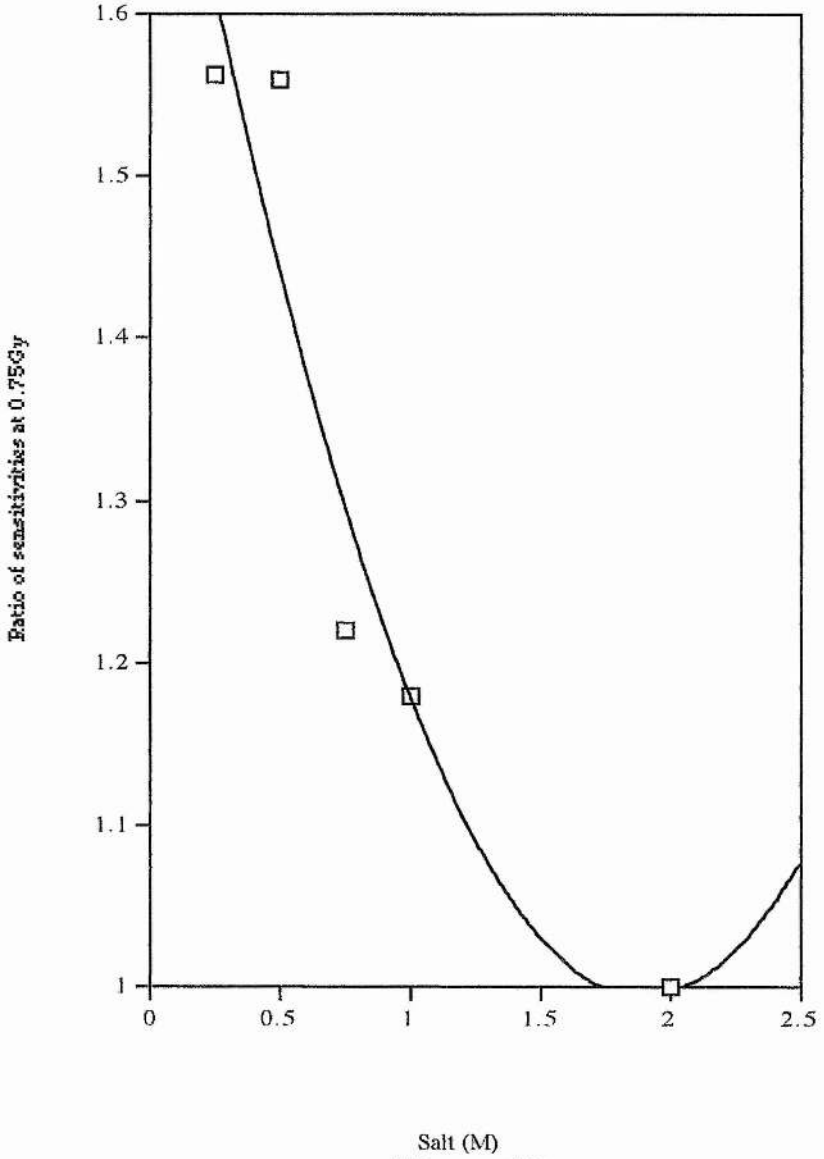

Figure 15:
Graph showing the ratio of the relative sensitivity of *xrs*-5 to CHO KI for different NaCl concentrations at a single IR dose.

(B) The micronucleus assay

Reversion of the mutant to wt occurs spontaneously, and therefore it was necessary to assess whether or not reversion had occurred in the *xrs*-5 cells in culture. The cytokinesis block micronucleus assay was used to assess whether or not reversion had occurred. The micronucleus assay was performed as described in Materials and Methods chapter section (4).

Figure 16 shows the results of micronucleus assays for six CHO KI-derived cell lines. Four mutant cell lines showed different frequencies of micronuclei from the wild type CHO KI (fresh stock *xrs*-5 designated as *xrs*5-89, *xrs*5-RC2, *xrs*-6, *xrs*6-Ku80) and one (old *xrs*-5 designated as *xrs*5-91) was only slightly increased from the wild type after exposure to 2 & 4 Gy. Thus the *xrs*5-91 had partially reverted to the wild type and it was this stock which was used in the unwinding experiments described above. The impact on the data was negligible as the *xrs*5-91 cells had not reverted to the wt radioresistance phenotype although the micronucleus data does indicate that the chromatin structure was in a state of flux and however reversion may partially explain the lower response of *xrs*5-91 nuclear monolayers to IR (Figs.13 and 14). Partial reversion may indicate that the *xrs*-5 chromatin structure was became more prone to IR-induced damage as the structure was less stable due to the interaction of reversion and more efficient ongoing repair; however without the use of repair and/or reversion inhibitors the effects of reversion could not be determined. Although the value for *xrs*6-87.1 was higher (50 micronuclei at 4 Gy) than the wild type, a new batch of cells (*xrs*6-87.2) had to be thawed out and the micronuclei assay repeated (Figure 17).

Figure 17 shows that these new stock of *xrs*6-87.2 cells developed more micronuclei per 100 binucleate cells (62 at 2 Gy) than the wild type parent (2 at 2 Gy). The low level of micronuclei in the wild type could be indicative of different efficiencies of repair in the wt and or the difference in rate of uptake of the drug (cytochalasin B) by the mutant. Thus some wt cells would be able to undergo mitosis leading to a low binucleate index. On the whole the binucleate index (data not shown) was at a level expected for the cell lines investigated. The supposition for higher repair efficiency in the mutant could be tested by performing the alkaline unwinding assay in the presence of repair inhibitors. Repair inhibitors such as araA, or araC and hydroxyurea would show a significant increase in the formation of micronuclei as inhibited repair would enhance the formation of IR-induced acentric aberration which can be packaged as micronuclei. The mode of action of araC and hydroxyurea is further discussed in the Perspectives chapter.

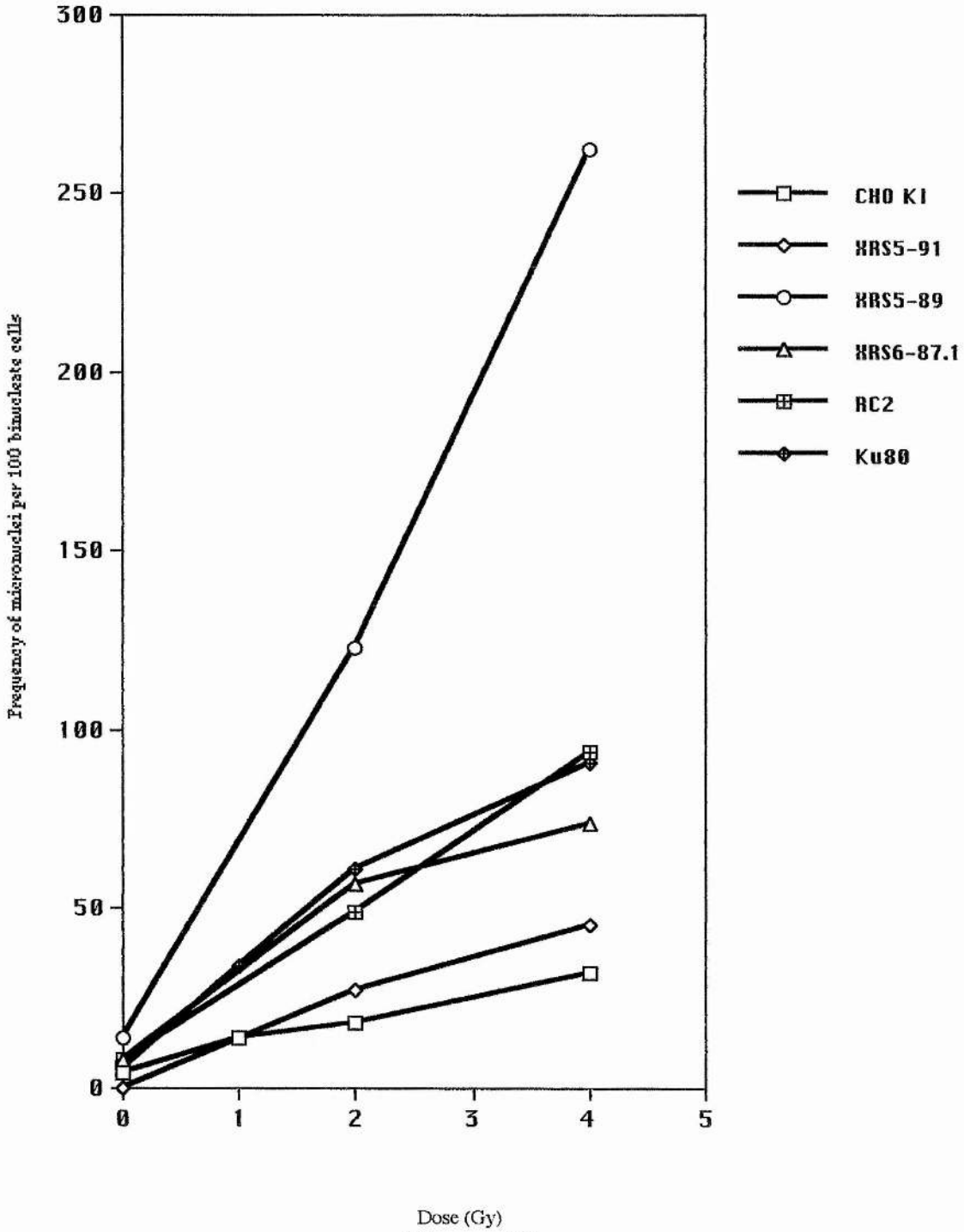

Figure 16:
Graph showing frequency of micronuclei per 100 binucleate cells for the Chinese hamster ovary wild type(wt), mutants and revertant.

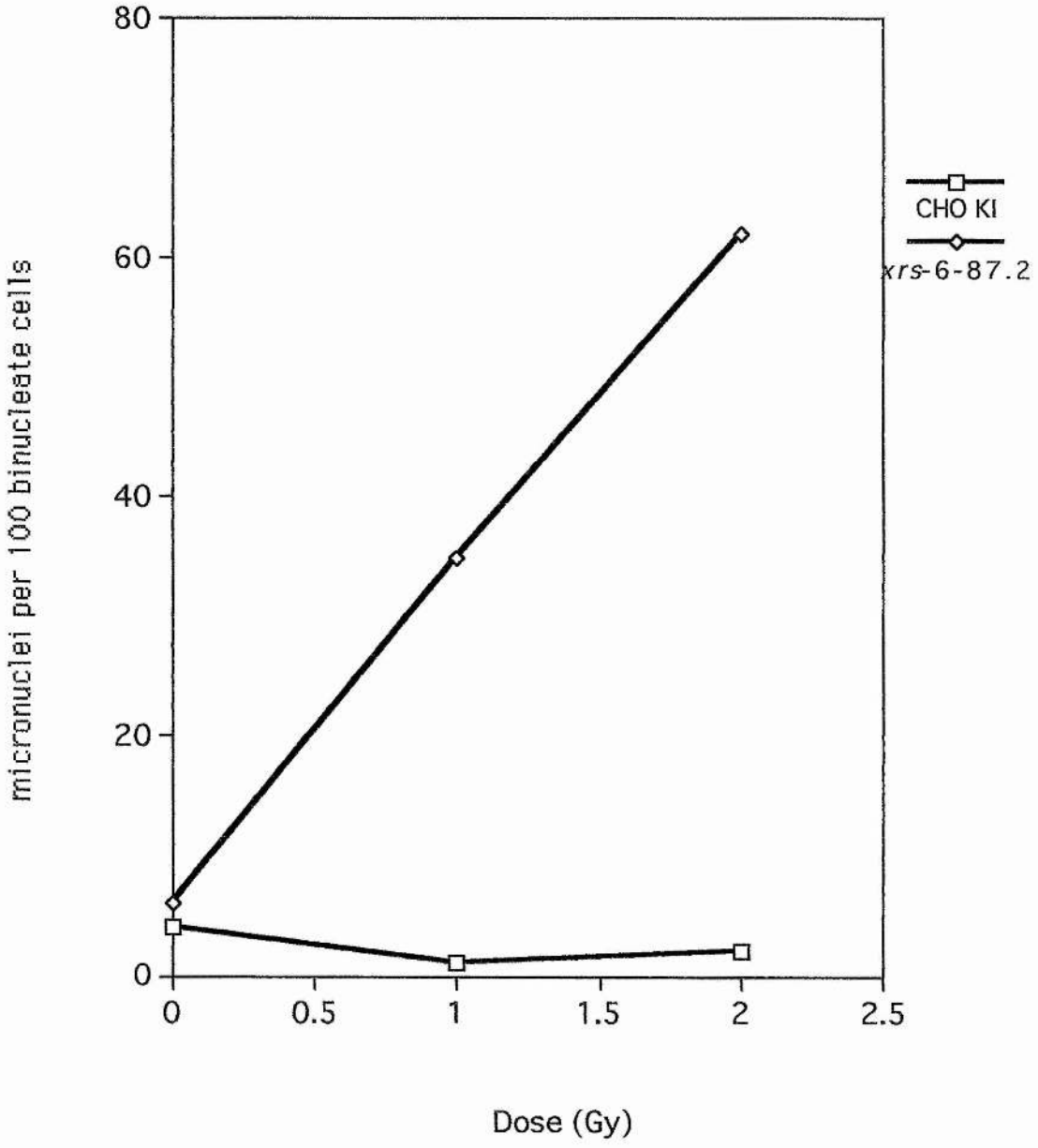

Figure 17:
Graph showing frequency of micronuclei per 100 binucleate cells for new XRS-6 and CHO KI.

Figure 18 shows a photomicrograph of a group of 11 wt cells, after exposure to 2 Gy and cytochalasin B, showing 7 binucleate cells , three mononucleate cells and one putative trinucleate cell as follows: (A) a binucleate cell without micronuclei; (B) a macro-mononucleated cell; (C) a binucleate cell with three micronuclei; and, (D) a binucleate cell with a micronucleus. The latter binucleate cell shows the joining of the two macronuclei by a chromatin bridge (indicated by two small arrows) which can be seen clearly also in another binucleate cell with two micronuclei.

CONCLUSION

The main conclusions of the radiobiology study were :

(1) DNA damage was greater in *xrs*-5 cells than the wt CHO KI cells under varying conditions of IR dose (0.25-0.75 Gy) and concentration of NaCl in extraction buffers between 0.25 and 0.75M NaCl. Maximal unwinding, as assessed by Fss, was achieved with 0.75M NaCl and 0.75Gy (Figs.9 & 10) but less in *xrs*-5 than CHO KI at 1 and 2M NaCl (Fig.13);
(2) The shape of the fitted curves for each cell line may reflect a difference in chromatin conformational state, thus CHO KI Fss values form a quadratic curve and *xrs*-5 form a quintic sine wave (Fig.14).
(3) Following from (2) the unwinding profile of the wt, CHO KI, parent follow a quadratic expression of the form ($y= mx^2$) and the mutant, a fifth order cosine function which is fundamentally biphasic. At high salt in the extraction buffer (1 and 2M NaCl) both cell lines exhibit a linear form.
(4) The micronucleus assays showed that the *xrs*-5 and -6 cell lines had partially reverted to the wild type. Therefore unwinding between the true mutants and the wild type might need to be repeated in the presence of repair inhibitors to re-assess the effect of reversion. Hence the observations made about the IR dose and NaCl concentration in extraction buffer variation experiments might be effected by partial reversion and thus any interpretation would need to be treated with caution. Despite this caveat the observations were valid and suggested that partial reversion did not adversely effect the aquisition of the unwinding data nor invalidate the interpretations that there is an increased susceptibility in the mutant to IR-induced DNA damage which may be due to chromatin conformation changes in the mutant.

These changes could be due to structural (Yasui *et al* 1991) or histone H1 modifications either by phosphorylation or the induction/repression of H1 subtypes , (Johnson & Bryant 1997). Modifications of Histone HI or it's subtypes may reflect in chromatin condensation differences as this Histone (HI) was considered to be a prerequisite for stable chromatin assembly and modification could lead to instability or continuous activation/ gene expression state (Oleinick & Chiu 1994).

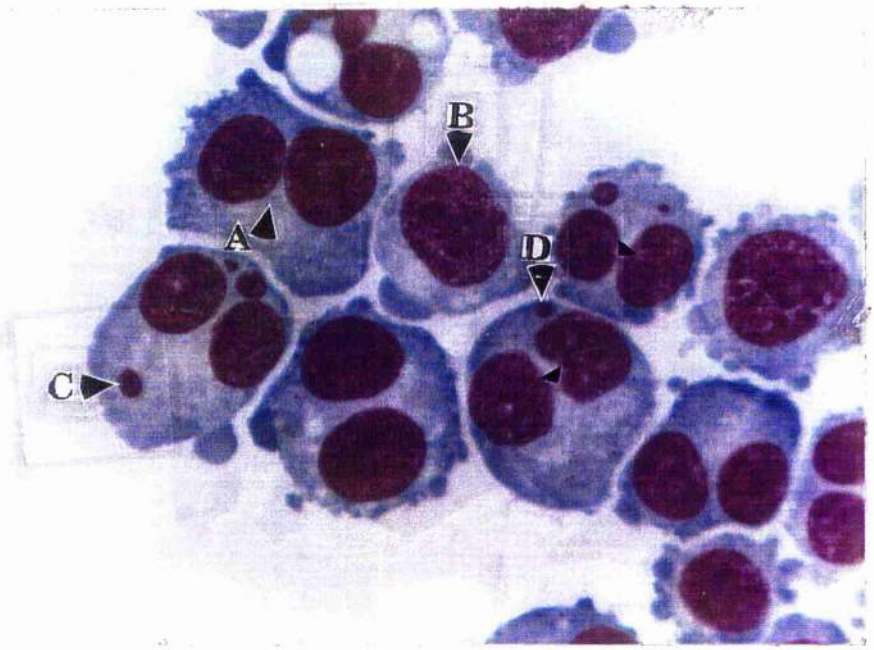

Figure 18:
Photomicrograph of binucleate cells containing micronuclei after inhibition of cytokinesis by the drug Cytochalasin B. Scale bar indicates 2.4 μm.

The increased radiosensitivity of the mutant (*xrs*-5) is due mainly to anomalies in chromatin conformation (Schwartz *et al* 1995, Johnson & Bryant 1994). It was suggested that the chromatin loops are less tightly supercoiled in *xrs*-5, and hence the structure can be easily unwound by high monovalent ions (NaCl) than the wt. The ease with which high salt can deplete the radioprotective proteins from the 'relaxed' chromatin could reflect the looseness of the bound protein in *xrs*-5 compared to wt.

The finding that maximium Fss values resulted from the use of a γ-irradiation dose of 0.75 Gy confirms the deduction of Mateos *et al* (1994) that optimal chromatid aberrations (breaks) occurred at this dosage. This would be consistent with the theory of dsb conversion processing as the duplex would be at its most plastic and hence unwinding would be optimal as more single strand 'nicks' can act as sites for unwinding initiation.

A greater susceptibility to IR-induced DNA damage in mutant as compared to wt has been observed, which could be attributed to chromosomal proteins (25,27). The next stage of this investigation therefore was to study chromosomal proteins, specifically histone H1, maturation promoting factor and the cyclin dependent kinases which have been implicated from the literature to be involved in chromatin condensation.

Chapter 4:
Protein Studies.

The remit was to investigate possible differences in chromatin conformational protein between CHO KI and *xrs*-6. Specifically:
(1) Are the histonal proteins, for example H1, modified in respect of phosphorylation, acetylation or methylation between the mutant and wild type cell lines?
(2) If histones are invariant, are the nonhistonal proteins different between the two cell lines with respect to expression levels at different cell cycle stages or post-translational modification?
(3) If the protein changes in the mutant are transient, then do these changes indicate a certain degree of plasticity about the *xrs* families chromatin structure?

These vexing questions may be tackled by taking two approaches- the use of electrophoretic separation by (a) mass (SDS-PAGE) and by (b) charge (Acid-Urea PAGE) of mitotic chromosomal proteins prepared by the mitotic shake-off method. The mass separated proteins would be subjected to analysis by (I) SDS-PAGE and Western Analysis, and (II) Acid-Urea PAGE.

(I) SDS-PAGE and Western Analysis

Mitotic CHO KI and *xrs*-6 cells were cultured, harvested and chromosomal protein were extracted and analysed as described in the Protein protocol sections (A) to (C) in the Materials and Methods chapter. Two methods were used to monitor the efficiency of extraction; (a) Giemsa stained light microscopy and, (b) protein quantitation and gel electrophoresis.

(a) *Microscopic monitoring of extraction*

Disrupted cells were stained with 3-6% Giemsa, after fixing with methanol, to check that the chromosomes were undamaged and to ensure that the majority of cells were mitotic i.e.a high mitotic index as displayed in Fig.19. For CHO KI the mitotic index was 84% and for *xrs*-6, 75%. Homogenisation of CHO KI cells required 60 strokes, whereas *xrs*-6 required 30 strokes. This difference reflects the greater resistance of the CHO KI cell membrane to shearing and compression forces. The CHO KI cell membrane may be more resistant to compression as cellular architecture is unmodified unlike that of the *xrs* family e.g. *xrs*-5 (Yasui *et al* 1991), specifically in *xrs*-5 an altered nuclear periphery in particular separation of the inner and outer layers of the nuclear envelope which could correlate not only with radiosensitivity but also with ease of cell membrane disruption in the whole *xrs* family .

Figure 19 shows the photographs of six *xrs*-6 cells following mild homogenisation. Two mitotic and one non-mitotic cells are indicated. In one mitotic cell, the outline of the nuclear membrane is visible (arrow A) as the tangled daughter chromatid pairs are polarised to the extremities of the cell (arrow B). One

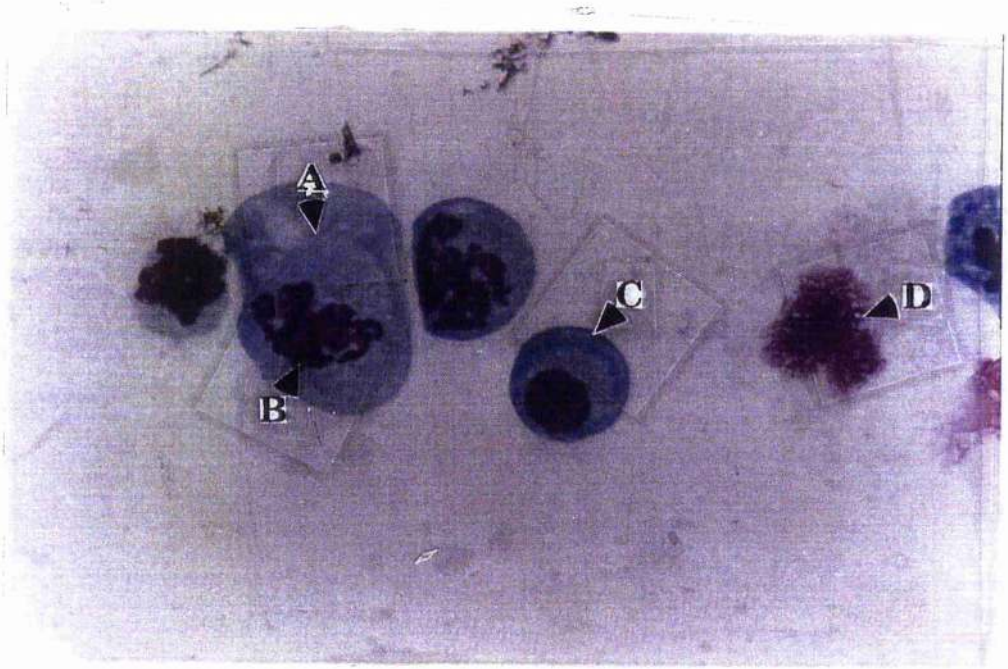

Figure 19:
The photomicrographs of mitotic and non-mitotic *xrs*-6 cells following exposure to Colcemid and treatment with 10% Non-Ident P40 detergent (NP40) in reswelling buffer. Fig.19(A) shows the nuclear membrane of a mitotic cell, Fig.19(B) shows the mitotic chromosome tangles, Fig.19(C) shows a non-mitotic cell, and, Fig.19(D) shows a NP40 disrupted mitotic cell. Scale bar indicates 2.5 μm

undivided cell with a single macronucleus and nuclear membrane can be seen (arrow C). One salt-ruptured *xrs*-6 cell exhibits DNA loops (arrow D) exuding from a central nucleus which has been swollen and the membrane disrupted by NP-40 detergent.

(b) *Protein quantitation and gel electrophoresis*

In order to ensure that the protein extraction was efficient and there was sufficient protein for Western analysis 5-10 μl aliquots of extract were analysed by a micro-Bradford assay and Coomassie stained SDS-PAGE. The protein concentration for CHO KI and *xrs*-6 was determined to be 200 μg protein per ml of homogenate.

Figure 20 shows the results of a SDS-PAGE analysis, where (M) refers to the pre-stained BioRad protein molecular weight markers (Daltons); (C) refers to the wt parent CHO KI cell line; and (X-6) refers to the mutant, *xrs*-6. Fig.20(A) shows a positive image of the gel and Fig.20(B) shows the corresponding negative print. These two images show that there was equal loading, and, that the protein banding pattern and intensities were approximately the same for both cell lines. A negative scanned image was included for clarity as not all the protein bands could be discerned from the positive scanned image: the magnification required to produce an A4-positive image caused a loss of resolution, because the pixels that form the image merged in the darkly-stained regions. From 20(A) it was concluded that at this level of analysis there was no discernible difference between the polypeptide profiles of wt and mutant.

Analysis of histone content in protein extracts by Western blotting

The treatment of protein extracts, electrophoretic separation, Western blotting and monoclonal antibody probing are described in the Protein protocol section (D) and (E) in the Materials and Method chapter.

Figure 21 showed the immunoblot for the gel shown in Figure 20 in which the gel was Western transferred and analysed by monoclonal antibody probing. The immunoblot was probed with an anti-Histone monoclonal antibody used was raised in Balb/c mice hyperimmunized to purified nuclear fractions from HeLa cells. These monoclonal antibodies recognise a conserved epitope present on histones H1, H2A, H2B, H3 and H4 from several species e.g. man, cow, rat, Xenopus, opossum and hamster. The immunoblot showed a series of bands that cross-reacted with the anti-Histone for both cell lines. The arrow points to a strong immunoreaction band about 30 000 Da in wt which was considerable reduced in band intensity for the mutant *xrs*-6. This band also was shown to be absent in *xrs*-5 by Johnson & Bryant (in press) by two-dimensional gel electrophoresis and corresponded in size to Histone HI. The size band could be HMG 1/2 or HMG 14/17 based on Johnson & Bryant's work. Alternatively another candidate conserved protein could be the maturation (mitosis) promotion factor (MPF) which is composed of the *cdk* proteins (P^{34CDC2}), 34 kDa in size,complexed with Cyclin B

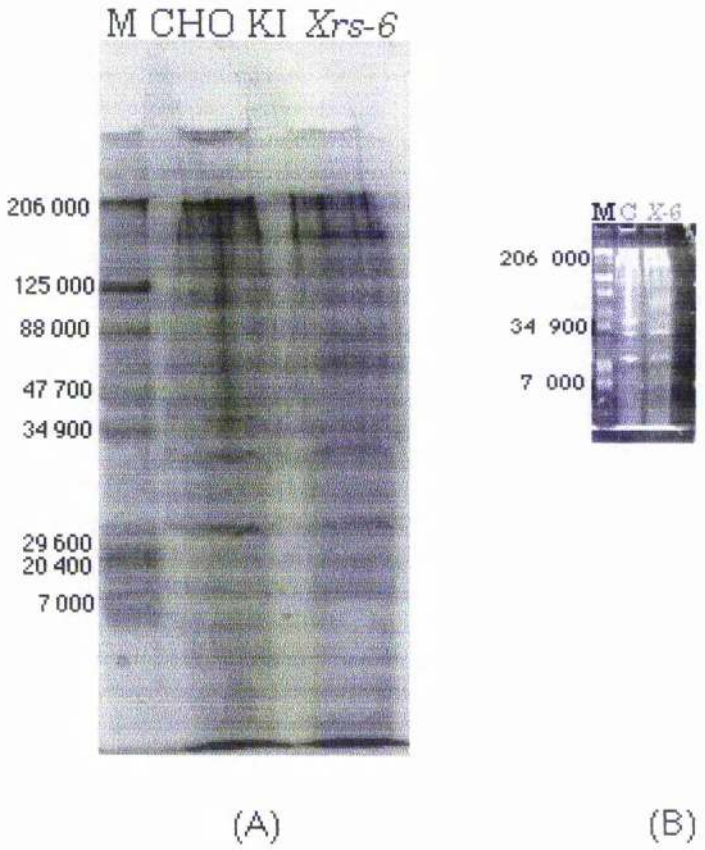

Figure 20:
Scanned SDS-PAGE gel of extracted chromosomal proteins from CHO KI and *xrs*-6 mitotic cell cultures.

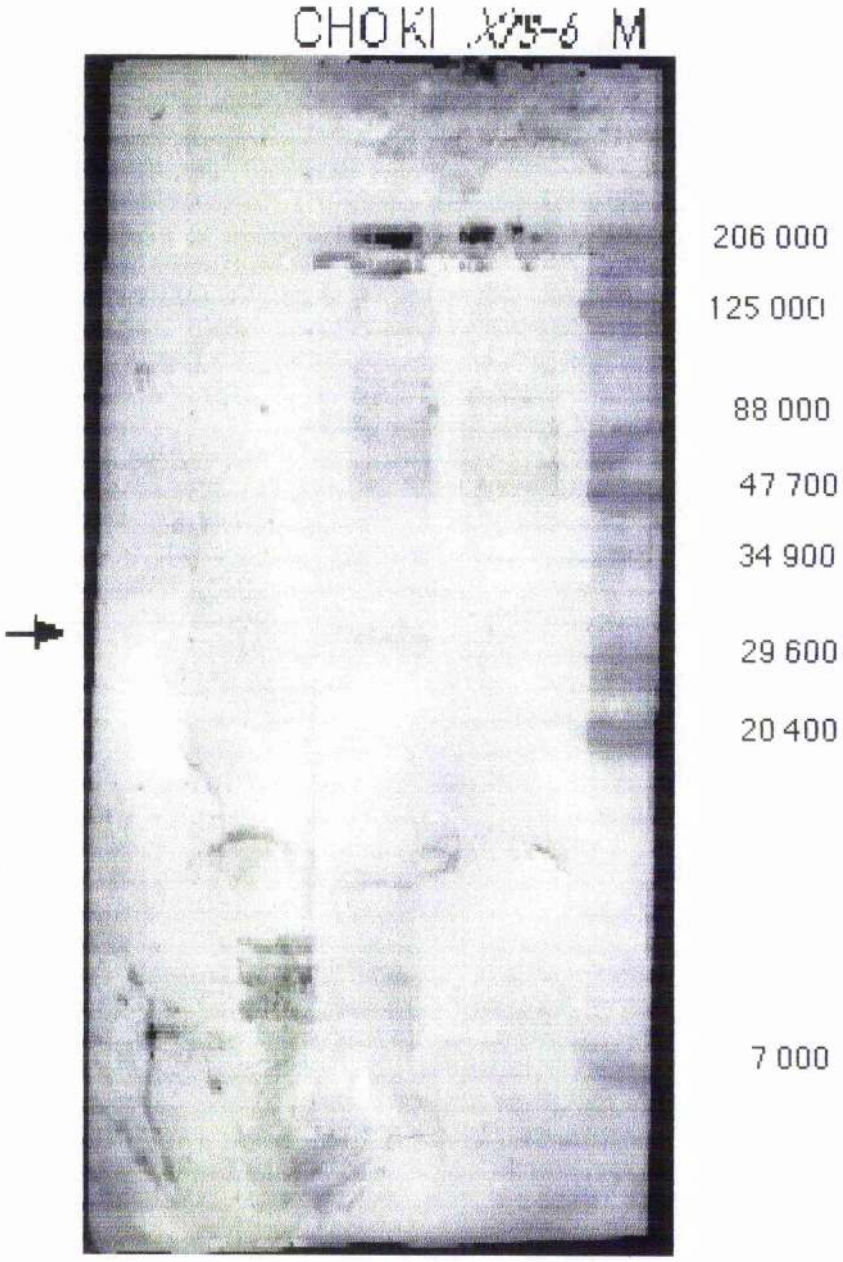

Figure 21:
Scan of the immunoblot for wt and mutant chromosomal proteins isolated from the cells shown in Figure 19. The mouse anti-HeLa core histone monoclonal antibody probe detected a reduced intensity band (Lane *Xrs*-6) and a high intensity band (Lane CHO KI) at 31 kDa (arrowed). Higher molecular weight chromosomal proteins are present from 35-80 kDa. The bound antibody probe was stained with a DAB rabbit antimouse antibody.

controlling entry into mitosis. MPF has been shown to be a tyrosine dephosphatase (9). The high molecular weight bands could be members of the cyclin-dependent protein kinases (*cdk*) and/or the cyclins ranging in molecular weight from 32-54 kDa.

(II) **Acid-Urea Triton PAGE (48).**

In order to determine whether or not there were any changes to the histones *per se* between CHO KI and *xrs*-6 with respect to quantity,or modifications, it was necessary to isolate and characterise by electrophoretic mobility as a result of charge differences (48). Bonner *et al* (1980) developed a technique for the the exploitation of the charge properties of the histone groups for their separation whereby the acidic (Aspartate and Glutamate) and basic (Lysine and Arginines) compositions of the five histone groups determines the movement of the protein in an electric field. The more negative the net charge (provided by the sum of the acidic and basic residues) then the closer the migrating band is to the cathode thus the band order from the anode would be: H2A, H1, H3, H2B,and, H4 according to increasing net negative charge. Electrophoretic mobility is provided by acetate ions, and any retardation of electrophoretic mobility due to secondary protein folding is inhibited by 1M urea in the gel and 6M urea in the boiling mix, and, separation of the histonal proteins was enhanced by the non-ionic detergent possibly by reducing the net charge of non-histonal proteins.

Due to unfamiliarity with the method the stained gel was not of sufficient quality to reproduce in this dissertation so that a representative image based upon Bonner *et al* (1980) was displayed in Fig.22. Figure 22 shows two composite images of Acid-Urea-Triton X100 (AUT) gels of acid extracted histones. Fig.22(A) shows the composite image of the expected histone distributions in an AUT gel. Fig.22(B) shows the observed image of histone distribution. The discrepancy could be due to the harshness of the extraction method which appeared to remove all the histones except histone H4 at 15 kDa. The recovered bands image appeared to be histone H4 and there appeared to be no difference between wt, mutants (*xrs*-5 & -6) and the revertant (*xrs*-6 KU80) with respect to the quantity of histone H4 present in extracts. Although the images were not photographs of actual gels the band distributions shown in Figure 22(B) does represent what was observed. If the opportunity were to arise to repeat this gel then an appropriate image would be substituted.

(III) **Protein Sequence Comparisons**

The protein extracts from wt cells shown in Fig.21. were sequenced by the Edma degradation method because it was noted from the Western analysis that

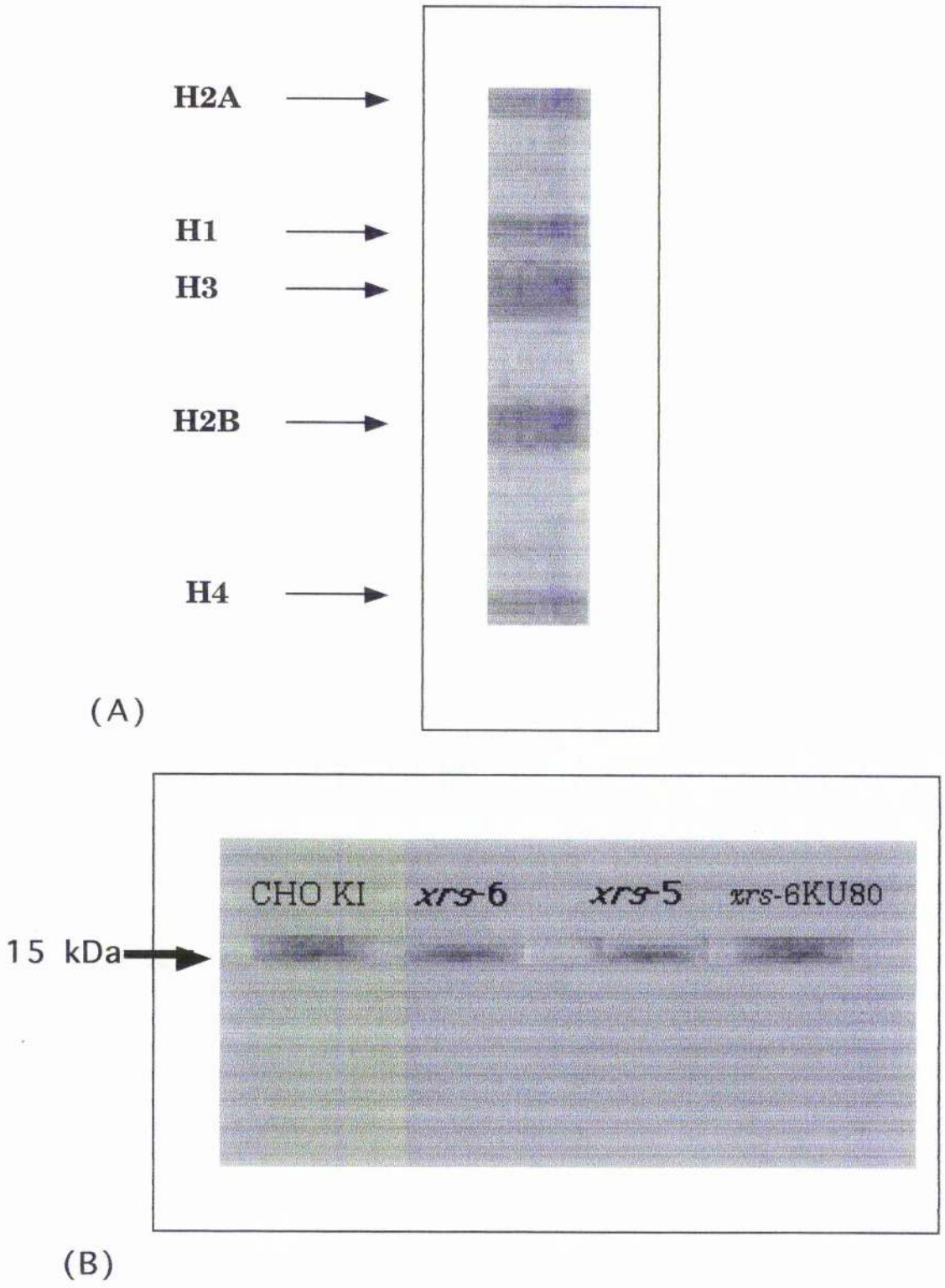

Figure 22:
Photographic images of representative Acid-Urea-Triton X100 gels stained with Coomassie blue. Figure 22(A) shows the idealised AUT gel showing the expected distribution of histones according to Bonner *et al* (1980). Figure 22(B) shows the observed facsimile of an actual AUT gel with one histone (H4) at 15 kDa (arrowed) for the four cell lines studied.

there was a difference in the protein profiles of *xrs* mutant and wild type parent. Initially, as a prerequisite for identifying the extracted 31 kDa protein (arrowed) the wild type parent, CHO KI was to be sequenced and subsequently, the mutant protein extracts were to be sequenced. It had been thought that urea was present with the boiling mixture: as such this chaotrope was known to covalently modify the N-terminus of proteins, consequently extra purification steps were introduced as descibed below.

The extracts, denoted as C,Cp and Cp2, were loaded onto a sequencing gel then transferred to PVDF membrane. The membrane was Coomassie stained and three strongly stainning bands of molecular weight range 15-20 kDa were excised (Fig.23). Figure 23 shows the thermal transfer print of the sequencing gel from which these three bands designated 1-3 were thought to contain enough protein for sequence analysis. The excised proteins were digested with trypsin and the digests concentrated by lyophilisation, and separated by microbore HPLC. The fractions collected were analysed by capillary electrophoresis, only fraction 22 of excised bands 2 and 3 had sufficient material for Edman degradation protein sequencing. These fractions yielded the following peptide sequences:

Cp Band 2 **ALNNQFAXXIDK**
Cp Band 3 **XIENYET**

These sequences were used in a protein sequence database search, **SwissProt**, using the **FASTA *search engine*** and a good match was found with human cytokeratin. The unknown residues designated as **X** were due to problems in loading (Band 2) and resolution of serine residues in position 1 (Band 3).

Although cytokeratin has been identified as a component of the nuclear matrix (34) the match with human cytokeratin could only be assumed to be a contamination of the sample during the prolonged preparative stage for sequencing (G.D.Kemp personal observation). In particular the contamination could have occurred at the trypsin/lyophilisation step. One of the weaker matches for Band 2 was to Chinese Hamster vimentin (63.6 % identity in 11 amino acid residues).

In summary the SDS-PAGE experiments have shown there was a qualitative protein difference between the distribution of chromosomal proteins of CHO KI and *xrs*-6. These differences are most marked by the reduction in the intensity of a histone-related protein band at 31 kDa.

The Acid-Urea-Triton X100 experiments showed there was no apparent differences in quantity of histone (H4) between protein extracts of wt (CHO KI) and mutants (*xrs*-5, *xrs*-6, *xrs*-6 KU80).

The sequencing of two darkly Coomassie-stained bands had shown that they were possible human cytokeratin II contaminants introduced during the trypsin/lyophilisation step. A third band (1) was trypsin-sensitive.

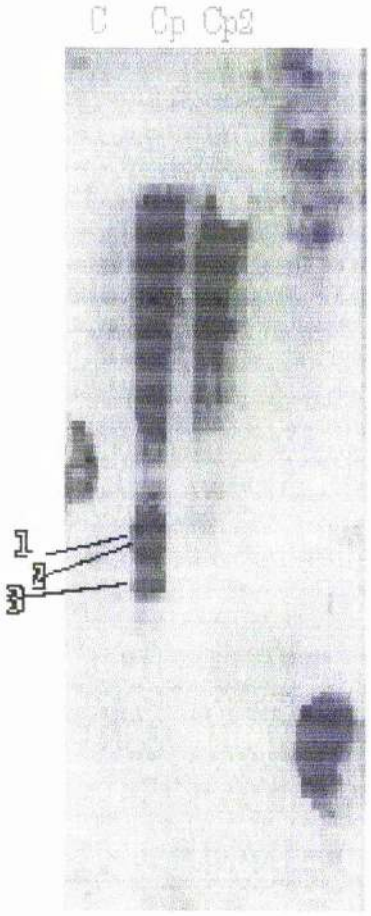

Figure 23:
A thermal transfer print of a PVDF membrane stained with Coomassie Blue and showing a sequencing gel of three CHO KI protein extracts. Three bands are indicated of around 15-20 kDa in size (designated 1,2 & 3) which were excised for Edman degradation sequencing.

If the opportunity were to arise a more stringent protein isolation would be required initially to produce more template for Edman degradation without urea to avoid possible contaminants arising from the trypsin/lyophilisation step.

CONCLUSION

The main conclusions of the protein study were :

(i) There was a difference in the distribution of high molecular weight histone-like chromosomal proteins in the mutant, *xrs*-6 as compared to the wild type parental cell line, CHO KI, (Fig.21);
(ii) One 31 kDa (Fig.21) polypeptide was less abundant in protein extracts from mutant compared to wt;
(iii) In Figure 21 the bands were detected which might correspond to HMG 1/2, HMG 14/17 or P^{34CDC2};
(iv) There was no apparent relative quantitative difference between histone H4 protein (15 kDa) in all the cell lines tested (Fig.22B). This is expected as the cell line has not been reported to lack nucleosomes and assembly of a nucleosome requires avid binding of histone H3 and H4. Nucleosome abnormalities would arise in the latter stages of assembly of the nucleosomal complex i.e. histone H1/ HMG1 or HMG2 binding, but as the isolation procedure was not optimal defects to these components of the nucleosomal architecturecan not be ruled out;
(iv) The two sequenced protein bands (Fig.23) showed a good match with human cytokeratin II. As suggested by G.D.Kemp, matching of the sequenced bands with human cytokeratin II could only be as a result of contamination.

To answer the three questions posed at the start of this chapter; (1) no apparent initial difference was detected in the histonal proteins but this must await confirmation by more refined AUT experiments; (2) there are electrophoretic mobility and anti-histone monoclonal antibody binding diffferences in the high molecular weight histone-like non-histonal proteins which could be Ku (70-80 kDa) and *cdk* family proteins (31-60 kDa); and, (3) there is little evidence from this small study to answer this question (See Perspective chapter for a discussion on the possible rôle of transistional chromosomal proteins and chromosomal plasticity).

Chapter 5:
Perspective.

(1) Radiobiology Studies.

It was concluded from the results shown in Chapter 2 that:-
(a) alkaline unwinding in both CHO KI and *xrs*-5 follow an inherent biphasic nature; however the shape of the fitted curves were different, with a quadratic curve for CHO KI and a quintic sine wave for *xrs*-5. i.e. This difference may be a reflection of a difference in conformational state.
(b) For salt treated & irradiated *xrs*-5 cellular (no extraction buffer), nuclear (0.25-0.75M NaCl concentration in the extraction buffer) and nucleoid monolayers (1 and 2M NaCl concentration in the extraction buffer) were more sensitive to IR-induced DNA damage than the wild type CHO KI cells, with maximal Fss values under the conditions used at 0.75M NaCl and 0.75Gy (Figs.9 & 10).
(c) Under hypertonic conditions (1 & 2M NaCl in the extraction buffer) both cell lines exhibited saturation kinetics i.e. reflecting that there was either efficient fast repair or nucleoid chromatin was more resistant to salt-mediated alkaline unwinding or in the mutant, the effects of partial reversion, and
(d) The micronuclei assays showed that the *xrs*-5 and -6 cell lines had partially reverted to the wild type and it was these cells that had been used in the radiobiology experiments in Chapter 3. The effect of partial reversion was discussed briefly in Chapter 3 and one possible consequence of using partially reverted cells is highlighted in conclusion (c).

If these results are valid then three possible mechanisms to account for the skewed biphasic graphs shown in Figs.9, 10 and 14 in Chapter 3:
(i) A two staged ongoing repair
(ii) Three different cell populations with different unwinding characteristics
(iii) Supercoiling polarity changes.

Each of these mechanisms will now be discussed:

(i) *Ongoing Repair* (the **'two speed'** hypothesis)

In this hypothesis, the skew of the Fss values is explained by ongoing repair of the γ-radiation-induced DNA damage despite the hypothermic conditions (4°C). Warming up between manipulations was cited in Chapter 3 as a cause of the skew at 0.5 Gy (Figs.9 and 10) and 1M NaCl in extraction buffer (Fig.14). Repair was possible in this assay because the microtitre plates might be at 4°C but the instrumentation (dispensing tips) was not cooled to the same temperature and the assay was not performed in a 'cold (4°C) room'. These conditions would have allowed some local temperature increases for repair to be initiated. To confirm or refute this possibility an additional experiment might be to perform the assay in 'cold room'

conditions and with repair inhibitors e.g. hydroxyurea. in conjunction with araC. Both these drugs acts at replication checkpoints and should abolish the aberrant plateau, although their mechanisms of action are different. The drug araC competitively inhibits DNA polymerase α at repair sites, while hydroxyurea inhibits ribonucleotide reductase resulting in depletion of intracellular dCTP pools. When used in tandem hydroxyurea can enhance the action of araC (68, 69,70,71). Repair could only occur if the lysis conditions were not optimal as repair could not occur in lysed cells but could occur in cell suspensions or cell monolayers and if the repair hypothesis is correct then lysis conditions were not optimal. Thus repair can not occur in nucleoid monolayers but it can not be discounted from nuclear and cell monolayers as denudation of the protein from the chromatin occurs gradually at lower NaCl concentrations so repair proteins could be active upto 0.75M NaCl. Therefore repair inhibitors might remove the skew at 0.5 Gy but it might not remove the skew at 1M NaCl which might be due to salt-resistant nuclear matrix proteins or reversion The findings presented in Chapter 2 are supported by work (72) that repair at hypothermic temperatures (0°C) was biphasic and specifically repair in mammalian cells (73,59 and 74) was also biphasic. Double-strand break (dsb) repair in mammalian cells has two components that can be separated according to the number of DSB and rate (speed) at which the breaks are repaired. These components are:-

(a) fast, and;

(b) slow.

The efficacy of the fast component, as shown in Figure 8, may be the cause of the skew in the Fss curves observed in Figs.9, 10 and 14.a biphasic character. The The rapid component has a $t^{1/2}$ value of 3-10 min and the slow component a $t^{1/2}$ value of 40 min- 4h. The slow repair is dependent on growth conditions and multiplicity of dsb (75). It is believed that during the fast component exchange aberrations are produced (76) and during the slow component, chromatid and chromosomal breaks (77). The trend for decreased unwinding (Fig 9-10 and Fig.14) in hypertonic Ljungman (nucleoid) lysis buffer might reflect efficient fast ssb repair at 4°C.

(ii) *Different Cell Populations* (the **'one country two systems'** hypothesis).

The skewed Fss values might be due to two (three) different cell populations (**two systems**) co-existing (**one country**) with three different susceptibilities to IR-induced damage:

(a) faster growing cells which are more sensitive to IR-induced damage and so may contains replication fork DNA;

(b) static population of cells which are either entering or exiting replication less sensitive to damage; and,

(c) slow growing cells which are asynchronous and might represent G1/G2 interface cells and their DNA would be torsionally constrained hence these cells would produce least sensitive to IR damage.

If the unwinding assay reflected the changes in population (**'one country'**) then it would be possible to confirm this hypothesis and also to confirm that reversion had indeed occurred by a clonegic survival assay or a growth curve which produces an **'S'** or sigmoidal curve whereby the 'tail' of the curve would be elongated if there was a slower growing population (revertant clones) of cells.

Repair is not excluded from the **'one country two systems'** hypothesis as there is a possibility that fast ssb repair might be active causing the observed right-handed skew.

(iii) *Supercoiling polarity changes* (the **'AC/DC'** hypothesis)

It could be argued that the skew of the Fss values could be the resultant of unwinding equilibria between relaxed DNA loops and torsionally stressed superhelical loops of replicating chromatin. This possibility arises from the hydrodynamic properties of DNA (Cook & Brazell 1975, (62)). These properties are summarised in the following expressions:

$$\alpha = \beta + \tau \qquad (4)$$

$$\Delta\tau = -\Delta\beta \qquad (5)$$

Where (α) is the topological winding number which is a constant in the absence of strand scission, and it is composed of two determinants;(β), the duplex winding number and (τ), the superhelix winding number. From equation (4) any positive change in superhelical turns (τ) results in a negative change in either strand of the duplex i.e. thus as the alkaline lysis causes unwinding then (τ) increases from negative (-1) to zero then to positive while (β) decreases from (1) to (0) in the absence of γ-irradiation.

Biophysically in unirradiated cell monolayers, exposed to mild alkaline lysis, their chromatin loops change from positive supercoiling to negative supercoiling through an intermediate relaxed form i.e. a biphasic response. At high dose γ-irradiation the chromatin loops enter the relaxed state and loses all supercoiling but at low dosage the transition to a different polarity of supercoiling might occur in some monolayers. The presence of monovalent and divalent ions can speed up the transition but hypertonic (nucleoid) solutions may synergistically enhance the low irradiant to produce an irreversibly relaxed form (Cook & Brazell 1975, Cook *et al* 1976).

An estimate of strand breakage and relative DNA cross linkage was obtained from the Ljungman (1991) and Ahnström & Erixxon (1981) papers using the following equations:

$$\text{SSB}/10^9 \text{ Daltons} = K \log \text{Fds} \qquad (6)$$

$$\text{Relative number of DNA cross-links (RelXLIN)} = (-) \log (\text{Fss}) \qquad (7)$$

Where SSB/10^9 Daltons represents the single strand breakage in one DNA strand of 10^9 Daltons in size, Fds and Fss are the fractions of double- and single-strands, K is the duplex unwinding constant,-1.8, and the negative logarithmic value of Fss converts the small value of Fss into a positive integer and the value represents the possible number of DNA loci for IR-damaged ssb to interact or be acted upon by repair enzymes.

The constant value K is derived from the exponent of a good solvent in the Zimm model for coiled polymers (60) and is related to relaxation time denoted as τ, and thus represents the duplex unwinding constant. In terms of this study relaxation of the supercoiled DNA, the K value, -1.8, represented the strand breakage at 0°C in the presence of 0.03M NaOH /0.15M NaCl and it is calculated as the quotient of -12, the value used by Ljungman (1991), and a value (6.7) representing the factor between 1M NaCl and 0.15M NaCl. Therefore as K= -1.8 and is related to (τ), the superhelix unwinding number (62), then the unwinding assay manipulates (τ) by making it equal to zero.

The hypothesis that fits best the experimental data is the one of ongoing fast ssb repair, although cell populations differences might explain some of the complexities of the right-handed skew, although not the suppression of the nucleoid (1 and 2M NaCl in extraction buffer) curve in both wt and mutant (Figures 9 & 10). An accumulation of relaxed form chromatin as suggested by mechanism (iii) might cause a reduction in the nucleoid signal. Two mechanisms indicate that repair is occurring at 0 (4)°C but the third explanation could explain the disparity of the hypertonic solutions in terms of DNA hydrodynamics.

Although there is noise in the system, i.e. the staistical errors, the noise is nonrandom and consistently (n=6) follows the signal. Therefore the **biphasic pattern must be inherent in the system** and the **effect of noise seems negligible**. Although any interpolations or extrapolations needs to be checked to avoid over interpretation and use of a complementary method would be help to prevent misinterpretation of the unwinding data e.g. cytofluorimetry (FCM) with propidium iodide as this method provides a complimentary measurement of supercoiling changes.

That maximium Fss values were incurred with 0.75M NaCl in the lysis medium indicates that protective proteins were removed most effectively at this concentration.

Reversion of the mutant to the wild type was suspected from an micronucleus experiment to demonstrate the micronucleus assay using the mutant and wt cells as examples of negative and positive control cells. These experiments had indicated that the frequency of micronuclei per 100 binucleate cells was lower than expected and Figure 16 (old *xrs*-5) graphs display a re-count of the microscope slides from that experiment. Previous indicators of reversion (G2 assay) had not indicated that reversion had occured and as such the unwinding experiments described in Chapter 3

had used these cells. Partial reversion as cited in Chapter 3, does not effect the observation that the mutant was more susceptible to IR-induced DNA damage than wt or explain the skew of the Fss values adequately, partial reversion does provide another explanation for the low Fss values of nucleoid monolayers (0.75M NaCl in extraction buffer) as shown in Fig.13 and of the 0.75 and 0.5M NaCl (in extraction buffer) Fss values at 0.5 and 0.75Gy as shown in Figure 10. The skew of the Fss values and particularly the low Fss values under nucleoid conditions (1 and 2M NaCl in extraction buffer) is consistent with an ongoing repair hypothesis. Therefore the effects of partial reversion on the interpretation of the unwinding data is negligible. If there had been time then undoubtedly the unwinding experiments would have been repeated with the fresh stock of mutants (*xrs*5-89 and *xrs*6-87.2) which would have shown more pronounced differences between wt and mutant nevertheless there was a **strong evidence** to show that the **mutant** was **more sensitive to IR-induced DNA damage after partial protein removal by monovalent ions (NaCl)** than the **wild type.**

That ongoing repair occurred in presumptive nucleoids and/or lysed cells implies that: (a) lysis conditions were not optimal, and (b) presence of NaCl-resistant (**repair?**) proteins in the chromatin structure.

(2) Protein Studies.

The radiobiology study had indicated a chromatin conformational difference between mutant (*xrs*-5) and wt which was deduced to arise from modification of the chromosomal proteins, and so experiments were performed to compare proteins which may be involved in the increased susceptibility of mutants in the *xrs* family to IR-induced DNA damage compared to wt. A previous study on *xrs*-5 (63) had already shown a protein difference between the mutant and wt CHO KI but not whether there were protein differences in other members of the *xrs* family so *xrs*-6 was chosen for the purpose comparative analyses. *Xrs*-6 had been as well characterised as *xrs*-5 and as a reference point the Ku80 protein was absent from these mutants. Although *xrs*-6 had been examined in radiobiology studies the unwinding results were inconclusive and as the objectives of the project had altered reducing the available time thus an initial comparative protein analysis between *xrs*-6 and wt CHO KI was performed. Synchronous cells were chosen as a cell cycle comparator as any change in distribution of chromosomal strutural proteins would expected to occur at defined stages of chromatin assembly or disassembly which occur mostly at intercyclic points such as G1/S or G2/M. The *xrs* family has been shown to have an enhanced mitotic delay after irradiation (87) and thus M stage was chosen as the cell cycle stage for comparison. Any protein difference could then be used as a probe to investigate expressional differences in asynchronous cells in wt and mutant. The results in Chapter 3 showed that; (i) there was a difference in the distribution of high

molecular weight histone-related chromosomal proteins in the mutant, *xrs*-6 as compared to the wild type parental cell line, CHO KI was detected, (Fig.21); (ii) by Western analysis, the protein extracts from the mutant had decreased immunoreactivity with a monoclonal antibody to histones specifically, a 31 kDa (Fig.21, arrowed), compared to the wild type CHO KI; (iii) the histone positive bands in Figure 21 may represent members of the cyclin dependent kinases in particular the arrowed band might be P^{34CDC2} or protein A. The other high molecular weight proteins around 65-70 kDa might include Ku protein and the DNA-PK_{cs} complex which would be expected to be missing in *xrs*-6; (iv) there was no apparent relative quantitative difference between histone H4 protein (15 kDa) in all the cell lines tested (Fig.22B); and, (v) the two protein bands (Fig.23 (2) and (3)) were extracted, but the sequencing was unsuccessful due to contamination of the samples during the preparative stages of the sequencing.

The consensus viewpoint is that chromatin condensation propagates unrepaired double-strand break lesions through mitosis into G2 leading to chromatid or chromosomal breaks or gaps. Condensation is a histone-driven process and stability of the chromatin structure is reliant upon histone H1. Differences in H1 composition or activity could lead to structural instability in the mutant and thus make the nuclear matrix radiosensitive.

To investigate this supposition chromosomal proteins were isolated and probed by Western analysis with antibodies to histones, and, a method for histone isolation was attempted. The antibodies had found a multiplicity of high molecular weight histone-like proteins but one (31 kDa) band was strongly stained in CHO KI which was less intensely stained in *xrs*-6. The size of these bands (31-60 kDa) exclude them being isoforms of the five histone classes, histones H1, H2A, H2B, H3 and H4 although from the antibody probing it appears to have a histone related sequence. This is preliminary evidence for the involvement of a histone related protein in the increased sensitivity of mutant to IR -induced damage compared to wt. Johnston & Bryant (in press (63)) found an array of polypeptides and two polypetides (31.8 & 32.8 kDa), by two dimensional analysis of protein extracts from CHO KI and *xrs*-5, appeared to be absent in *xrs*-5. They showed that in South Western blots that the array of *xrs*-5 polypeptides differentially bound radiolabelled double-stranded DNA as compared to CHO KI.

In terms of the present study the protein that is reduced in intensity (Fig.21), in the mutant *xrs*-6, is similar in size to MPF however there is no strong evidence for this polypeptide being MPF. Although this polypeptide has been implicated in the promotion of mitosis and in checkpoint control after low dose γ-irradiation (1 Gy (51)), and, other workers had reported that the *xrs* family have enhanced mitotic delayed after UV irradiation (78). Thus in the *xrs* family any diminution of control factors could allow for proliferation. MPF is a seryl and threononyl protein kinase and consists of two subunits:- a cyclin dependent kinase (Cdk), Cdc2, and a mitotic cyclin (cyclin B). MPF-kinase activity is high in mitosis and low in interphase. MPF-kinase

activity drives chromosome condensation, nuclear envelope breakdown and cytoskeletal rearrangement to form the mitotic spindle by phosphorylation of microtubule-associated proteins at the centrosome during metaphase-anaphase transition. Additionally MPF phosphorylation of seryl residues of the nuclear lamin molecule catalyses the disassembly of the nuclear matrix leading to breakdown of the nucleus. MPF phosphorylation of seryl and threononyl residues of histone H1 might lead to chromosome condensation. One burst of MPF has been shown to produce one round of replication followed by an arrest i.e.**re-replication block.** MPF-kinase activity is regulator of cell size in fission yeast and cell size was shown to be roughly proportional to ploid (the number of copies of the genome in a cell) thus the small size denoted by Nussenzweig *et al* (1996) with Ku80 homozygous recessive mice might be due to differences in ploidy. MPF-kinase activity is high in mitosis and low in interphase. MPF and Cdk is activated by cyclins but activation requires both cyclin binding and Cdk regulation. In yeast Cdc2 is regulated by *wee1,cdc25,* and, *cdc13*. Cdc13 protein is homologous to mitotic cyclin (cyclin B). When cyclin B binds Cdc2 is downregulated by tyrosyl phosphorylation at sites adjacent to the catalytic site by the Wee1 protein kinase and upregulated by the synergistic threononyl phosphorylation by MO15 (Cdk7) protein kinase and tyrosyl phosphate degradation catalysed by Cdc25. Mammalian equivalents of these kinases have been identified (9). MPF has been shown to associate with G1 cyclins to drive cells past the G1 checkpoint (START) by forming a **start kinase** complex and this complex has been shown in yeast to activate DNA polymerase (δ), DNA ligase and DNA topoisomerase. Start kinase has also been associated with the activation of nucleotide synthesis enzymes, chromosome structural proteins (histones) and replication origin initiation factors. In mammalian cells Cdc2 is designated as P^{34CDC2} and has been shown by peptide alignment to have a conserved seven amino acid residue sequence, **PSTAIRE**. Possibly two or three of these residues might be cross-reacting with the anti-histone monoclonal antibody e.g. **RE**.

The numerous high molecular weight histone-like bands in Figure 21 around 35-90 kDa indicate that the antibody was non-specific recognising histone variants as well as the five major histone types. The consensus peptide sequence by Boehringer Mannheim must represent a common amino acid residue in most chromosomal proteins isolated from the two hamster cell lines. This peptide might represent an evolutionary conserved sequence. The sequence has not been published and as such Boehringer Mannheim were reluctant to release the sequence for comparative analysis so supposition would indicate that the conserved sequence could be *HMG*-related. Boehringer Mannheim were reluctant to release the sequence as either it has not been characterised or patented.

Inability in obtaining all histones by the method of Bonner *et al* (1980) from both cell lines indicates that conditions were not optimal for the isolation of histonal proteins however it was suspected that there was no difference between the histones of *xrs* family and CHO KI. Confirmation of this viewpoint would necessitate

refinement of the Bonner *et al* (1980) method. The lack of success in the isolation of histonal proteins by the acid urea Triton X100 method (48) might have been due to the excessive storage and thawing of nuclear extracts which resulted from numerous abortive attempts at gel preparation. Thus the resultant gel, shown in Figure 22(B), was a composite diagrammatic representation rather than an actual photograph. However, the bands do reflect the distribution of bands observed in the Coomassie-stained acid urea detergent gel. Therefore the AUT gel did resolve bands which were in the correct size range for histones and the composite image was a true reflection of the AUT gel and an interpretation of the image was valid.

Histones have been shown to have a rôle in radioprotection (Ljungman et al 1992) but not a DNA repair rôle. Non-histonal proteins (NHP) have both a radioprotectant and a radiorepair rôle especially the *rad* family (e.g. *rad*-51, *rad*-52 & *rad*-53). Recently *rad*-51 has been associated with the 'caretaker' (52) genes, *BRCA*1 and *BRCA*2 (79). Non-histonal proteins have been involved in chromatin remodelling (CAFI) and thus by implication repair (50) but not for proofreading the topology of the nascent chromatin. Other NHP proteins, part of the transcription apparatus e.g.TFIII, perform this rôle and recruit topoisomerases II into the repair complex to correct any unsustainable topologically aberrances. Non-histonal proteins, such as Ku, may have a DNA damage sensing rôle in collaboration with damage mediators or repair enzymes in response to irradiation e.g. c-*abl* (80,81). Therefore c-Abl has been shown to downregulate DNA-PK activity by binding to the Ku component to facilitate cell killing by IR. Recently Ku has been shown in *Saccharomyces cerevisae* to be involved in transcriptional silencing at telomeric ends by interacting with carboxy-terminal tail of Sir4 and through Sir4 to Sir3 and Sir2 (82,83) leading to the formation of heterochromatin via chromatin condensation. Therefore Ku could recruit other mediators of chromatin condensation e.g. topoisomerase II and P^{34CDC2} to sites of IR-induced DNA damage to protect the site for repair or by interacting with c-Abl signalling apotosis.

(3) Pleiotropy, Ku and the DNA-PK_{cs} Knockout mice: a case for survival by chromosomal plasticity, specifcally does the plastic nature of the chromatin reflect a survival strategy adopted by proliferative cells? c.f. tumorigenic cells)

Johnson and Bryant (submitted (63)) have postulated that the protein anomalies of the *xrs* chromosome structure represent pleiotropic effects resulting from defects in the dsb rejoining in the *xrs* family. This might be interpreted as there was a propensity for the ionising radiation damage in these mutants due to their chromatin structure being more plastic compared to wt. Chromosome structural plasticity has been observed in both wt and mutant cells under the microcope and these have been correlated with interstitial heterochromatic sites or 'hot sites' where the chromatin has been observed to undergo exchange type interactions or act as putative breakage points (84).

Microscopy observations of stained Chinese hamster ovary G2 chromatids have shown that they preferentially form clusters and seem to undergo exchange type interactions with or without irradiation (85). Different lesions and initiation points might reflect the plasticity of the chromatin structure allowing exchange interaction facilitating possible conversion of double-strand breaks to chromatid breaks or translocations. These observation could indicate that these exchanges may be a survival mechanism and as such did the *xrs*' apparent difference in DNA binding by chromatin structural proteins as compared to CHO KI shown by this radiobiology study (Chapter 2) represent the plasticity of the structure? Consequently the relative quantity difference between 31 kDa proteins might be a pleiotropic compensation for the Ku80 deficiency.

A number of whole animal studies (murine) have been done to investigate the *in vivo* effects of *xrs*-6 cell types i.e. Ku80 defective cells which have shown developmental and cell changes that may imply survival mechanisms in operation (30,86).

Jeggo (1997) reviewed the current knowledge of dsb and V(D)J rejoining by the Ku components and the protein kinase complex DNA-PK_{cs}. In this review the author examined the available evidence provided by studies on homologous recombination and ES- generated knockout mice (71). The author suggests that the immune system the same components for V(D)J recombination as for damage-induced site-specifc repair thus in these knockout mice both dsb repair and V(D)J rejoining, coupled to radiosensitivity, were defective. However as there was no change in cell cycle checkpoints and the mice were viable then Ku80 did not have an essential functional rôle. The growth retardation in these mice suggested that Ku80 might have a rôle in development possibly in the repair of endogenous damage. In order for developmental and/or repair to act sufficiently to ensure cell survival a certain threshold of chromatin structural plasticity must be accommodated.

In summary chromatin structural plasticity might be a pleiotropic compensation for Ku80 deficiency, but in terms of a cell survival mechanism it might allow for proliferation. Chromatin structural plasticity might be a mechanism by which tumorigenic cells survive the effects of radiotherapeutic agents.

Recently a paper by Badie *et al* (1997) (88) threw doubt upon the rôle of Ku80 in predisposition to radiosensitivity as they found that the their rodent cell lines 180BR and 180BRM derived from an acute lymphoblastic leukaemia (ALL) patient with hypersensitivity to IR had normal DNA-PK activity but defective DSB repair and sensitivity to IR. Therefore Ku80 (XRCC4) expression was normal in 180BR but the cell lines retained their IR-hypersensitivity. Thus it is possible for the IR sensitivity in these cell lines to be due to chromatin structural abnormalities (plasticity ?).

Conclusions

The aim of this study was to examine the chromatin structure proteins of CHO KI and *xrs* rôle in relation to ionising radiation-induced chromosomal aberrations by (a) radiobiological and (b) protein chemistry methods.

The radiobiology discussion section (1) has lead to following conclusions:

(A) The biphasic nature of both cell lines could be attributed to three factors; (a) ongoing 'slow single stranded break recombinogenic repair, (b) three different cell populations with different unwinding characteristics, and, (c) supercoiling polarity changes;

(B) The change from quadratic kinetics to quintic sine kinetics in the mutant (*xrs*-5) illustrates that the cell line was more susceptible to salt-induced conformational change (Fig.14) and the increased *xrs*-5 Fss indicates that the mutant was radiosensitive at 0.75 Gy.

(C) DNA unwinding may occur at *Pvu II* sites indicating the presence of 'hot spots' or fragile sites upon which IR-induced hydroxyl radicals can act.

The protein discussion section (2) has lead to two main conclusions:

(C) The uncharacterised 31 kDa histone-related chromosomal protein could be tentatively identified as P^{34CDC2} a component of the mitosis(maturation)-promoting factor.

(D) The histones are detectable at equivalent levels, which are 15 kDa in size.

Future Work

As time was limited it was not possible to repeat the unwinding experiments shown in Figures 9, 10 and 14 with a fresh stock of mutant but if time had been available then these experiments would have been performed. The major outcome of the unwinding study has been the observation of possible ongoing repair at 4°C during and post IR, producing the curves shown in Figures 9, 10 and 14. This hypothesis might be tested unequivocally using repair inhibitors e.g.hydroxyurea and/or araC in the unwinding experiments during and post IR with careful monitoring of the ambient temperature. Prior to the unwinding assay putative mutants would be checked to ensure reversion had not occurred. This would confirm that the graphs obtained in Figs 9, 10 and 14 were due to repair then the skew would be eliminated and the Fss values would become higher and the curves would be approximately

linear with dose of IR and be similar to Fig.7. A chase step with unlabelled medium for 1h would remove any possible bias toward replication fork DNA. Additionally an increase in sample size would be beneficial by a factor of 2 i.e. 96 wells instead of 48 wells for the single parameter (salt content or radiation dose) experiments.

There was evidence to show that MPF activity in *xrs*-5 was three times higher compared to CHO KI. Implying that there was prime facie evidence for a structural modification of the catalytic subunit P^{34CDC2}. Unequivocal evidence for the involvement of MPF as the 31 kDa polypeptide would require a bulk protein isolation step involving 5-6ml of mitotic cell suspension and gel purification to produce pure 31 kDa fraction or the use of a fraction purification column using an affinity column containing the anti-histone monoclonal antibody bound to sepharose beads and eluates being tested for MPF activity by MPF kinase and size by 12% SDS-PAGE. The pure protein may then be sequenced directly and characterised initially by sequence comparisons with the SWISSPROT database or by Enhanced Chemiluminiscent assay (Amersham) with PSTAIRE, KKIARE,PITALRE and PCTAIRE panel of anti-cdk monoclonal antibodies. Thus if the hypothetical polypeptide was MPF then it would have MPF kinase activity and would either have P^{34CDC2} related sequence or show immunoreactivity to anti-cdk monoclonal antibodies.

To test whether the quantity of histones was invariant then the intial isolation from nuclei would require a range of hydrochloric acids from 0.2 to 0.5M. which would ensure optimal histone extraction. The extracted histones would need to be loaded immediately onto a prepared AUT gel and resolved overnight at a low constant current 2mA to avoid denaturation and 'acid' Coomassie stained. Standard histones (10μg/ml stock) would need to be resolved as a 1 in 10 dilution with the samples as a size marker.

Bibliography

(1) **Kemp L.M., Sedgwick S.G. & Jeggo P.A.** (1984).
X-ray sensitive mutants of Chinese hamster ovary cells defective in double-strand break rejoining. *Mutation Research* **132**, 189-96.
(2) **Taccioli,G.E.,Gottlieb,T.M.,Blunt,T.,Priestley,A.,Demengeot,J., Mizuta,R.,Lehman,A.R.,Alt,F.W.,Jackson,S.P.,Jeggo,P.A.** (1994).
Ku80 product of the **XRCC5** gene and its role in DNA repair and V(D)J recombination. *Science* **265**, 1442-45.
(3) **Getts,R.C. & Stamato,T.D.** (1994).
Absence of a Ku-like DNA end binding activity in the *xrs* double-strand DNA repair-deficient mutant. *J.Biol.Chem.* **269**(23), 15981-84.
(4) **Bryant P.E.** (1990).
In: CHROMESOME ABERRATIONS: BASIC AND APPLIED ASPECTS. pp61-69.
(5) **Jeggo,P.A.,Kemp,L.M. & Holliday,R.** (1982).
The application of the microbial "tooth-pick" technique to somatic cell genetics, and its use in the isolation of X-ray sensitive mutants of Chinese ovary cells. *Biochimie* **64**, 713-15.
(6) **Jeggo,P.A. & Kemp,L.M.** (1983).
X-ray-sensitive mutants of Chinese hamster ovary cell line Isolation and cross-sensitivity to other DNA-damaging agents. *Mutation Research* **112**, 313-27.
(7) **Jeggo,P.A.** (1985).
X-ray sensitive mutants of Chinese hamster ovary cell line: radio-sensitivity of DNA synthesis. *Mutation Research* **145**, 171-76.
(8) **Kemp,L.M. & Jeggo,P.A.** (1986).
Radiation-induced chromosome damage in X-ray-sensitive mutants (*xrs*) of the Chinese hamster ovary cell line. *Mutation Research* **166**, 255-63.
(9) **Alberts, B. *et al*** (1994).
MOLECULAR BIOLOGY OF THE CELL 3rd.Ed.,Garland Publishing,London.
(10) **Gasser, S. M. and Laemmli, U. K.** (1986).
The organisation of chromatin loops: Characterisation of a scaffold attachment site. *EMBO J.*, **5**, 511-518.
(11) **Pienta, K. J. and Coffey, D. S.** (1984).
A structural analysis of the role of the nuclear matrix and DNA loops in the organisation of the nucleus and chromosome. *J. Cell Sci. Suppl.* , **1**, 123-135.
(12) **Jackson,D.A. and Cook,P.R.**(1986).
Replication occurs at a nucleoskeleton. *EMBO J.* **5**, 1403-11.
(13) **Jackson,D.A.,Dickinson,P. and Cook,P.R.**(1990).
The size of chromatin loops in HeLa cells. *EMBO J.* **9**, 567-71.
(14) **Jackson,D.A.,Hassan,A.B.,Errington,R.J. and Cook,P.R.**(1993).
Visualisation of focal sites of transcription within human nuclei. *EMBO J.* **12**, 1059-65.
(15) **Wolffe,A** (1995).
CHROMATIN STRUCTURE AND FUNCTION 2nd Ed.Academic Press,London. Ch2 pp6-104.
(16) **Zentgraf,H. and Franke,W.W.**(1984).
Differences of supra nucleosomal organisation in different kinds of chromatin: cell type-specific globular subunits containing different numbers of nucleosomes. *J.Cell Biol.*,**99**, 272-86.
(17) **Worcel,A.** (1978).
Molecular architecture of the chromatin fibre. *Cold Spring Harbor Symp.Quant.Biol.* **42**, 313-24.
(18) **Woodcock,C.L., Frado,L.L. and Rattner,J.B.** (1984).
The higher-order structure of chromatin: evidence for a helical ribbon arrangement. *J.Cell Biol.***99**, 42-52.
(19) **Feslsenfeld,G. and McGhee,J.D.** (1986).
Structure of the 30 nm fibre. *Cell* **44**, 375-7.
(20) **Sedat, J. and Manuelidis,L.** (1978).
A direct approach to the structure of mitotic chromosomes. *Cold Spring Harbor Symp.Quant.Biol.* **42**, 331-50.
(21) **Zdzienicka, M.Z.** (1995).
Mammalian mutants defective in the response to ionising radiation-induced DNA damage. *Mutation Research* **336**, 203-13
(22) **Cornforth, M.N. & Bedford,J.S.** (1993).
In: ADVANCES IN RADIATION BIOLOGY. Ed. J.T.Lett, W.K.Sinclair. Pbl: Academic Press, London Vol.**17** pp423-96.
(23) **Jeggo,P.A. & Holliday,R.** (1986).
Azacytidine-induced Reactivation of a DNA repair gene in Chinese hamster ovary cells. *Molecular and Cellular Biology* **6**(8), 2944-49.
(24) **Jeggo,P.A. & Smith-Ravin,J.** (1989).
Decreased stable transfection frequencies of six X-ray-sensitive CHO strains, all members of the *xrs* complementation group. *Mutation Research* **218**, 75-86.
(25) **Schwartz,J.L. *et al*** (1995).

Altered metaphase chromosome structure in xrs-5 cell is not related to its radiation sensitivity or defective DNA break rejoining. *Mutation Research* **328**, 119-26.

(26) **He,D.M.,Lee,S.E. and Hendrickson,E.A.**(1996).
Restoration of X-ray and etoposide resistance, Ku-end binding activity and V(D)J recombination to the Chinese hamster *sxi*-3 mutant by a hamster Ku86 cDNA. *Mutation Research* **363**, 43-56.

(27) **Yasui,L.S.,Ling-Indeck,L.,Johnson-Wint,B.,Fink,T.J. & Molsen,D.** (1991).
Changes in the nuclear structure in the radiation-sensitive CHO mutant cell, *xrs*-5. *Radiation Research* **127**, 269-77.

(28) **Yasui,L.S.** (1992).
Cytotoxicity of ^{125}I decay in the DNA double strand break repair deficient mutant cell line, *xrs*-5. *Int.J.Radiat.Biol.* **62**(5), 613-18.

(29) **Collins,A.R.** (1993).
Mutant rodent cell lines sensitive to ultraviolet light,ionising radiation and cross-linking agents: a comprehrensive survey of genetic and biochemical characteristics. *Mutation Research, DNA Repair* **293**, 99-118.

(30) **Nussenzweig,A.,Chen,C.,da Costa-Soares,V.,Sanchez,M.,Sokol,K.,Nussenzweig,M.C. and Li,G.C.** (1996).
Requirement for Ku80 in growth and immunoglobin V(D)J recombination. *Nature* **382**(6591), 551-5.

(31) **Roti-Roti,J.L., Wright,W.D., and Taylor,Y.C.** (1993).
In: ADVANCES IN RADIATION BIOLOGY. Ed. J.T.Lett, W.K.Sinclair. Pbl: Academic Press, London Vol.**17** pp227-59.

(32)**Vogelstein,B.,Pardoll,D.M. & Coffey,D.S.** (1980).
Supercoiled loops and eucaryotic DNA replication. *Cell***22**, 79-85.

(33) **Mullenders,L.H.F.** *et al* (1987).
The localisation of ultraviolet-induced excision repair in the nucleus and the distribution of repair events in higher order chromatin loops in mammalian cells. *J.Cell Sci.Suppl.***6**:243-62.

(34) **Hakes ,D.J. and Berezney,R.**(1991).
DNA binding properties of the nuclear matrix and individual nuclear matrix proteins. *J.Biol.Chem.* **266**(17), 11131-40.

(35) **VanderWaal,R.,Thampy,G.,Wright,W.D. and Roti-Roti,J.L.**(1996).
Heat-induced modifications in the association of specific proteins with the nuclear matrix. *Radiation Research* **145**,746-53.

(36) **Cook,P.R.,Brazell,I.A. and Jost,E.** (1976).
Characterisation of nuclear structures containing superhelical DNA. *J.Cell Sci.*, **22**, 303-324.

(37) **Oleinick,N.L. & Chiu,S.-M.** (1994).
Nuclear and chromatin structures and their infulence on the radiosensitivity of DNA. *Radiation Protection Dosimetry* **52**(1-4):353-58.

(38) **Ahnström,G. & Erixxon,K.** (1981).
Measurement of strand breaks by alkaline denaturation and hydoxyapatite chromatography. In: DNA REPAIR. Eds. Friedberg,E.C. & Hanawalt,P.C. Pbl: Marcel Dekker Inc., Vol.**1**, pp403-418.

(39) **Ljungman,M.** (1991).
The influence of chromatin structure on the frequency of radiation induced DNA strand breaks: a study using nuclear and nucleoid monolayers. *Radiat.Res.***126**, 58-64.

(40) **Ljungman,M.,Nyberg,S.,Nygren,J.,Eriksson,M. and Ahnström,G.** (1991).
DNA-bound proteins contribute much more than soluble intracellular compounds to the intrinsic protection against radiation-induced DNA strand breaks in human cells. *Radiat.Res.* **127**, 171-76.

(41) **Nygren,J.,Ljungman,M. and Ahnström,G.** (1995).
Chromatin structure and radiation-induced DNA strand breaks in human cells: soluble scavengers and DNA-bound proteins offere a better protection against single- than double strand breaks. *Int.J.Radiat.Biol.* **68**(1), 11-18.

(42) **Goodhead, D. T.**, (1994).
Initial events in the cellular effects of ionising radiations: clustered damage in DNA. *Int. J. Radiat. Biol., 65, 7-17.*

(43) **Fenech,M. & Morley,A.A.**(1985).
Measurement of micronuclei in lymphocytes. *Mutation Research* **147**:29-36.

(44) **Tucker,J.D. and Preston,R.J.**(1996).
Chromosome aberrations, micronuclei, aneuploidy, sister chromatid exchanges, and cancer risk assessment. *Mutation Research* **365**, 147-59.

(45) **Bradbury,E.M.,MaClean,N. and Matthews,H.R.** (1981).
Components of eukaryotic chromatin. In: DNA, CHROMATIN AND CHROMESOMES. Pbl: Blackwell Scientific Publications, Oxford. Ch.**1**, pp11-34.

(46) **Allfrey, V.G.**(1977).
Postsynthetic modifications of histone structures. In: CHROMATIN AND CHROMOSOME STRUCTURE. Eds. Li,H.J. & Eckert, R. Publ.Academic Press, New York pp167-91.

(47) **Dixon,G.H.,Candido,E.P.M.,Honda,B.M.,Loui,A.J.,Macleod,A.R. and Sung,M.T.**(1974).
The biological rôles of post-synthetic modification of basic nuclear proteins. *CIBA Found. Symp.: The Structure and Function of Chromatin* **28**, 229-58.

(48) **Bonner,W.M.,West,M.H.P. and Stedman, J.D.** (1980).

Two-dimensional gel analysis of histones in acid extracts of nuclei, cells and tissues. *Eur.J.Biochem.* **109**, 17-23.

(49) **Goodwin,G.M.,Walker,J.M. and Johns,E.W.**(1978).
The high mobility (HMG) nonhistonal chromosomal proteins. In: THE CELL NUCLEUS. Eds. Busch,H. Publ. Academic Press, New York pp181-219.

(50) **Gaillard,P-H.L. *et al*** (1996).
Chromatin assembly coupled to DNA repair: a new role for chromatin assembly factor I. *Cell* **86**:887-96.

(51) **Barth H.***et al* (1996).
Radiation with 1 Gy prevents the activation of the mitotic inducers Mitosis-Promoting Factor (MPF) and cdc-25-C in HeLa cells. *Cancer Research* **56**:2268-72.

(52) **Kinzler,K.W. and Vogelstein,B.** (1997).
Cancer-susceptibility gene: Gatekeepers and Caretakers. *Nature* **386**(6627), 761-63.

(53) **Zhao,K.,Käs,E.,Gonzalez,E. and Laemmli,U.K.**(1993).
SAR-independent mobilization of histone H1 by HMG-I/Y *in vitro*: HMG-I/Y is enriched in H1-depleted chromatin. *EMBO J.* **12**(8), 327-47.

(54) **Wolffe,A.P.,Khochbin,S. and Dimitrov,S.**(1997).
What do linker histones do in chromatin? *BioEssays* **19**(3), 249-55.

(55) **Tubiana,M. *et al*** (1990).
INTRODUCTION TO RADIOBIOLOGY.,Taylor & Francis,London pp1-173.

(56) **Britten,R.J. Pavich,M. & Smith,J.** (1976).
A new method for DNA purification. *Carnegie Institution Yearbook.* **68**, 400-02.

(57) **Ljungman,M.** (1989).
Pretreatment with UV light renders the chromatin in human fibroblasts more susceptible to the DNA-damaging agents bleomycin, gamma radiation and 8-mehtoxypsoralen.*Carcinogenesis* **10**(3), 447-51.

(58) **Bryant,P.E. & Blöcher,D.** (1980).
Measurement of the kinetics of DNA double strand break repair in Ehrlich ascites tumour cell using the unwinding method. *Int.J.Radiat.Biol.* **38**(3), 335-47.

(59) **Costa,N.D. and Bryant,P.E.**(1991).
Elevated levels of DNA double-strand breaks (DSB) in restriction endonuclease-treated XRS5 cells correlate with the reduced capacity to repair DSB. *Mutation Research* **255**(1), 219-26.

(60) **Zimm,B.H.**(1956).
Dynamics of polymer molecules in dilute solution:viscoelasticity, flow birefrigence and dielectric loss. *J.Chem.Phys.* **24**, 269-78..

(61) **Quake,S.R.,Babcock,H. and Chu,S.**(1997).
The dynamics of partially extended single molecules of DNA. *Nature* **388**(6638), 151-54.

(62) **Cook,P.R. and Brazell,I.A.**(1975).
Supercoiling in Human DNA. *J.Cell Sci.* **19**, 264-79.

(63) **Johnston,P.J. and Bryant,P.E.** (1997).
Altered DNA binding activities of proteins extracted from the ionising radiation sensitive mutant *xrs5*. Submitted to Int.J.Radiat.Biology.

(64) **Johnston,P.J. and Bryant,P.E.** (1994).
A component of DNA double-strand break repair is dependent on the spatial orientation of the lesions within the higher-order structures of chromatin. *Int.J.Radiat.Biol.***66**(5),531-6.

(65) **Mateos,S., Slijepcevic,P.,MacLeod,R.A.F. and Bryant,P.E.**(1994).
DNA double strand break rejoining in XRS5 cells is more rapid in the G2 than in the G1 phase of the cell cycle. *Mutation Research* **315**, 181-87.

(66) **Narayanswami,S. and Hamkaic,B.A.** (1989).
Preparartion of whole-mount metaphase chromosomes. In: PROTEIN STRUCTURE- A PRACTICAL APPROACH. Ed. Creighton,T.E.Pbl. IRL Press,Oxford University Press. pp217-18

(67) **Bradford,M.**(1976).
Anal. Biochem. **72**, 248.

(68) **Snyder,R.D.,Van Houten,B. and Regan,J.D.** (1982).
The accumulation of DNA breaks due to incision: comparative studies with various inhibitors. In: DNA REPAIR AND INHIBITION-Nucleic Acid Symposium Series 13. Eds. **Collins,A.R.,Downes,C.S. and Johnson,R.T.**. Pbl.IRL Press, Oxford Ch.**2**, 13-33.

(69) **Fenech,M.,Rinaldi,J.,and Surralles,J.**(1994).
The origin of micronuclei induced by cytosine arabinoside and its synergistic interaction with hydroxyurea in human lymphocytes. *Mutagenesis* **9**(3), 273-7.

(70) **Brunborg,G.,Holme,J.A. and Hongslo,J.K.**(1995).
Inhibitory effects of paracetamol on DNA repair in mammalian cells. *Mutation Research* **342**(3-4), 157-70.

(71) **Slamenová,D.,Gábelová,A.,Ruzeková,L',Chalupa,I.,Horváthová,E., Farkasová,T.,Bozsakyová,E. and Stetina,R.**(1997).
Detection of MNNG-induced DNA lesions in mammalian cells; validation of comet assay against DNA unwinding technique, alkaline elution of DNA and chromosomal aberrations. *Mutation Research* **383**, 243-52.

(72) **Ogorek,B. and Bryant,P.E.**(1985).
Repair of DNA single-strand breaks in X-irradiated yeast: II Kinetics of repair as measured by the DNA-unwinding method. *Mutation Research* **146**, 63-70.

(73) **Fonck,K.,Barthel,R. and Bryant,P.E.**(1984).
Kinetics of recombinational hybrid formation in X-irradiated mammalian cells: a possible first step in the repair of DNA double-strand breaks. *Mutation Research* **132**,113-18.

(74) **Johnston,P.J. and Bryant,P.E.** (1991).
Lack of interference of DNA single-strand breaks with the measurement of double-strand breaks in mammalian cells using the neutral filter elution assay. *NARS* **19**(10), 2735-38.

(75) **Bryant,P.E.,Warring,R. and Ahnström,G.**(1984).
DNA repair kinetics after low doses of X-rays. A comparison of results obtained by the unwinding and nucleoid sedimentation methods. *Mutation Research* **131**(1), 19-26.

(76) **Holmberg,M. and Gumauskus,E.**(1986).
The role of short-lived DNA lesions in the production of chromosome-exchange aberrations. *Mutation Research* **160**, 221-9.

(77) **MacLeod,R.A.F. and Bryant,P.E.**(1990).
Similar kinetics of chromatid aberrations in X-irradiated *xrs*-5 and wild type Chinese hamster ovary cells. *Mutagenesis* 5(**4**), 407-10.

(78) **Jeggo,P.A.** (1990).
Studies on mammalian mutants defective in rejoining double-strand breaks in DNA. *Mutation Research* **239**, 1-16.

(79) **Sharan,S.K.,Morimatsu,M.,Albrecht,U.,Lim,D-S.,Regel,E.,Dinh,C.,Sands,A.,Eichele,G., Hasty,P. and Bradley,A.** (1997).
Embryonic lethality and radiation hypersensitivity mediated by Rad51 in mice lacking Brca2. *Nature* **386**(6627), 804-10.

(80) **Kharbanda,S.,Pandey,P.,Jin,S.,Inoue,S.,Bharti,A.,Yuan,Z-M.,Weichselbaum,R.,Weaver,D. & Kufe,D.** (1997).
Functional interaction between DNA-PK and c-Abl in response to DNA damage. *Nature* **386**(6626), 732-35.

(81) **Shafman,T.,Khanna,K.K.,Kedar,P.,Spring,K.,Koslov,S,Yen,T., Hobson,K.,Gatel,M.,Zhang,N.,Watters,D.,Egerton,M.,Shiloh,Y.,Kharbanda,S.,Kufe,D. & Lavin,M.F.** (1997).
Interaction between ATM protein and c-Abl in response to DNA damage. *Nature* **387**(6632), 520-23.

(82) **Jackson,S.P.**(1997).
Silencing and DNA repair connect. *Nature* **388**(6645), 829-30.

(83) **Tsukamoto,Y.,Kato,J.-i. and Ikeda,H.**(1997).
Silencing factors participate in DNA repair and recombination in *Saccharomyces cerevisae*.. *Nature* **388**(6645), 900-03.

(84) **Slijepcevic,P. and Natarajan,A.T.**(1994).
Distribution of radiation-induced G1 exchange and terminal deletion breakpoints in Chinese hamster chromosomes as detected by G banding. *Int.J.Radiat.Biol.* **66**(6), 747-55.

(85) **Slijepcevic,P.,Xiao,Y.,Dominguez,I and Natarajan,A.T.**(1996).
Spontaneous and radiation-induced chromosomal breakage at interstitial telomeric sites. *Chromosoma* **104**, 596-604.

(86) **Jeggo,P.A.**(1997).
DNA-PK: at the cross-roads of biochemistry and genetics. *Mutation Research* **384**, 1-14.

(87) **Weibezahn,K.F.,Lohrer,H. and Herrlich,P.**(1985).
Double -strand break repair and G2 block in Chinese hamster ovary cells and their radisensitive mutants.
Mutation Research **145**, 177-83.

(88) **Badie,C.,Goodhardt,M.,Waugh,A.,Doyen,N.,Foray,N.,Calson,P.,Singleton,B.,Gell,D.,Salles,B., Jeggo,P.,Arlett,C.F. and Malaise,E-P.**(1997).
A DNA Double-Strand Break defective fibroblast cell line (180BR) derived from a radiosensitive patient represents a new mutant phenotype.
Cancer Research **57**, 4600-07.